FABRICATION, CHARACTERIZATION AND WELDING OF AA7075 METAL MATRIX COMPOSITE USING FSW PROCESS

Thesis

Submitted in fulfillment of the requirement of

DOCTOR OF PHILOSOPHY

to

J.C. BOSS UNIVERSITY OF SCIENCE & TECHNOLOGY, YMCA, FARIDABAD

By

DHAIRYA PARTAP SINGH

(Registration No. YMCAUST/Ph 22/2010)

Under the supervision of

Dr. Vikam Singh
Professor
Mechanical Engineering Dept.

Dr. Sudhir Kumar
Professor
Mechanical Engineering Dept.

Department of Mechanical Engineering
Faculty of Engineering and Technology
J.C BOSS University of Science & Technology, YMCA,
Sector-6, Mathura Road, Faridabad, Haryana, India
JULY 2019

CANDIDATE'S DECLARATION

I hereby declare that this thesis entitled **FABRICATION, CHARACTERIZATION AND WELDING OF AA7075 METAL MATRIX COMPOSITE USING FSW PROCESS** by **DHAIRYA PARTAP SINGH**, being submitted in fulfillment of the requirements for the Degree of Doctor of Philosophy in Mechanical Engineering under Faculty of Engineering and Technology of J.C Boss University of Science & Technology, YMCA, Faridabad, is a bonafide record of my original work carried out under guidance and supervision of **Dr. VIKRAM SINGH, Professor, Mechanical Engineering**, **J.C Boss University of Science & Technology, YMCA, Faridabad** and **Dr. SUDHIR KUMAR, Professor, Mechanical Engineering**, Greater Noida Institute of Technology, Greater Noida and has not been presented elsewhere.

I further declare that the thesis does not contain any part of any work which has been submitted for the award of any degree either in this university or in any other university.

Dhairya Partap Singh
YMCAUST /Ph 22/2K10

ACKNOWLEDGEMENT

It gives me great pleasure to express my heartfelt gratitude towards my esteemed supervisor **Dr. Vikram Singh,** Professor, Mechanical Engineering Department, YMCA University of Science and Technology, Faridabad. His supervision indeed helped me to overcome arising problems throughout this research. Without his continuous motivation, constant monitoring and constructive criticism this would not have been possible.

I would like to express my sincere and great appreciation to my esteemed supervisor, teacher and mentor **Dr. Sudhir Kumar**, Professor, Mechanical Engineering Department, Greater Noida Institute of Technology, Greater Noida. His invaluable continued guidance, motivation, constant inspiration and above all for his ever co-operating attitude that enabled culmination of this huge task possible. His suggestions and attention to the minutest details made it possible to give this study its present form. He has been the primary guiding force and inspiration behind this study. I feel privileged on being associated with such an esteemed research supervisor.

I am highly grateful to **Dr. Dinesh Kumar,** Vice Chancellor, YMCAUST, Faridabad for giving me the opportunity to conduct this study.

I am extremely thankful to **Prof. Tilak Raj,** Chairperson, Mechanical Engineering Department, YMCAUST, Faridabad for providing all kinds of possible help and advice during the course of this work.

I cannot forget to thank **Dr. M. L. Aggarwal, Dr. Hari Om, Dr. Rajiv Saha, Dr. O.P Mishra, Dr. Mahesh Kumar** and **Mr. Rajender Kumar Tyal** for constant valuable discussions and suggestions.

This work would not have seen light of the day without the kind co-operation of my friends **Mr.** Ravi Kushwah, Mr. Arun Kumar and Mr. Sachin Kumar Lecturer, BSACET, Mathura. I am highly grateful to him for the invaluable help, guidance and constant encouragement. His suggestions became an important part for the completion of this work. His excellent writing skill became an invaluable inspiration for me. I would fail in my duty to appreciate his support if any word could be found suitable to explain it.

A word of special thanks to my ex-students **Mr. Rahul Chaudhary** and **Mr. Visnu Kumar** for their support and help during my experimental work.

Still remain many whose names do not feature above. But their anonymity, however in no way suggests that their contribution has gone unacknowledged.

Hand that rocks the cradle rules the world. I bow my head to my beloved parents **Sh. Surendra Pal Singh** and **Smt. Bimlesh Singh** whose love and care have been the keys to my success. No words can express what their undemanding love, sacrifices, dedication and prayers have done to help me become what I am today. I thank them for always being there to support me.

I also express deep gratitude to my brother, **Mr.Shorya Pratap Singh**, his wife **Mrs. Geeta Singh,** and his daughter **Shelli** for their constant love, and care, and being there to support me. A special thanks to my dear wife, **Manju Singh** and my little champs **Aradhya** and **Himanshu** for supporting me in every step of my life, encouraging me, trusting me, conducting me through my troubles and always being my best allies.

Finally, I remember and thank the all-powerful **ALMIGHTY GOD**, who gave me energy, skill and enthusiasm to complete the task. I pray to him to empower me to scale new heights, to kindle my mind with knowledge, to dispel the darkness of ignorance and to lead the life gifted by him fruitfully.

Dhairya Partap Singh

YMCAUST/Ph 22/2K10

ABSTRACT

Aluminum metal matrix composites have been widely used in aerospace industries. These AMC offer serious challenges for joining by conventional welding due to their unique combination of properties such as high strength to weight ratio and high hardness. These AMC are referred to as difficult to weld since they possess a greater challenge due to their abrasive behavior, high stress generation and large HAZ developed during in conventional welding process. Therefore non-traditional welding technique provides the effective solutions to these problems. Friction stir welding (FSW) is a non-traditional and solid state welding technique. It is more efficient and economical welding method which produces very less defects as compared to the other liquid state welding techniques. High weld quality can be obtained by this technique.

The main objective of this research is to fabricate AA7075/10%wt.SiC composite and determine the optimal process parameters of friction stir welding technique. In this research composite were prepared by mechanical stir casting process. Characterization was done SEM, EDAX, XRD and Thermal analysis. SEM analysis revealed that a fairly uniform and homogeneous distribution of reinforcing particles of SiC with matrix alloy. EDAX analysis confirmed that elements like Mg, Si, Zn and Cu were present in major quantity. The XRD patterns of cast composite confirmed the presence of the base alloy 7075 and other constituents of matrix alloy. The presence of hard phase constituents SiC were confirmed at respective peaks. Thermal analyses confirmed that there are no degradation and material loss in the composites. Experiments were performed with four process parameters such as tool rotation speed(T.R.S), welding speed(W.S), axial force(A.F) and tool geometry considering three levels of each. The process parameter's levels were selected by pilot experiments. The Welding experiments were conducted using L_{27} orthogonal array and responses such as tensile strength, percentage elongation, hardness and joint efficiency were measured. A combination of orthogonal array and design of experiments was used to give best possible welding process parameters that give optimal responses. Experimental results reveal that the tool rotation speed, welding speed and axial force were the significant process parameters affecting the welding performance. The predicted optimal value of tensile strength, percentage elongation

hardness and welded joint efficiency was 307.48 MPa, 4.344%, 123.736 HV and 95.621% respectively. The research proposed a grey-based Taguchi method to solve the multi-response problems. A combination of orthogonal array, design of experiments and grey relational analysis were used to predict best possible welding process parameters that give maximum response. The output response characteristics were tensile strength and hardness of welded joints. The result demonstrated that the tool rotational speed has the strongest effect on multi performance characteristics among the other process parameters. The value of grey relation grade was 0.7371 with initial parameters ($A_1B_1C_1D_1$) was improved to 0.8268 with optimal process parameters ($A_2B_2C_2D_1$). This increment in grade reflected that welded joint quality was improved using optimal process parameters. The results revealed that combination of Taguchi design of experiment and grey relational analysis improved the quality of welded joints. The confirmation tests have been performed to verifying the results.

TABLE OF CONTENTS

Declaration		i
Certificate		ii
Acknowledgements		iii
Abstract		v
Table of Contents		vii
List of Tables		xi
List of Figures		xv
Nomenclature		xix
CHAPTER-1	INTRODUCTION	1-12
1.1	COMPOSITE MATERIAL	1
1.1.1	Classification of Composite	1
1.1.2	Metal Matrix Composite	2
1.1.3	Fabrication Technique of Metal Matrix Composite	3
1.1.3.1	Liquid phase fabrication technique	3
1.1.3.2	Solid phase fabrication technique	4
1.1.3.3	Power metallurgy technique	4
1.1.4	Advantage of Metal Matrix Composites	4
1.1.5	Disadvantage of Metal Matrix Composites	5
1.1.6	Application of Metal Matrix Composites	5
1.2	Welding of Metal Matrix Composite	5
1.2.1	Conventional Welding	5
1.2.2	Unconventional Welding	5
1.2.3	Friction Stir welding process	6
1.2.3.1	Basic principle of operation	6
1.2.3.2	Advantage of Friction Stir Welding	7
1.2.3.3	Disadvantage of Friction Stir Welding	7
1.2.3.4	Application of Friction Stir Welding	8
1.3	ORGANIZATION OF THE THESIS	10-11

CHAPTER-2	LITERATURE REVIEW	12-25
2.1	OVERVIEW	12
2.2	LITERATURE OF METAL MATRIX COMPOSITE	13-18
2.3	LITERATURE OF FRICTION STIR WELDING	19-25
2.4	IDENTIFICATION OF GAPS IN THE LITERATURE	25
2.5	OBJECTIVE OF RESEARCH	26
2.6	FLOW CHART OF ENTIRE RESEARCH	27
CHAPTER-3	EXPERIMENTAL SET-UP	28-37
3.1	SELECTION OF MATERIAL	28
3.1.1	Selection of Matrix Material	28
3.1.2	Selection of Reinforcement	28
3.2	COMPONENTS OF MECHANICAL STIR CASTING	29
3.2.1	Graphite Crucible	29
3.2.2	Stirrer and Blades	29
3.2.3	Muffle Furnace and Temperature controller	30
3.2.4	D.C Motor	31
3.2.5	Nitrogen Gas	32
3.3	EXPERIMENTAL SET-UP OF MECHANICAL STIR CASTING	32
3.4	FABRICATION PROCEDURE OF METAL MATRIX COMPOSITE	35
3.5	FABRICATION OF FSW TOOL	36
3.6	EXPERIMENTAL SET-UP OF FSW	37
CHAPTER-4	SELECTIONS OF PROCESS PARAMETERS AND RESPONSES	38-49
4.1	SELECTION OF PROCESS PARAMETERS OF MECHANICAL STIR CASTING PROCESS	38
4.1.1	Stirrer design	38
4.1.2	Stirring speed	38
4.1.3	Stirring Temperature	38
4.1.4	Stirring Time	38
4.1.5	Reinforcement pre-heat temperature	39

4.2	CAUSE AND EFFECT DIAGRAM OF MECHANICAL STIR CASTING	39
4.3	RESPONSES OF FABRICATED COMPOSITE	40
4.3.1	Characterization of Metal Matrix Composite	40
4.3.1.1	Microstructure	40
4.3.1.2	SEM and EDAX analysis	41
4.3.1.3	X-Ray diffraction analysis	42
4.3.1.4	Thermal analysis	43
4.3.1.5	SEM fractography	44
4.3.1.6	Mechanical behaviour	44
4.3.1.6.1	Tensile strength testing	44
4.3.1.6.2	Impact strength testing	45
4.3.1.6.3	Hardness	46
4.4	CAUSE AND EFFECT DIAGRAM OF FRICTION STIR WELDING	47
4.5	SELECTION OF PROCESS PARAMETERS AND THEIR RANGES OF FRICTION STIR WELDING	47
4.5.1	Tool Rotation Speed	48
4.5.2	Welding Speed	48
4.5.3	Axial Force	48
4.5.4	Tool Geometry	49
4.5.5	Tilt Angle	49
4.5.6	Tool Diameter	49
CHAPTER-5	OPTIMIZATION TECHNIQUE	57-65
5.1	DESIGN OF EXPERIMENTS	57
5.1.1	Taguchi approach	57
5.1.2	Experimental design strategy	57
5.1.3	Signal to Noise ratio	58
5.1.4	Steps in experimental design and analysis	58
5.1.4.1	Selection of Orthogonal Array (OA)	58
5.1.4.2	Data analysis	59
5.1.4.3	Analysis of Variance (ANOVA)	60
5.1.4.4	Determination of confidence intervals	61

5.2	CONDUCT OF EXPERIMENTS FOR RESPONSE CHARACTERISTICS	62
5.2.1	Responses	63
5.3	MULTI RESPONSE OPTIMIZATION TECHNIQUE	64
5.3.1	Planning for Optimizing Multi Response Characteristics	64
5.3.2	Grey relational analysis (GRA)	65
CHAPTER-6	RESULTS AND DISCUSSION	66-135
6.1	CHARACTERIZATION OF AA7075/SIC COMPOSITE	66
6.1.1	Microstructures	66
6.1.2	Scanning Electron Microscopy (SEM) and Energy Dispersive X-ray Analysis (EDAX) analysis	67
6.1.3	X-Ray diffraction analysis	69
6.1.4	Thermal analysis	70
6.1.5	SEM Fractography	71
6.2	RESULTS OF WELDING RESPONSE CHARACTERISTICS	72
6.2.1	Signal to noise ratio(S/N ratio)	72
6.2.2	Analysis of Tensile Strength	72
6.2.2.1.	Effect of Tool rotation speed	76
6.2.2.2	Effect of welding speed	77
6.2.2.3	Effect of axial force	77
6.2.2.4	Effect of tool geometry	78
6.2.2.5	Analysis of variance (ANOVA)	79
6.2.2.6	Interaction Plot for Tensile Strength	79
6.2.2.7	Estimation of optimum performance characteristic for Tensile Strength	82
6.2.2.8	Confirmation of experiments	85
6.2.3	Analysis of Percentage Elongation	86
6.2.3.1	Effect of Tool rotation speed	89
6.2.3.2	Effect of welding speed	89
6.2.3.3	Effect of axial force	89
6.2.3.4	Effect of tool geometry	90

6.2.3.5	Analysis of variance (ANOVA)	90
6.2.3.6	Interaction Plot for Percentage Elongation	92
6.2.3.7	Estimation of optimum performance characteristic for Percentage Elongation	94
6.2.3.8	Verification of Optimal Parameters Through Confirmation Test	97
6.2.4	Analysis of Hardness	98
6.2.4.1	Effect of Tool rotation speed	101
6.2.4.2	Effect of welding speed	102
6.2.4.3	Effect of axial force	102
6.2.4.4	Effect of tool geometry	102
6.2.4.5	Analysis of variance (ANOVA)	103
6.2.4.6	Interaction plots for hardness	104
6.2.4.7	Estimation of optimum performance characteristic for Hardness	107
6.2.4.8	Verification of Optimal Parameters through Confirmation Test	110
6.2.5	Analysis of Welding Joint Efficiency	110
6.2.5.1	Effect of Tool rotation speed	114
6.2.5.2	Effect of welding speed	114
6.2.5.3	Effect of axial force	114
6.2.5.4	Effect of tool geometry	115
6.2.5.5	Analysis of variance (ANOVA)	115
6.2.5.6	Interaction Plots for Joint Efficiency	117
6.2.5.7	Estimation of optimum performance characteristic for Tensile Strength	119
6.2.5.8	Verification of Optimal Parameters through Confirmation Test	122
6.3	MULTI RESPONSE OPTIMIZATION	123
6.3.1	Analysis of Grey Relation Grade	123
6.3.1.1	Data Pre-Processing	124
6.3.1.2	Grey Relational Deviation, Coefficient and Grey Relational Grade	124

6.3.1.3	Response Table for grey relation grade	127
6.3.1.4	Effect of Rotational Speed on Grey Relation Grade	129
6.3.1.5	Effect of Welding Speed on Grey Relation Grade	129
6.3.1.6	Effect of Axial Force on Grey Relation Grade	129
6.3.1.7	Effect of Tool Pin Profile on Grey Relation Grade	130
6.3.2	Analysis of variance (ANOVA)	130
6.3.3	Interaction Plots for Grey Relational Grade	131
6.3.4	Optimization of Process Parameters for Grey Relational Grade	134
6.3.5	Verification of Optimal Parameters Through Confirmation Test	135
CHAPTER 7	CONCLUSION	136-139
7.1	CONCLUSION	136
7.2	INDUSTRIAL APPLICATION OF FSW PROCESS	138
7.2	LIMITATION AND SCOPE FOR FUTURE WORK	139
	REFERENCES	140-151

LIST OF TABLES

Table No	Caption	Page No
3.1	Chemical Composition of AA7075	28
4.1	Selected process parameters and their ranges	56
5.1	Taguchi's orthogonal array	62
5.2	Measured responses of friction stir welding pocess	63
6.1	Weight and atomic % AA7075/SiC	68
6.2	Tensile Strength and S/N ratio results of Friction Stir Welding	73
6.3	Response Table for Means	74
6.4	Response Table for S/N ratio	74
6.5	Pooled ANOVA for Means	78
6.6	Pooled ANOVA for S/N ratios	79
6.7	Response table for Tensile Strength	82
6.8	Comparison of optimal predicted value and confirmation experiment result	85
6.9	Percentage Elongation and S/N ratio results of Friction Stir Welding	86
6.10	Response Table for Means	87
6.11	Response Table for S/N ratio	87
6.12	Pooled ANOVA for means	91
6.13	Pooled ANOVA for S/N ratios	91
6.14	Response table for Percentage Elongation	95
6.15	Comparison of optimal predicted value and confirmation experiment result	97
6.16	Hardness and S/N ratio results of Friction Stir Welding	98
6.17	Response Table for Means	99
6.18	Response Table for S/N Ratio	99
6.19	Pooled ANOVA for Means (Hardness)	103
6.20	Pooled ANOVA for SN ratios (Hardness)	104
6.21	Response table for Hardness	107
6.22	Comparison of optimal predicted value and confirmation	110

	experiment result	
6.23	Joint Efficiency and S/N ratio results of Friction Stir Welding	111
6.24	Response Table for Means	112
6.25	Response Table for S/N ratio	112
6.26	Pooled ANOVA for Means	116
6.27	Pooled ANOVA for S/N ratios	116
6.28	Response table for Joint Efficiency	120
6.29	Comparison of optimal predicted value and confirmation experiment result	122
6.30	Multi responses(Tensile Strength and Hardness) results of Friction Stir Welding	123
6.31	Pre-processing (normalized) and deviation	125
6.32	Grey relational coefficient and Grey relational grade	126
6.33	Response Table for grey relation grade	127
6.34	Pooled ANOVA for grey relation grade	130
6.35	Comparison between initial and optimum welding parameters	135

LIST OF FIGURES

Figure No	Caption	Page No
1.1	Classification of composites on the basis of matrix	1
1.2	Classification of composite on the basis of reinforcement	2
1.3	Operation of friction stir welding	6
1.4	Automotive application of Friction Stir Weldin	8
1.5	Automotive application of Friction Stir Weldin	9
1.6	Automotive application of Friction Stir Weldin	9
2.1	Classification of Literature Review	12
2.2	Flow chart of entire research	27
3.1	Graphite Crucible	29
3.2	View of Stirrer and its blades	30
3.3	Muffle Furnace	31
3.4	Experimental Set-up of Stir Casting	33
3.5	Fabricated composite	33
3.6	Variation of tensile strength of composites with % of SiC reinforcement	34
3.7	Fabrication Procedure of composite	35
3.8	Fabrication of Square pin profile tool	36
3.9	Fabrication of Hexagonal pin profile tool	36
3.10	Fabrication of Octagonal pin profile tool	36
3.11	Friction stir welding Set-up	37
4.1	Cause and Effect Diagram of Mechanical Stir Casting	39
4.2	Photographic view of Grinding and Polishing Machine	40
4.3	Photographic View of SEM Analysis Set-Up	41
4.4	Photographic View of X-Ray Diffraction Machine	42
4.5	Photographic View of Differential Thermal Analysis Set-Up	43
4.6	Photographic View of Tensometer	44
4.7	Photographic view of Charpy Impact Testing machine	45
4.8	Photographic view of Vicker Hardness Testing System	46
4.9	Cause and Effect Diagram of Friction Stir Welding	47

4.10	Scatter plot of tensile strength vs. tool rotation speed	50
4.11	Scatter plot of tensile strength vs. welding speed	50
4.12	Scatter plot of tensile strength vs. axial force	51
4.13	Scatter plot of tensile strength vs. tool geometry	51
4.14	Scatter plot of tensile strength vs. tilt angle	52
4.15	Scatter plot of tensile strength vs. tool diameter	52
4.16	Scatter plot of hardness vs. tool rotation speed	53
4.17	Scatter plot of hardness vs. welding speed	53
4.18	Scatter plot of hardness vs. Axial force	54
4.19	Scatter plot of hardness vs. tool geometry	54
4.20	Scatter plot of hardness vs. tilt angle	55
4.21	Scatter plot of hardness vs. tool diameter	55
5.1	Procedure of grey relation analysis	64
6.1	Optical microstructure of AA7075/10wt% SiC composite at 100X magnification	66
6.2	Optical microstructure of AA7075/10wt% SiC composite at 400X magnification	67
6.3	SEM analysis of AA7075/10 %wt.SiC(20–40 μm)	68
6.4	EDAX profile of AA7075/10% wt SiC	68
6.5	X-ray diffraction curves of AA7075/10wt%SiC Composite	69
6.6	TG, DTG and DTA curv of AA7075/10% wt.SiC Composite	70
6.7	SEM fractography of AA7075/10%wt.SiC	71
6.8	Effects of Process Parameters on Tensile strength (Main effects)	75
6.9	Effects of Process Parameters on Tensile strength S/N (ratio)	76
6.10	Interaction plot for tensile strength (Means)	80
6.11	Interaction plot for tensile strength(S/N ratio)	80
6.12	Normal probability plot of the residuals for tensile strength(Means)	81
6.13	Normal probability plot of the residuals for tensile strength (S/N ratio)	81
6.14	Effect of process parameters on percentage elongation (Main effects)	88
6.15	Effect of process parameters on percentage elongation (S/N	88

	Ratio)	
6.16	Interaction plot for Percentage Elongation (means)	92
6.17	Interaction plot for Percentage Elongation (S/N ratio)	93
6.18	Normal probability plot residuals (Means)	93
6.19	Normal probability plot residuals(S/N ratio)	94
6.20	Effects of Process Parameters of Hardness (Means)	100
6.21	Effects of Process Parameters of Hardness (S/N ratio)	101
6.22	Interaction plot for hardness (Means)	105
6.23	Interaction plot for hardness (S/N Ratio)	105
6.24	Normal probability plot of the residuals for hardness (Means)	106
6.25	Normal probability plot of the residuals for hardness (S/N ratio)	106
6.26	Effects of Process Parameters on Joint Efficiency (Main effects)	113
6.27	Effects of Process Parameters on joint efficiency (S/N ratio)	113
6.28	Interaction plot for Joint Efficiency (Means)	117
6.29	Interaction plot for Joint Efficiency(S/N Ratio)	118
6.30	Normal probability plot of the residuals for Joint Efficiency (Means)	118
6.31	Normal probability plot of the residuals for Joint Efficiency (S/N Ratio)	119
6.32	Main effect plot for grey relation grade (Means)	128
6.33	Main effect plot for grey relation grade (S/N Ratio)	128
6.34	Interaction plot for Grey Relation Grade (Means)	131
6.35	Interaction plot for Grey Relation Grade (S/N Ratio)	132
6.36	Normal probability plot of the residuals for Grey relation grade	132
6.37	Percentage contributions of process parameters	133

LIST OF ABBREVIATIONS

Symbol	Description
FSW	Friction Stir Welding
MMC	Metal Matrix Composite
TRS	Tool Rotation Speed
WS	Welding Speed
TG	Tool Geometry
AF	Axial Force
TA	Tilt Angle
TS	Tensile Strength
PE	Percentage Elongation
HV	Hardness Value
JE	Joint Efficiency
CI	Confidante Interval
ANOVA	Analysis of Variance
OA	Orthogonal Array
SEM	Scanning Electron Microscope
EDS	Energy Dispersive X-ray Spectroscopy
XRD	X-ray Diffractometer
GRA	Grey Relational Analysis
GS	Grain Size
HAZ	Heat affected zone
HB	Higher is better
DOF	Degree of freedom
SS	Sum of Square
MS	Mean Square
F	Fisher Ratio
PC	Percentage Contribution

CHAPTER-1

INTRODUCTION

1.1 COMPOSITE MATERIALS

A composite material is a system of materials, which consists of two or more materials on a macroscopic level. Generally, it is a combination of metal matrix (metals and polymers etc.) and reinforcements (particulates, fibers and flanks etc.) The matrix holds the reinforcement to form require shape and size while the reinforcement improves the overall mechanical properties of composite materials [1-7].

1.1.1 Classification of Composites

These are classified in different ways by many researchers but in the simplest and effective way, it may be classified, which is based on accordingly to matrix and reinforcement type. A effective classification of composite materials on the basis of matrix and reinforcement are explained by figure 1.1and figure 1.2 respectively.

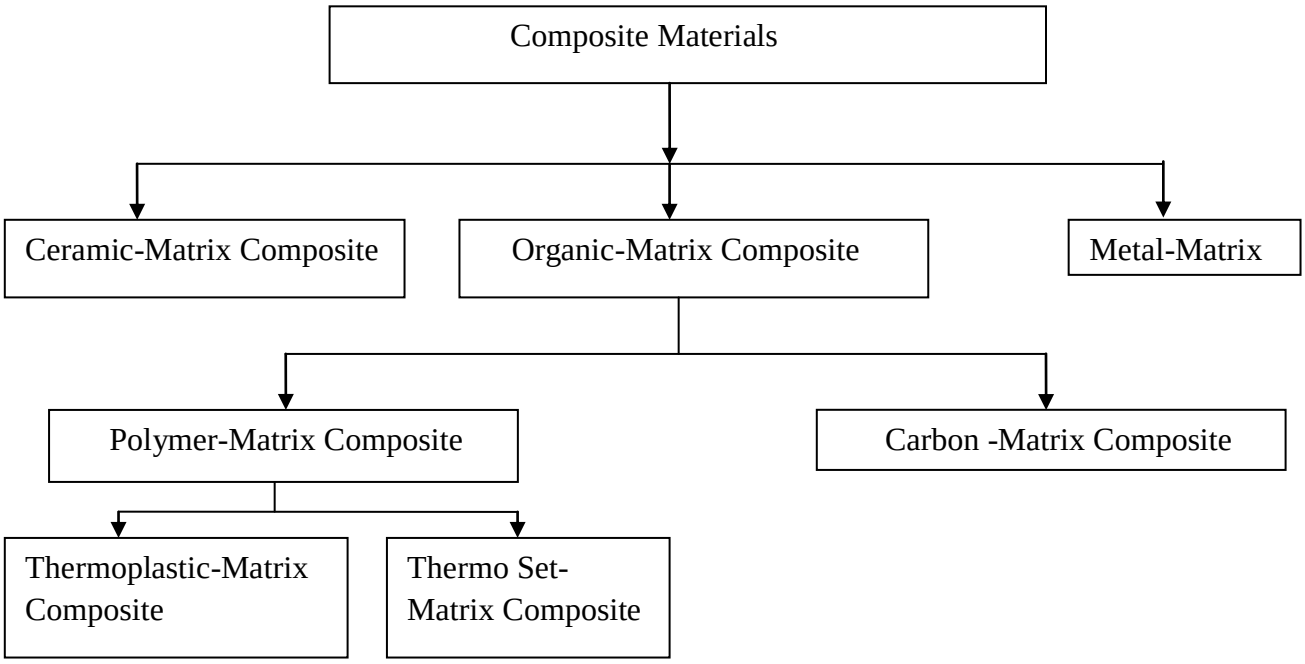

Figure 1.1 Classification of composites on the basis of matrix

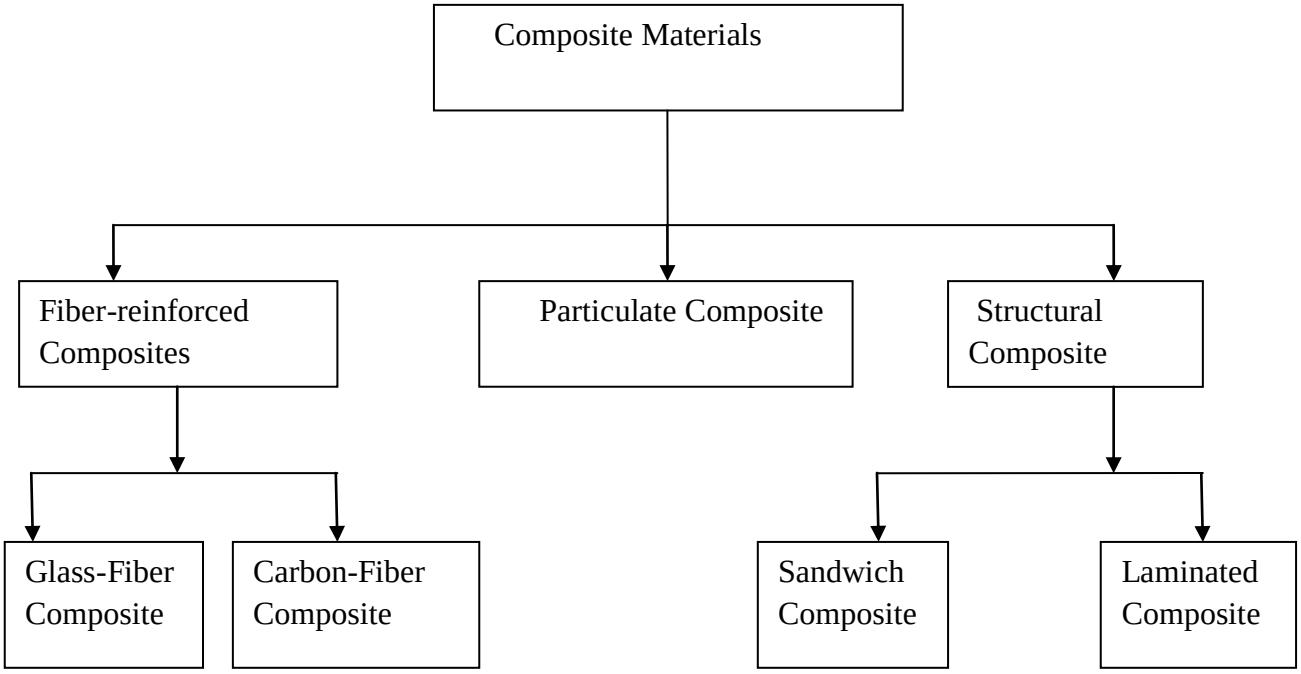

Figure 1.2 Classification of composite on the basis of reinforcement

1.1.2 Metal Matrix Composite

The utilization of metal matrix composite has been increased day by day in many areas due to their effective mechanical properties. Metal matrix composite produces higher strength, light in weight, high stiffness and anti corrosion property than matrix aluminum alloy. Due to these excellent properties, metal matrix composites has the potential to replace conventional materials in the field of automobile, aerospace and manufacturing industries produce a different type of new materials those poses superior mechanical properties. Basically, metal matrix composite consists of two or more components one is metal matrix part and other is reinforcement [8-12]. Commercially, matrix is available in form of like Al, Cu, Ag, Mg and Ti etc. and reinforcements like SiC, B_4C and Al_2O_3. For fabrication of metal matrix composites, some basic problems arise in proper mixing of the reinforcement like Al_2O_3 and SiC with liquid material due to poor wetability of reinforcement. So, proper selection of material matrix, reinforcement and fabrication technique play a very vital role in fabrication of composite [13-17].

1.1.3 Fabrication Technique of Metal Matrix Composite

There are different types of techniques used for fabrication of metal matrix composites. The fabrication technique can be classified into three major categories which are as follows.

- Liquid phase fabrication technique
- Solid phase fabrication technique
- Powder metallurgy

1.1.3.1 Liquid Phase Fabrication Technique

In liquid phase fabrication technique, reinforced particles are mixed into the metal matrix when it is in liquid state. Metal Matrix Composite can be fabricated by this technique at very low production cost and easier to handle than other fabrication technique [18-21]. It is further classified into three major categories which are as follows.

Liquid Metal Infiltration

Infiltration is a liquid state method for fabrication of metal matrix composite, where a preformed dispersed phase (ceramic particles, fibers) are mixed in a molten matrix metal, which fills the space between the dispersed phase inclusions [21-24]. This method is suitable for fabricated composite material due to its simplicity and possibility of introducing small particles into metal matrix.

Spray Process

In this process, atomized stream of molten metal droplets are sprayed together with the reinforcing phase at high velocity and collected on a substrate where metal solidification is completed and form a desired composite [25-27]. The important process parameters in spray processing are initial temperature, size distribution and velocity of the metal drops, temperature and feeding rate of the reinforced particulate.

Stir Casting Process

Reinforced particles (ceramic particles, short fibres) mechanically mix into the molten metal pool and transferring the mixture directly into the mould, composite

prepared after solidification. Reinforced particulates are distributed in the matrix material during the melt stage of casting process which depends on the stirring speed, heating temperature, stirring time, particle preheated temperature, effectiveness of mixing and minimizing of gas entraption [28-31].This process is very simple and most cost effective method of liquid state fabrication technique.

1.1.3.2 Solid Phase Fabrication Technique

In solid phase fabrication technique, the metal matrix is in the form of sheets and reinforced material is in the form of fibers by direct pressing both metal matrix and reinforcement for proper casting.

1.1.3.3 Powder Metallurgy

Powder metallurgy is a solid state fabrication method. It is based on the typical blending of matrix powders and reinforcement particulate. In this method, two or more metallic and or non-metallic powders are properly blended together in a machine and then compacted at high pressure by a die [32-35]. This compacted powder will still in green state further, this powder is taken out of the die and then sintered at high temperature. Sintering is used to facilitate the bonding between powder particles by high heating. In this process, heating temperature should be just below the melting temperature to develop proper solid state diffusion. The final product is then used as metal matrix composite material after some require secondary operations. It is capable for relatively mass fabrication of composites.

1.1.4 Advantages of Metal Matrix Composites [36-37]

- Higher strength to weight ratio
- Higher corrosion resistant
- Higher design Flexibility
- Higher stiffness to density
- Higher temperature capability
- No moisture absorption

- Higher fatigue resistance
- Higher abrasive resistance
- Higher electrical and thermal conductivities
- Higher radiation resistance
- Lower coefficient of thermal expansion

1.1.5 Disadvantages of Metal Matrix Composites

- Higher cost
- Complex Fabrication

1.1.6 Applications of Metal Matrix Composites

- Automobile industry such as disc brakes, drive shaft and panels etc
- Sports equipments
- Electrical cables
- Aeronautical and aerospace components.

1.2 WELDING OF METAL MATRIX COMPOSITES

There are different types of welding used which are as under.

1.2.1 Conventional Welding

Metal matrix composites are new engineering material having high hardness and toughness compare to other alloys as due hard and advanced ceramics are mix with matrix part. These materials are very difficult to weld by conventional welding process such MIG, TIG and plasma arc welding etc due to abrasive nature of Metal matrix composites.

1.2.2 Unconventional Welding

Unconventional Welding like Electronic Beam welding, Laser Beam welding and Explosive welding are the major classification of unconventional category. This process is applicable only those metals having enough impact resistance, and ductility. Operator

requires more protection compare to other conventional welding process. This process is applicable where the geometries of work piece must be simple and flat but cost is higher.

1.2.3 Friction Stir Welding (FSW) Process

Friction stir welding (FSW) is a solid state joining process. It was first invented by TWI (The welding Institute) (UK) in December 1991. It uses a non-consumable tool to weld two edges of work pieces without melting. By the action of friction, heat is generated between rotating tool and the work piece which produces a softened region near the rotating tool. Tool moves forward along the joint line, it mechanically intermixes the two pieces of work piece and axially force applied by the rotating tool shoulder continuously. It is environmental friendly process because there are no smoke and toxic fumes generated during and after the welding. This process is higher energy saver compared to other conventional fusion welding.

1.2.3.1 Basic Principle of Operation

In this process, a rotating cylindrical tool with desired tool pin geometry is fed into a butt joint between two highly clamped work pieces and a tool shoulder produces an axial force to work piece. The tool pin is slightly shorter (96-98% of work piece thickness)[38]. According to figure 1.3, Rotating tool probe inserted into the work-piece, after a short dwell time, the tool is moved forward along the joint line at the desire welding speed. The basic principle and operation are shown in the figure 1.3.

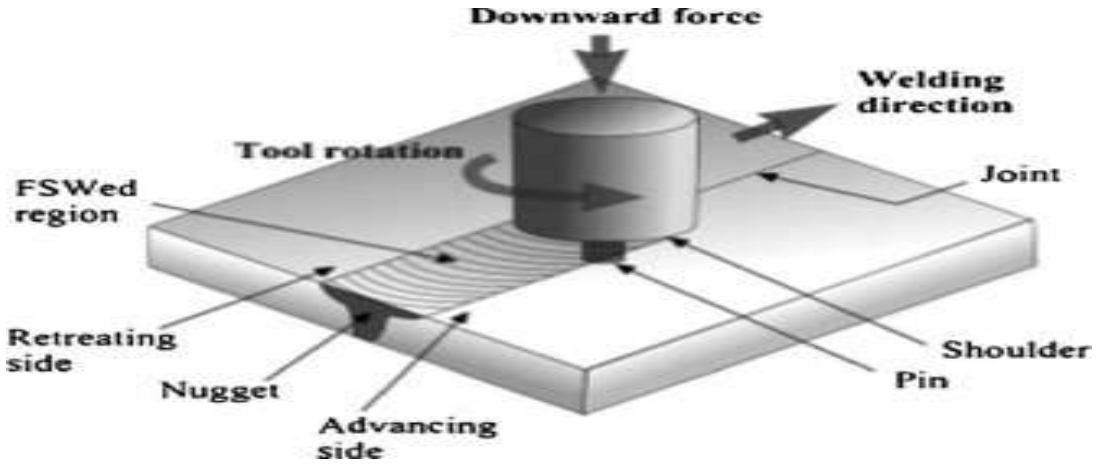

Figure 1.3 Operation of friction stir welding (http://en.wikipedia.org)

According to the figure 1.3, the tool advances in the forward direction and then reaches the retreating side hence, advancing side in friction stir welding process is the location from where the solid material starts to transform in to semi-solid form and flows around the tool pin plunged into the material. The semi-solid material retreated and cooled in the retreating side. Therefore advancing side having more solid state nature at any point of time/location compare to retreating side during friction stir welding process, thus advancing side generate higher friction stress (unbalanced frictional force) which ultimately generates more heat of plastic deformation compare to retreating side.

1.2.3.2 Advantages of Friction Stir Welding

There are so many advantages of Friction Stir Welding which are as follows [39].

- It is a solid state welding process so there are no problems with hot cracking and porosity, etc
- It has good mechanical properties in the as-welded condition.
- It has produced low distortion.
- Since, It uses a non-consumable tool to weld so there is no requirement of filler wire or no shielding gas require for aluminum alloys.
- This process is safe, due to the absence of toxic fumes or the spatter of molten material.
- It produces no UV rays, therefore it is environment friendly.
- It is easy to automatic and reduces to need for skilled welders.
- It can operate in all positions (horizontal and vertical), because there is no weld pool here.
- This process is highly energy efficient.

1.2.3.3 Disadvantages of Friction Stir Welding

However, some limitations of the process have been identified:

- At the last of operation exit hole always left when withdrawing tool from the process.
- It requires significant axial force and welding speed, therefore clamping arrangement must is necessary.
- It is less flexible than manual and arc welding.

1.2.3.4 Applications of Friction Stir Welding

There are wide applications of Friction Stir Welding process. Figure 1.4,Figure 1.5 and Figure 1.6 shows the practical automotive application, which are given below [40].

- This process is used in railway industries to build railway tankers and container bodies.
- It is used in shipping, marine and automotive industries, e.g. fabrication of car door (Toyota and Honda), wheel rims and suspension arms etc.
- It is used in aerospace industries for fabrication of floors, wing and fuselage.
- This process can also be utilized for electric motor housing, cooking equipments, kitchens, gas storage tanks and gas cylinders etc.
- This Process widely used in making furniture, doors, and light structures and land transport etc.

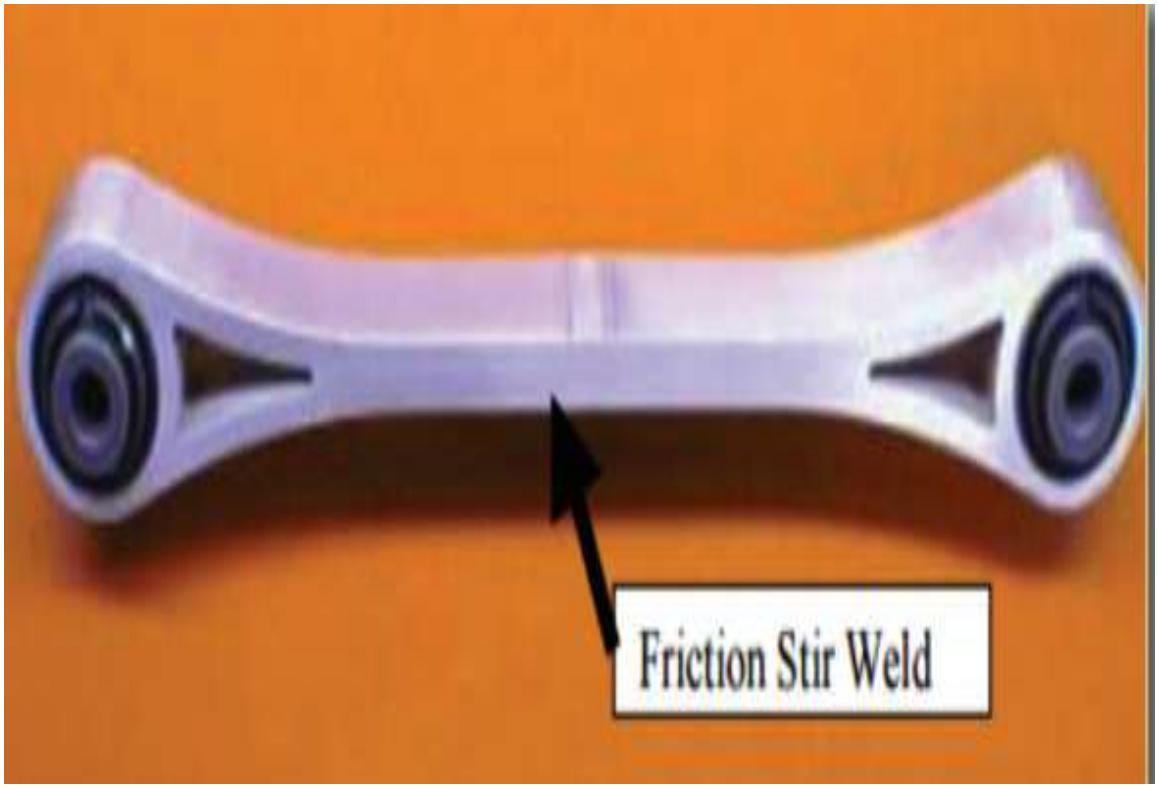

Figure 1.4 Friction stir welded vehicle aluminium link arm (http://en.wikipedia.org)

Figure 1.5 Tailor welded blank (Audi B pillar structure) (http://en.wikipedia.org)

Figure 1.6 Friction stir welding in series (http://en.wikipedia.org)

1.4 ORGANIZATION OF THE THESIS

The thesis has been organized in different chapters are as follows.

Chapter 1

Introduction to composite material and classification based on the basis of metal matrix and the nature of reinforcement. Various fabrication methods for composite, the strengthening mechanism and advantage of metal matrix composites (MMC) with applications. Welding of MMCs by conventional and unconventional methods. The problems being faced in conventional welding of AA7075/10wt.SiCp and need to develop a process for welding is also explained. Advantage of friction stir welding, its principal and applications are as discuss.

Chapter 2

This chapter deals with literature review related to stir casting process, friction stir welding, material characterizations, mechanical properties and optimizations of friction stir welding parameters, and multi characteristic optimization. Identification of gaps in the literature also explained.

Chapter 3

This chapter deals with the experimental set up of mechanical stir casting process and its components for fabrication of metal matrix composite having 10wt% of SiC reinforcement. In this chapter, experimental set up of friction stir welding and its components also discuss.

Chapter 4

In **t**his chapter discuss the selection of process parameters and responses of mechanical stir casting process and friction stir welding process. The different phases of work plan have been explained. Discussed about the selection of metal matrix alloy Al 7075 and reinforcement material SiC for the fabrication of composite. Explain the characterization of metal matrix composite like mechanical properties, optical microstructure, X-RD analysis, EDAX analysis and thermal analysis. Cause and effect diagrams also explain for mechanical stir casting and friction stir welding process.

Chapter 5

In this chapter, discuss the single and multi response optimization technique. The main experiment is carried out using L_{27} OA, Taguchi method Grey relation analysis used to optimize the process parameters.

Chapter 6

This chapter deals with results and discussion of whole experimental work such as composite characteristic are discussed regarding mechanical properties, microstructure, EDAX analysis XRD analysis, Thermo analysis and fractrography. Discuss the effect of friction stir welding process parameters on the Tensile strength, Percentage of tensile elongation, Hardness and weld Joint efficiency. The analysis of variance (ANOVA) is performed to know the contribution of effective process parameters on the response characteristics. Analysis for process parameter optimization is carried out using Taguchi method and grey relation analysis and the conformation experiments are carried out to validate the results.

Chapter 7

This chapter deals with summary and conclusion of whole research and Implications for both academicians and professionals are also spelt out.

CHAPTER-2

LITERATURE REVIEW

2.1 OVERVIEW

This chapter presents the study of metal matrix composite, friction stir welding technique, Taguchi single response optimization technique and grey relation analysis multi response optimization technique which is explained by figure 2.1. Whole literature was divided into different categories related to design, fabrication, and characterization of metal matrix composite.

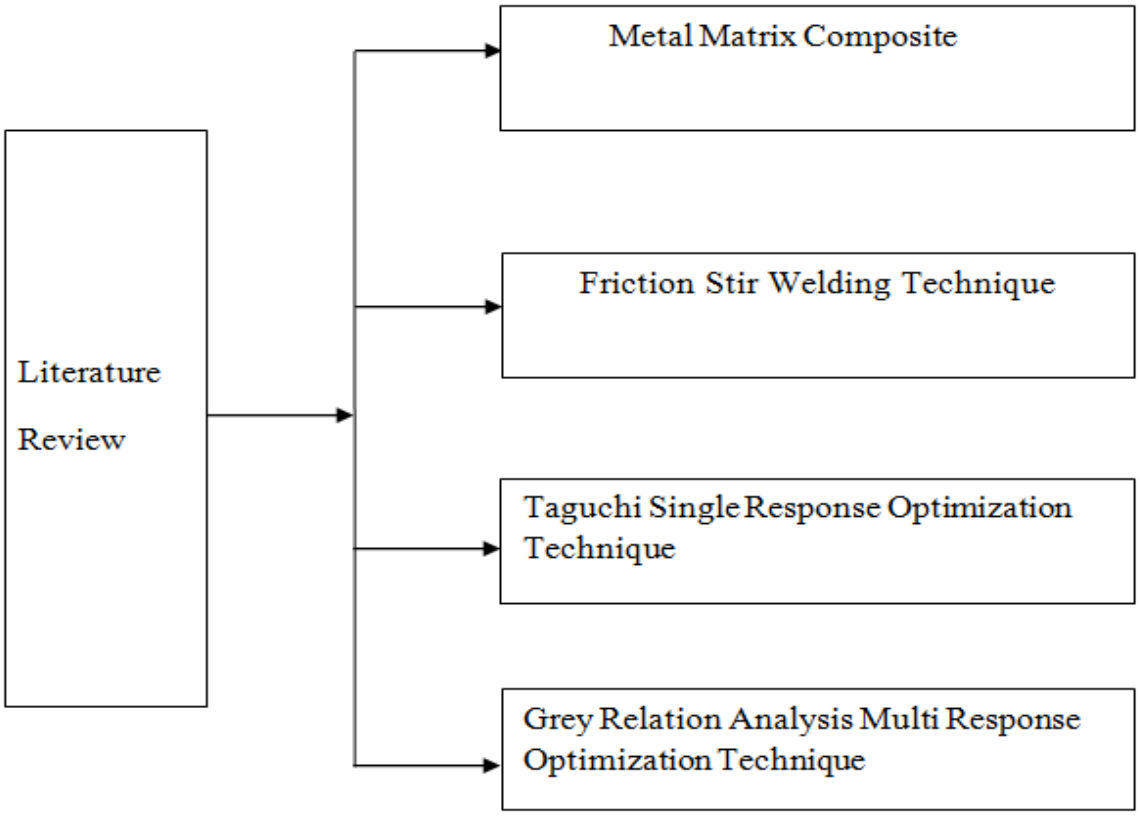

Figure 2.1 Classification of Literature Review

2.2 LITERATURE OF MECHANICAL STIR CASTING

Clyne et al. [1995] studied the metal matrix composite. It is the combination of metal and reinforcement. There are so many metals used for this purpose. Mg, Al and Ti are general matrix metals with characteristics like higher strength to weight ratio. For the selection of reinforcement, particle size play a vital role to make metal matrix composite. The typical reinforcing ceramics is SiC, Al_2O_3, and B_4C. These can be used as short whiskers, long fibers, or particles in either an irregular or spherical shape or size [40].

Ralph et al. [1997] studied various casting processes. Out of these processes stir casting technique was most economical for fabrication of metal matrix composite. This is quite easier compared to other fabrication technique of metal matrix composite. It is also used for large production rate and allow to fabricate large size component. Cost of fabrication of metal matrix composite is almost one third to half compared to other fabrication technique [41].

Hashim and Looney [1999] studied numerous composite materials by using different type of matrix, reinforcement size, shape and volume as well as suitable processing technique depending upon the requirement and applications. In order to achieve the optimum properties of the metal matrix composite, the distribution of the second phase in the matrix alloy must be uniform, and the wettability or bonding between these substances should be optimized [42].

Mitra et al. [2004] fabricated aluminium metal matrix composite which is oxidized or unoxidize with SiC reinforcement with varing magnesium concentration. The result revealed that magnesium segregated at the interface and prevents the formation of Al_4C_3 compound [43].

Pathak and Singh [2006] explained the effect of silicon carbide particles which was dispersed in the grain boundary regions and fragmented dendrites in the synthesized silicon carbide particles, aluminium-silicon alloy. Mechanical properties and wear resistance increased with the addition of SiC particles in the matrix [44].

Kalkani and Yimaz [2008] fabricated the AA7075 with different weight percentage (10%,15%,20%wt.) of reinforcement silicon carbide particulates using squeeze casting process.. In this study, 10% weight silicon carbide as reinforcement had higher mechanical strength as compared to other combination of AA7075/15%wt.SiC. and AA7075/20%wt.SiC[45].

Reddy and Zitoun [2010] explained the material selection criteria of high strength and good corrosion resistance aluminum alloys for the matrix materials. The mechanical properties have been determined for different metal matrix composites produced from Al 6061, Al 6063 and Al 7072 matrix alloys reinforced with silicon carbide particulates. The yield strength, ultimate strength, and ductility of Al/SiC metal matrix composites are in the descending order of Al 6061, Al6063 and Al 7072 matrix alloys. Mg has improved the wettability between Al and SiC particles by reducing the SiO2 layer on the surface of the SiC. The fracture mode is ductile in nature [46].

Kumar et al. [2013] fabricated AA7075/10%SiC composite with particulates size by mechanical stir casting technique. Experiments were carried out at stirring speed 500,650 and 750 rpm, for stirring period of 10mins.The result showed that composite produced at stirring speed of 650rpm and stirring time of 10mins has uniform distribution of SiC Particulates. Compare the mechanical properties (Tensile strength and hardness) of fabricated composite with base alloy and results revealed that Tensile strength and hardness increased by 12.74% and 10.48% respectively [47].

Bharath et al. [2014] studied MMCs are preferred to other conventional materials in the fields of aerospace, automotive and marine applications owing to their improved properties like high strength to weight ratio, good wear resistance etc. In the present work an attempt has been made to synthesize metal matrix composite using 6061Al as matrix material reinforced with ceramic Al_2O_3 particulates using liquid metallurgy route in particular stir casting technique. The addition level of reinforcement is being varied from 6 - 12wt% in steps of 3wt%. For each

composite, reinforcement particles were preheated to a temperature of 200^0C and then dispersed in steps of three into the vortex of molten Al6061 alloy to improve wettability and distribution. Microstructural characterization was carried out for the above prepared composites by taking specimens from central portion of the casting to ensure homogeneous distribution of particles. Hardness and tensile properties of the prepared composite were determined before and after addition of Al_2O_3 particulates to note the extent of improvement. Microstructural characterization of the composites has revealed fairly uniform distribution and some amount of grain refinement in the specimens. Further, the hardness and tensile properties are higher in case of composites when compared to unreinforced 6061Al matrix, also increasing addition level of reinforcement has resulted in further increase in both hardness and tensile strength [48].

Kumar [2017] studied various MMCs are found in many applications such as aerospace, space, electrical and automotive industries due to their good physical, mechanical and corrosion properties. But MMCs suffer from insufficient process stability, reliability and in-adequate economic efficiency. To overcome these problems, the hybrid metal matrix composites (HMMCs) were developed. The reinforcement materials in aluminum alloy improve the mechanical properties. In this work, the mechanical behavior of Aluminum Hybrid Metal Matrix Composites (HMMCs) has been investigated. Al7075 alloy was selected as matrix alloy and Silicon Carbide (SiC) and Titanium Carbide (TiC) were used as reinforcements for fabrication of HMMCs by liquid metallurgical technique (Stir Casting Technique). The mechanical properties such as yield strength, ultimate tensile strength, Brinell hardness and Impact strength were conducted for HMMCs specimen as per ASTM standard. The mechanical properties are increased for the combination of reinforcement TiC and SiC and impact strength was decreased [49].

Laxmi and Kumar [2017] explained the composite materials those having many advantages over other conventional materials due to their higher specific properties such as tensile, flexural and impact strengths, stiffness and fatigue properties, which enable the

structural design to be more versatile. Due to their many advantages they are widely used in aerospace industry, mechanical engineering applications (internal combustion engines, thermal control and machine components), electronic packaging, automobile, and aircraft structures and mechanical components. The problem is associated with the study of mechanical properties of aluminium- Silicon carbide metal matrix composites (MMCs) of aluminium alloy of grade 6061 with the addition of 10% 15% and 20%by weight composition of Silicon carbide (SiC) by stir casting technique. The changes in physical and mechanical properties will be taken into consideration. For the achievement on the above, an experimental setup will be prepared to facilitate the preparation of required MMCs. The experiment has to be carried out by preparing the sample of 10% ,15% and 20%composition of Silicon carbide by stir casing process and then study the mechanical properties i.e. hardness. A brief analysis of microstructure has to be conducted on scanning electron microscope (SEM) to verify the dispersion of reinforcement in the matrix [50].

Koppad et al. [2017] analyzed the current research scenario, in the field aluminium based hybrid composites, to explore the materials for automotive and aerospace applications this is achieved with the help of stir casting technique. Stir casting is one of the simple and effective method to produce metal matrix composites with more uniform distribution of matrix and reinforcement constituents. This approach involves mechanical mixing of the reinforcement particulates/particles into a molten metal bath. A crucible is heated to malt aluminum metal, with a motor and blades is placed in the crucible that helps to get uniform molten metal. The reinforcement is poured into the crucible above the melt surface and at a controlled rate, to ensure a smooth and continuous feed. As the blades rotate at moderate speeds, it generates a uniform mixing of the reinforcement particles into the melts to produce homogenous composites. In this paper authors discussed about construction and experimentation of stir casting setup for metal matrix composites [51].

Kunjir et al. [2018] discussed a large variety of heating techniques/furnaces are available for fabricating the MMC. There may be many method for supplying heat to the

work but heat is produced either by combustion of fuel or electric resistance heating. Taking into consideration the effect of cost, safety, simplicity and ease of construction we are going for an electrical resistance heating furnace with indirect heating provisions. The stir casting furnace has two main parts that enable to perform all its operations, they are: Furnace Elements and Control Panel. In Metal matrix composites, the Aluminium Matrix Composites are gaining increasing attention for applications in aerospace, defence and automobile industries. This paper shows the design and fabrication of stir-casting furnace and aluminium melted and casted to form [52].

Sahu et al. [2018] explained that aluminum matrix composites (AMCs) and hybrid aluminum matrix composites (HAMCs) becomes choice for automobile and aerospace industries due to its tunable mechanical properties such as very high strength to weight ratio, superior wear resistance, greater stiffness, better fatigue resistance, controlled co-efficient of thermal expansion and good stability at elevated temperature. Stir casting is an appropriate method for composite fabrication and widely used industrial fabrication of AMCs and HAMCs due to flexibility, cost-effectiveness and best suitable for mass production. Distribution of the reinforcement particles in the final prepared composite regulates the anticipated properties of AMCs and HAMCs. However, distribution of reinforcements is governed by stirring process parameters. The study of effect of stirring parameters in the particle distribution and optimal selection of these is still a challenge for the ever-growing industries and research [53]**.**

Prasad et al. [2018] discussed the demand of aluminum hybrid metal matrix composites has increased in recent times due to their enhanced mechanical properties for satisfying the requirements of advanced engineering applications. The performance of these materials is greatly influenced by the selection of an appropriate combination of reinforcement materials. The reinforcement materials include carbides, nitrides, and oxides. The ceramic particles, such as silicon carbide and aluminum oxide, are the most widely used reinforcement materials for preparing these composites. In this paper, an attempt has been made to prepare an Al6061 hybrid metal matrix composite (HAMMC) reinforced with particulates with different weight fractions of SiC and Al_2O_3 and a

constant weight fraction (5%) of fly ash by a stir-casting process. The experimental study has been carried out on the prepared composite to investigate the mechanical properties due to the addition of multiple reinforcement materials. The density and mechanical properties, such as ultimate tensile strength, yield strength, impact strength, and the hardness and wear characteristics of the proposed composite, are compared with those of unreinforced Al6061. The experimental investigation is also aimed at observing the variation of properties with a varying weight percentage of the reinforcement materials SiC and Al_2O_3 simultaneously with the fly ash content maintained constant. The outcome of the experimental investigation revealed that the proposed hybrid composite with 20% of total reinforcement material exhibits high hardness, high yield strength, and low wear rate but no considerable improvement in impact strength [54].

Ganesan et al. [2018] investigated examination has been centered on the use of welding slag of electrode E6013 in a valuable way by scattering it into aluminium alloy Al6061 to produce a composite by stir casting technique. The mechanical property studied is the hardness of the produced composites. The experimental results showed significant changes in each composition. The hardness tend to increase when compared to the unreinforced Al6061 [55].

Dhas et al. [2018] produce an aluminum metal matrix composite with high strength, low weight with good thermal resistance. For preparing metal matrix composite AA6061 is used as matrix and activated carbon is used as reinforcement and it is cast using modified stir casting technique. The reinforcement activated carbon is added in various weight ratios from 2% to 8% of the matrix. The casted metal matrix composites are taken as per ASTM standard by using wire cut process for various tests. Microstructural test like SEM, EDAX, XRD and thermal tests like Fourier Transform infrared spectroscopy and Thermo gravimetric tests were taken .From testing results, it is noted that increase in the percentage of activated carbon up to 6%, shows a significant mixing of matrix and reinforcement it is evident in microstructure test result and also shows there is the formation of voids. Thermo gravimetric proves the fabricated

composite have good thermal resistance by adding activated carbon as reinforcement [56].

2.3 LITERATURE OF FRICTION STIR WELDING

Marzoli et al. [2006] investigated the effect of process parameters on AA6061/20% Al_2O_3 metal matrix composite. Microstructure has been analyzed by optical microscope and image analyzed with the help of image analysis software. Mechanical tests (micro hardness and tensile strength) have been also performed. Result revealed that Al_2O_3 particles distribution may be affect by tool rotating speed. Weld joint efficiency was evaluated and tensile failure always held outside the stir zone and produced defect free high strength weld joints [57].

Uzun [2007] fabricated the AA2124/25%SiC composite through friction stir welding process and characterized by the EDAX and microstructure analysis of AA2124/25_P SiC composite confirmed the presence of fine as well as coarse silicon particulates reinforced with aluminium alloy matrix. A zone which is adjacent of the weld nugget, called thermo mechanically affected zone has been plastically deformed. Heat affected zone formed between the thermo mechanically affected zone and unaffected base composite region. So, a similar micro structure on both advancing and retreating side of the base composite achieved [58].

Sarsılmaz [2009] studied the effect of friction stir welding process parameters such as tool rotational speed, welding speed, and tool pin geometry on tensile strength (TS) and micro hardness of welded joints. ANOVA (Analysis of variance) and main effect plots were used to determine the significant process parameters and set the optimal level for each parameter. A linear regression equation was also formed to predict each output characteristic [59].

Rajakumar et al. [2010] investigated the effect of friction stir welding's process parameters on the tensile strength of AA7075 alloy. The researcher was formed an empirical relationship between the friction stir welding process parameters and tensile

strength of the joint using statistical tools such as design of experiments, analysis of variance, and regression analysis [60].

Jayaraman et al. [2011] established an empirical relationship for base metal properties and optimized friction stir welding's process parameters on aluminium metal matrix composites. Friction stir welding tool pin geometry like straight cylindrical, cylindrical taper, threaded cylindrical, square, and triangular with combinations of 15, 18, and 21mm shoulders diameter were selected. Square pins provided superior tensile properties with least number of defects [61].

Kalaiselvan et al. [2014] fabricated AA6061/B_4C composite by mechanical stir casting Technique. Thickness of composite plates was 6 mm. The friction stir welding was carried out with tool rotational speed of 1000 rpm, welding speed of 1.3 mm/sec. and axial force of 10 kN. A tool used with square pin geometry and made of high carbon high chromium steel. Optical and scanning electron microscopy were used for characterize microstructure of welded joints. The weld zone showed fine grains and homogeneous distribution of B_4C particles and weld joint efficiency of 93.4% was achieved under the experimental conditions [62].

Babu et al.[2014] fabricated AA5083 and AA6061 joints using friction stir welding process by controlling the various welding parameters viz. rotational speed, welding speed and Tool axial force for two different tool profiles. Aluminum alloys 5083 and 6061 have similar properties and they both are widely used in marine industries and other transportation industries. In this work the effect of various parameters on the mechanical properties viz. tensile strength and impact strength were studied. In this study the Taguchi approach was used as a design of experiment to set optimum parameters. The experiments were done using Taguchi's L9 orthogonal array. Analysis of variance test was also performed to obtain the effect of the parameters on the weld strength. Both DOE and ANOVA were performed using MINITAB software. [63].

Asif et al. [2016] studied the optimal combination of process parameter for friction stir welding of UNS31803 duplex stainless steel using Taguchi and GRA approach. The main objective was to maximize mechanical properties like tensile strength, hardness and impact toughness and to minimize corrosion rate. Four process parameters namely heating pressure, heating time, upsetting pressure and upsetting time were considered for study. Experiments were conducted as per the L_9 Orthogonal Array results of ANOVA showed that heating pressure and upsetting time were the most significant factors affecting the quality characteristics. GRA was better than Taguchi method because it improved the multi response ratio by higher value [64].

Rana et al. [2016] derived a process from the friction stir welding (FSW) process, is an emerging novel, green and energy efficient processing technique to fabricate surface composite. In the present investigation, FSP technique has been used for fabrication of surface composites, using aluminium 7075 as parent metal and Boron Carbide (B_4C) powder particles as reinforcement. Aluminium 7075 has been selected as matrix phase, as being widely used by automotive and aerospace application and having the highest strength among all commercial Al alloys. In present paper, details about the fabrication of AA7075-B_4C surface composite for various combination of tool rotation, tool travel speed and number of passes have been discussed. The same being intended to improve hardness and thereby wear resistance. The fabricated surface composites are examined for microstructure using image analyser, and found friction stir processed zone with a few defects. It is also observed that the average hardness of friction stir processed surface composite was 40-70% higher than that of parent metal (75-80 HV). Wear Resistance is found to be improved by 100% compared to parent metal. The increase in same is attributed to B_4C particles dispersed in aluminium matrix and grain strengthening mechanism [65].

Jacob[2017] studied that metal matrix composite used for various applications in aerospace, renewable energy and automotive industries due to their superior strength, low cost, easy availability and high temperature resistance. The crack and propagation occurs in conventional materials without any appreciable indication in a short span. Hence

composite materials are preferred nowadays to overcome this problem. The process of metal matrix composites (MMC's) is to unite the enviable attributes of metals and ceramics. The Stir casting method is used for producing aluminium metal matrix composites (AMC's). A key challenge of the process is to spread the ceramic particles to achieve a defect free microstructure. By carefully selecting stir casting processing specification, such as stirring time, temperature of the melt and blade angle, the desired microstructure can be obtained. The focus of this work is to develop a high strength particulate strengthen aluminium metal matrix composites, and Al7075 was selected which can offer high strength without much disturbing ductility of metal matrix . The composites will be examined using standard metallurgical and mechanical tests. The cast composites are analysed to Laser flash analysis (LFA) to determine Thermal conductivity. Also changes in microstructure are determined by using SEM analysis [66].

Verma et al. [2017] analyzed that heat played a very vital role in friction stir welding (FSW) and hence, the study of heat flux characteristic during the process is essential for producing good quality weld. Moreover, life and capability of the tool depend on the heat dissipation throughout the process. The aim of present study is to experimentally explore the distribution of temperature during the friction stirred butt joint of aluminum 6082 plates. Eight L shaped thermocouples are placed at equally distance from the center line to measure the resulting temperature; four thermocouples on advance side (AS) and four on retreating side (RS). The experiment is conducted at constant rotational speed and feed rate and with varying tool tilt angle and dwell time. It is observed that the temperature on advancing side is on higher side as compared to retreating side [67].

Bozkurt et al. [2017] studied the effect of tool's material on friction stir butt welding of AA2124-T4 alloy matrix MMC. Uncoated tool, coated tool with a CrN, and coated tool with AlTiN were used to weld aluminum MMC plates. Macro structure and microstructure observations, ultimate tensile strength, wear resistance, and chemical analysis were carried out to determine the appropriate tool for joining these composite plates. Results showed that the good welded joints could be obtained when a tool is coated with AlTiN [68].

Singh et al. [2017] studied the experimental comparison of friction stir welding process and TIG welding process for 6082-T6 aluminium alloy joints. Most commonly used method for welding of aluminium alloy is TIG welding process. TIG welding process produces the sound joints but the newly developed method friction stir welding process gives better joints than TIG welding process. The effect of two welding processes on mechanical and metallurgical properties is studied in this research work. Mechanical properties of the welded joints were evaluated and it was found that friction stir welded joints have superior mechanical properties as compared to TIG welded joints. From the micro structure analysis it was observed that fine and equiaxed grains were observed in the friction stir welded joints and coarse grains were observed in TIG welded joints. SEM analysis also carried out to know the fracture behavior of the tensile tested joints [69].

Kohak et al. [2017] identified the applications of friction stir welding process in the field of aerospace, shipbuilding, automobile industries and in many applications of commercial importance. This is because of many of its advantages over the conventional welding techniques which include very low distortion, no fumes, no porosity or spatter, no consumables (no filler wire), no special surface treatment and no shielding gas requirements. FSW joints have improved mechanical properties and are free from porosity or blowholes compared to conventionally welded materials. In this work tapered cylindrical tool with three sided re-entrant probe made of Tungstun Carbide (Wc) is used for the friction stir welding (FSW) of aluminium alloy HE30 – HE30 and test the mechanical properties of the welded joint by tensile test. Finally, we were compare mentioned mechanical properties and make conclusion. The result will help welding parameter optimization in friction stir welding process. Like rotational speed, depth of welding, travel speed, Tool Axial force, type of material, type of joint, work piece dimension, joint dimension, tool material and tool geometry. The detailed mathematical model is simulated by Minitab15. Experiments were conducted by varying rotational speed, transverse speed, and constant Axial force using L9 orthogonal array of Taguchi method. We analyzed the effect of these three parameters on tensile strength. In this investigation, an effective approach based on Taguchi method, has been developed to

determine the optimum conditions leading to higher tensile strength. The present work aims at optimizing process parameters to achieve high tensile strength [70].

Magalhaes et al. [2018] identified a perspective on the current development of the friction stir welding (FSW) technology. The industrialization of the technology and related research were assessed by analyzing patent and scientific publications databases. The literature reviews on FSW and related technologies were also collected and analyzed. The work performed enabled to understand the main areas of industry/research where the FSW technology is being applied/explored and the geographical distribution of the main players in its implementation/research. The main FSW process variants, the materials already welded/processed using it, as well as the applications envisaged, were also analyzed. The data collected shows that the FSW technology, originally developed for the joining of light alloys, became a research tool with interest in several fields of engineering and material science [71].

Jain et al. [2018] analyzed the effect of FSW process parameters on weld quality of AA6082 and AA5083 alloys using Taguchi method and GRA approach. Four welding parameters were investigated, namely tool rotation speed (TRS), welding speed (WS), tool geometry(TG) and tool shoulder diameter (TSD). Analysis of variance (ANOVA) was used to investigate the effects of these welding process parameters on responses like elongation (EL) and Tensile strength (TS). Single response optimization was carried out using Taguchi Technique while grey relation analysis (GRA) was used for simultaneous optimization of two responses. In the multi-response optimization tool rotation speed was found to have the maximum effect followed by other process parameters [72].

Mohammed et al. [2018] investigated the effect of process parameters like thickness of the plate, axial load, rotational speed on hardness, percentage of elongation and impact strength. Genetic programming (GP) is a relatively new method of evolutionary computing with the principal advantage of this approach being to evaluate efficacious predictive mathematical models or equations without any prior assumption regarding the possible form of the functional relationship. This paper both defines and

illustrates how GP can be applied to the FSW process to derive precise relationships between the output and input parameters in order to obtain a generalized prediction model. A GP model will assist engineers in quantifying the performance of FSW, and the results from this study can then be utilized to estimate future requirements based on the historical data to provide a robust solution. The obtained results from the GP models showed good agreement with experimental and target data at an average prediction error of 0.72% [73].

Mahananda et al. [2018] studied Cast and wrought aluminum (Al) alloys, steels, along with titanium (W), copper (Cu) and magnesium (Mg) alloys, different metal cluster alloys and metal matrix amalgams are widely used in aerospace, automotive, marine, defense, construction etc. due to their high strength, low weight, high machinability, good conductivity of heat and electricity etc. Friction stir welding is preferred for joining these materials as it is a solid state forge welding process and problems related with welding of such can be subdued through this process. This welding process is a solid state welding procedure that uses a non-consumable rotating tool that is permitted to rub against the work piece hence generating frictional heat. When the weld constraints such as tool or work piece rotation speed, welding time, axial load are optimum the friction between the work piece and the tool generates enough heat to create a plastic deformation layer at the weld interface. The process doesn't involve any melting process and whole process occurs in solid state through plastic deformation and mass flow among the work pieces. This review paper explains the mechanism of the Friction stir welding as well as studies investigated over friction stir welding by researchers [74].

2.4 IDENTIFICATION OF GAPS IN THE LITERATURE

By the scrutiny of the published work on the fabrication, characterization and Welding of Metal Matrix Composite, the following gaps have been found:

1. Although, stir casting process has been used for fabrication of AA7075/10%wt.SiC composite, a very little work has been done to fabricate 7075 Al alloy SiC composite with varying wt.% of SiC, which also has minimum porosity.

2. Impact strength of AA7075/10%wt.SiC composite fabrication by stir casting has not been investigated.
3. Literature lacks some specific research that would focus on the impact of the friction stir welding process parameters specifically on the weld joint efficiency.
4. Optimization of process parameters during welding of AA7075/10%wt.SiC composites has not been studied.

2.5 OBJECTIVES OF RESEARCH

The present research has been undertaken with a main objective to overcome the problems during fabrication, characterization and welding of AA7075/10%SiC composites. The research work has been focused on the following aspects:

1. The development of detail experimental set-up of Stir Casting process.
2. Fabrication of AA7075 alloy with 10%wt.SiC particulate composite with minimum porosity by using Mechanical Stir Casting process
3. Characterization of newly developed AA7075/10%wt.SiC composites by mechanical properties (like tensile strength, Impact and hardness), Microstructures examination by optical microscope and scanning electron microscope, EDAX, XRD and Thermal analysis.
4. The development of detailed experimental setup of Friction Stir Welding Process and to optimize the welding process parameter for newly developed Al 7075/10%wt.SiC metal matrix composite for response characteristics like Tensile strength, Percentage of elongation, Hardness, weld joint efficiency.
5. To fractography of fractured welded surface of composite using SEM analysis.
6. Optimization of outcome responses by using Grey relation Analysis
7. Validate the experimental results.

2.6 FLOW CHART OF ENTIRE RESEARCH

Figure 2.2 Represents the Flowchart which shows, how the entire research has been carried out. It indicates the various methodology processes employed to carry out the research.

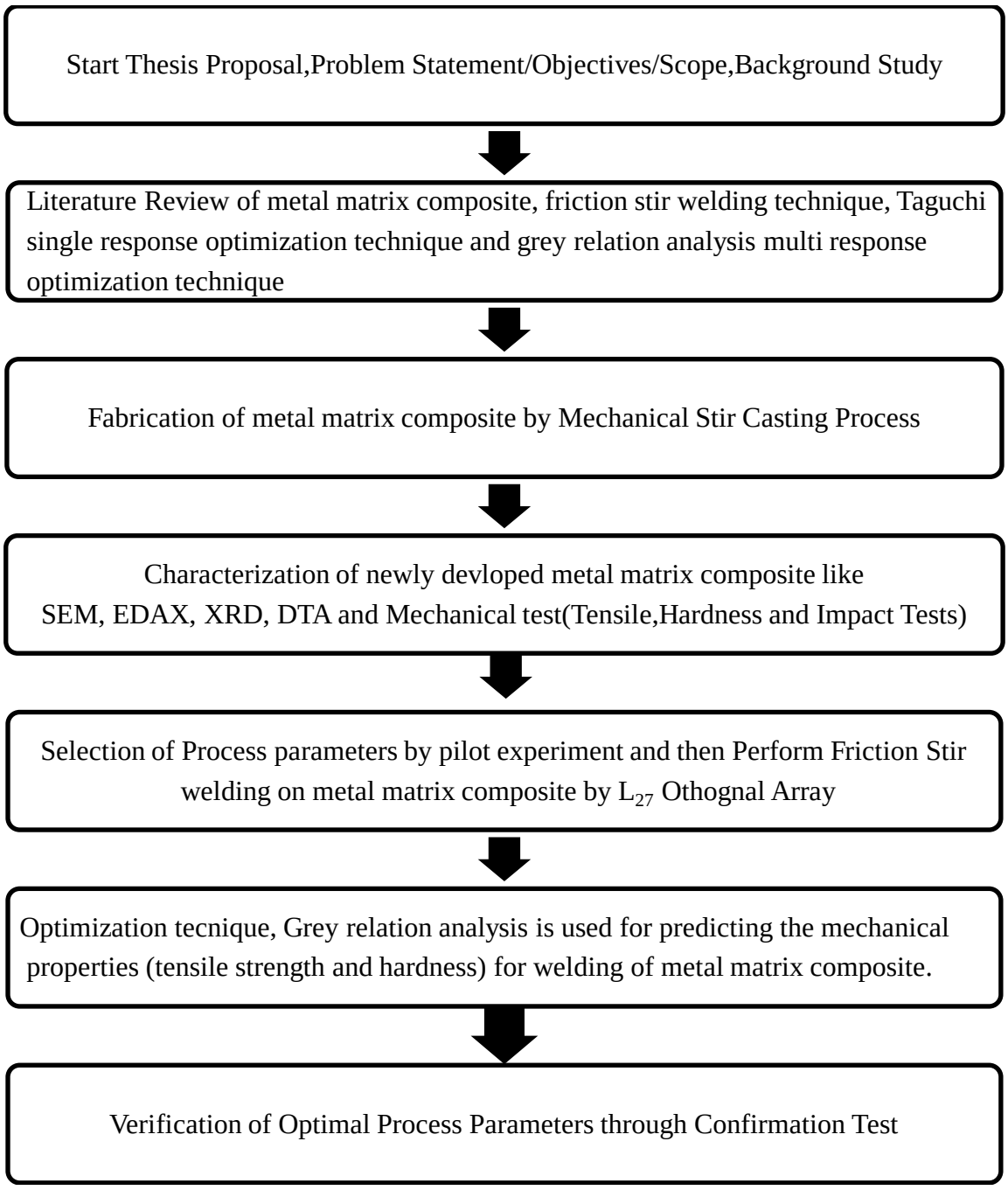

Figure 2.2 Flow Chart of Research work

CHAPTER-3

EXPERIMENTAL SET-UP

3.1 SELECTION OF MATERIAL

Matrix material (AA7075) and reinforcement (SiC) was selected. Details of these materials are follows.

3.1.1 Selection of Matrix Material

Aluminum alloy 7075 was selected as base material. It is the most widely used aluminum alloy and has gathered wide acceptance in the fabrication of light mass structures which require high strength to weight ratio, high wear resistance, high corrosion resistance and creep resistance. The chemical composition of the AA7075 is shown in Table 3.1.

Table 3.1 Chemical Composition of AA7075

Element	**Mg**	**Mn**	**Zn**	**Fe**	**Cu**	**Si**	**Cu**	**Al**
Wt%	2.1	0.12	5.1	0.35	1.2	0.58	1.2	Bal

3.1.2 Selection of Reinforcement

Al_2O_3, B_4C, SiC, TiB, and TiC reinforcements are commonly used in commercial applications. Out of these reinforcements, SiC have more good mechanical properties (elastic modulus, 350 – 450 GPa; hardness, 2,350 – 2,850 HV; compressive strength, 3,850 MPa), including high temperature strength, chemical corrosion resistance and thermal shock resistance. [61-63] It maintains its high mechanical strength in temperatures as high as 1,400°C. Hence, SiC has been selected as reinforcement with the size of 20-40 μm.

3.2 COMPONENTS OF MECHANICAL STIR CASTING SET-UP

For design of experimental set-up of mechanical Stir Casting, certain major components are used. Details of these components are as follows.

3.2.1 Graphite Crucible

A crucible is made of refractory material in which the metal is melted shown in figure 3.1. It can withstand very high temperatures (about 2750°C) and it is used for metal, glass, and pigment production as well as a number of modern laboratory processes. The diameter of the graphite crucible was 115 mm.

Figure 3.1 Graphite Crucible

3.2.2 Stirrer and Blades

Stirrer is used to mix the AA7075 and SiC reinforcement (20-40 μm) which is shown in figure 3.2. It is made of high speed steel with diameter 12 mm. Stirrer's blades design play a very vital role to find out the better particle distribution and strength of composite. During experimental work, a four-flat bladed angled 45^{o} was selected. Its length, height and thickness was 25mm, 10 mm and was 7 mm respectively. The stirrer was connected to a 1HP D.C motor. A manual lifting mechanism for the rotational drive

unit and stirrer assembly was used to remove the stirrer from the crucible to facilitate the stirrer positioning, cleaning and replacement. Height of the stirrer from the bottom of the crucible was adjusted.

Figure 3.2 View of Stirrer and its blades

3.2.3 Muffle Furnace and Temperature Controller

Muffle furnace is used to melt the AA7075 with size 6x6x12inch shown in figure 3.3. It was very fast heating furnace and consume very low power. The temperature controller was attached with furnace, played a vital role to control the temperature through the thermocouple that was placed inside the furnace. The temperature controller also regulated the current flow inside the furnace to maintain the required temperature and hence, avoids over-heating. When the temperature inside the furnace rose above the set temperature the temperature controller activated the electromagnet inside the contactor to cut the circuit and when temperature falls below the set temperature, the electro magnet was demagnetized to again complete the circuit to start heating. Hence, temperature of the furnace was maintained. It has a working range of 1000°C and connected with a 230V AC supply.

Figure 3.3 Muffle Furnace

3.2.4 D.C Motor

D.C motor was used to rotate the stirrer along with blade at different rpm. The specifications of motor are as follows.

Horsepower	1
Armature Voltage	90V
Field Voltage	90V
Rotation	1000rpm
Weight	38 lbs

3.2.5 Nitrogen Gas

Nitrogen is a colorless, odorless and tasteless gas that makes up 78.09% (by volume) of the air. It is nonflammable and it does not support combustion. It is widely used as shielded cover or protector from reactive materials and other outer impurities. It also does not react with molten metal, due to certain advantage; this gas was used in mechanical stir casting process to maintain the quality of casting.

3.3 EXPERIMENTAL SET-UP OF MECHANICAL STIR CASTING

Mechanical stir casting process was designed to fabricate Metal Matrix Composite. The experimental setup of mechanical stir casting is shown in figure 3.4. One kg of aluminium alloy 7075 was charged in graphite crucible. Furnace temperature was raised to 700^{o}C and allowed to get liquid state. After the melting of AA7075, the stirrer was placed in crucible 10 mm height from the base. The stirrer rotated at 650 rpm at this stage preheated SiC particulates are added into the vortex. A plunge of nitrogen gas (0.5kg/cm^{2}) was continuous supplied in the furnace during the process. Continuous stirring was carried out at 650 rpm for 10mins. After 10 mins heating was stopped and stirrer taken out from the crucible, molten material goes in to the mushy zone and after solidification ingots was taken out from crucible The above procedure was adopted for preparing composites with 5%,10% and 15weight% of SiC particulates. Fabricated composites are presented in figure 3.5

Figure 3.4 Experimental Set-up of Stir Casting

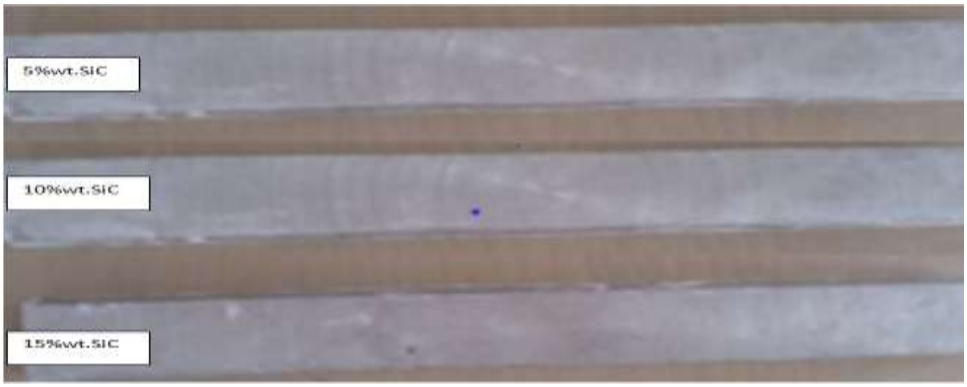

Figure 3.5 Fabricated composite with 5%,10% and 15% SiC Particulates

Out of above fabricated composites (5%,10% and 15% wt.SiC Particulates),10%wt. SiC Particulates composites were selected for further experiments. This is Cleary represented in figure 3.6. It indicates that the tensile strength is increases with increase in the percentage of SiC reinforcement from 5 to 10%wt. Further, tensile strength decreased when the percentage of reinforcement reached upto 15% due to sharp edge of reinforcement particulates, which acts as nucleation site. At nucleation point, more stresses would be developed which leads to fracture occur.

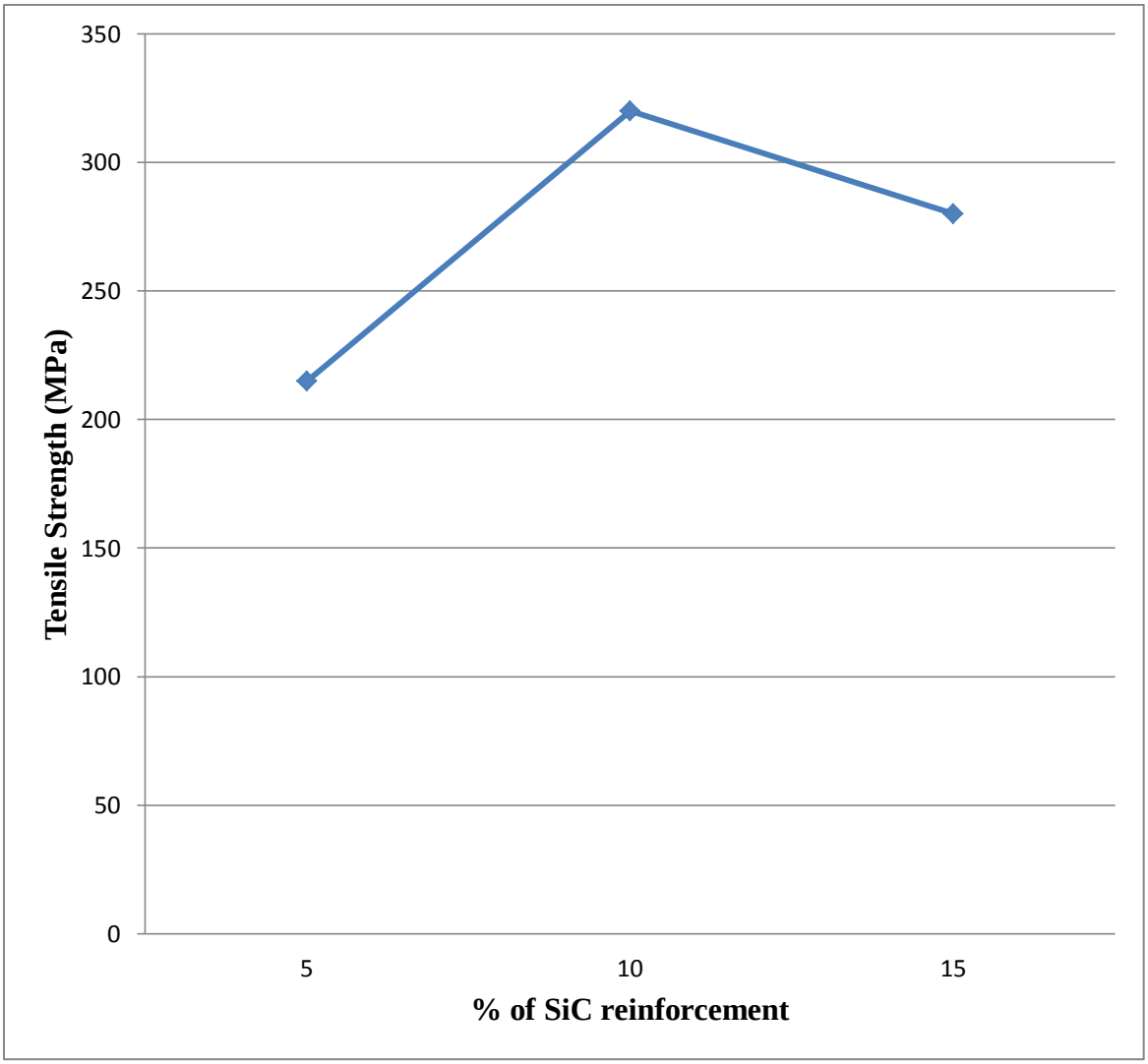

Figure 3.6 Variation of tensile strength of composites with %of SiC reinforcement

3.4 FABRICATION PROCEDURE OF METAL MATRIX COMPOSITE

Fabrication Procedure of metal matrix composite can easily explained by flow chart,which is shown by figure 3.7.

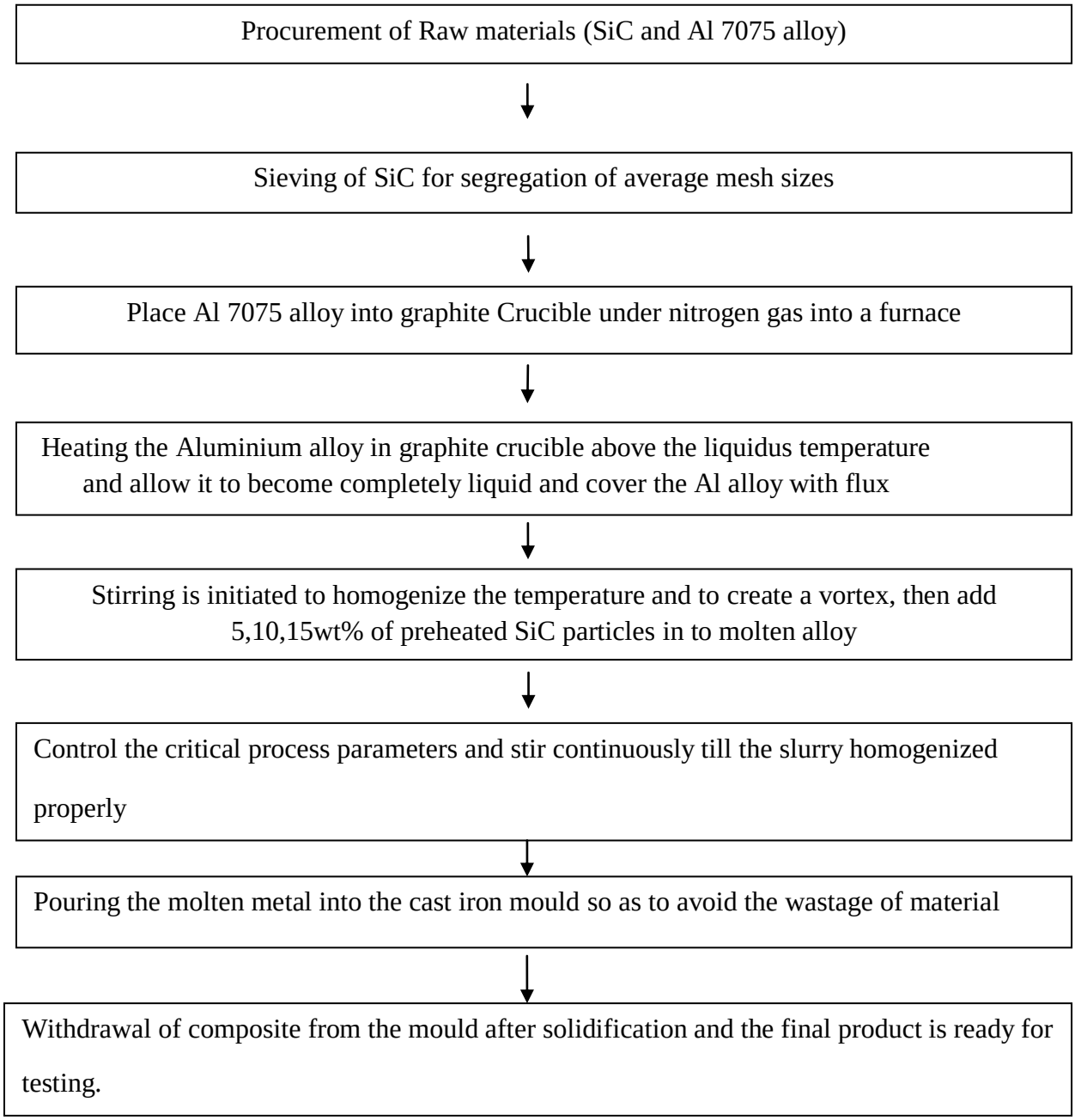

Figure 3.7 Fabrication Procedure of composite

3.5 FABRICATION OF FRICTION STIR WELDING TOOLS

Non consumable high speed steel tools with tool pin geometries like Square, Hexagonal and Octagonal were fabricated for friction stir welding process. The schematic diagram for the fabricated tools is shown in figure 3.8, figure 3.9 and figure 3.10 respectively. Tool classified into two major components, shoulder and pin. The total length of pin and pin diagonal length are 5.8 mm and 6 mm respectively. The total length of shoulder and diameter of shoulder are 60 mm and 18 mm respectively.

Figure 3.8 Square pin profile Figure 3.9 Hexagonal pin profile Figure 3.10 Octagonal pin profile

3.6 EXPERIMENTAL SET-UP AND PROCEDURE OF FRICTION STIR WELDING

Vertical milling machine was used for friction stir welding process which is shown in figure 3.11. In this process 5 H.P electric motor used for rotating the spindle. Tool rotation speed may vary according to the rotation of motor. A rotating tool with a desired pin profiled was plunged into a butt joint between two clamped work pieces until the shoulder touches the surface with sufficient thrust force. The tool's pin is slightly shorter (97% of work piece thickness) than the work piece thickness to achieve excellent weld quality. After a short dwell time, the machine table was moved at a predetermined welding speed. When the plunged tool reaches the last end of the work-piece the tool was retracted. This process was repeated for various combinations of welding process parameters, those were predefined.

Figure 3.11 Friction stir welding Set-up

CHAPTER-4

SELECTION OF PROCESS PARAMETERS AND RESPONSES

4.1 SELECTION OF PROCESS PARAMETERS OF MECHANICAL STIR CASTING PROCESS

For achieve uniform distribution of the reinforcement particulates into matrix and minimize porosity in the fabricated metal matrix composite, process parameters play a very important role. Details of these process parameters are as follows.

4.1.1 Stirrer Design

It is the primary parameter in stir casting process, that is essential for vortex formation. The blade angle and number of blades decide the flow pattern of the liquid metal. For composite fabrication, stirrer having four-flat blade angled at 45^{o}. Stirrer is immersed till two third depth of molten metal. [64-66]. All these are required for uniform distribution of reinforcement in liquid metal, perfect interface bonding and to avoid clustering.

4.1.2 Stirring Speed

Stirring speed is one of the most important process parameter as wettability is promoted by stirring i.e. bonding between matrix and reinforcement. The flow pattern of the molten metal is directly controlled by the stirring speed. The stirring speed is selected as 650 rpm. As solidifying rate is faster, it will increase the percentage of wettability [67].

4.1.3 Stirring Temperature

The viscosity of AA 7075 alloy is influenced by the processing temperature. Aluminium alloy 7075 melts around 640°C, at this temperature semisolid stage of melt is present. Particle distribution depends upon the change in viscosity. The viscosity of liquid is decreased by increasing processing temperature with increasing holding time for stirring which also promote binding between matrix and reinforcement. There is also

acceleration in the chemical reaction between matrix and reinforcement. The stirring temperature is selected as 700^{o}C [67].

4.1.4 Stirring Time

As stirring produce uniform distribution of reinforcement particles and interface bond between matrix (AA7075) and reinforcement (SiC), stirring time plays a crucial role in stir casting method. Less stirring takes more time, leads to non-uniform distribution of particles and excess stirring take less time, forms clustering of particles at some places. So, stirring time is selected as 10 minutes [67].

4.1.5 Reinforcement Pre-Heat Temperature

In order to remove moisture or any other gases present within reinforcement, it was preheated at a specified 750^{o}C temperature for 40 minutes. The wettability of reinforcement with matrix is promoted by preheating.

4.2 CAUSE AND EFFECT DIAGRAM OF MECHANICAL STIR CASTING

Various process parameters are shown in cause and effect diagram, which are presented in figure 4.1. Out of these process parameters, we have selected stirring speed, stirring temperature, stirring time, pressure of nitrogen gas and stirrer position.

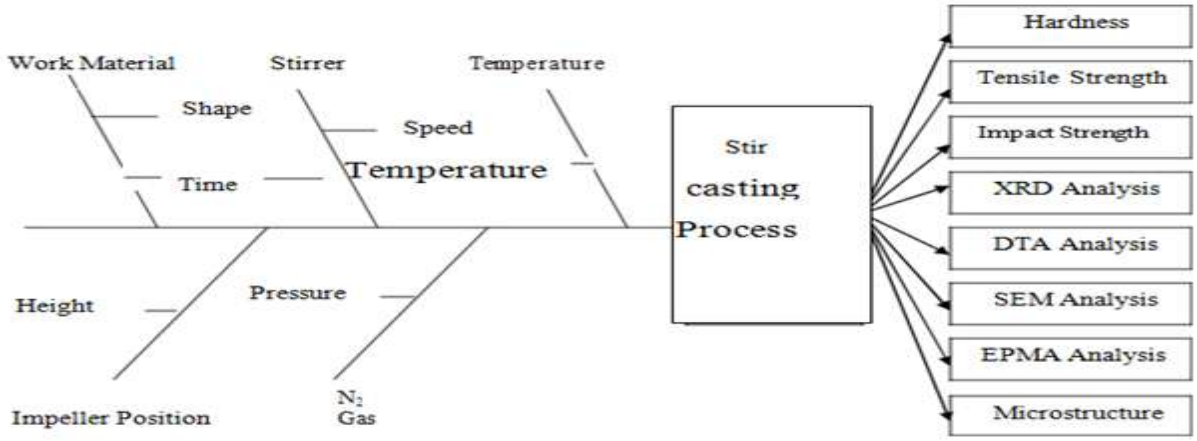

Figure 4.1 Cause and Effect Diagram of Mechanical Stir Casting

4.3 RESPONSES OF FABRICATED COMPOSITE

Detail characterization and description of newly developed metal matrix composite are as follows.

4.3.1 Characterization of Metal Matrix Composite

4.3.1.1 Microstructure

The specimens for microscopic examination were prepared by adopting standard metallographic procedure. The grinding and polishing machine were used for specimen preparation which is shown by figure 4.2. Well cleaned samples were etched with keller reagent to reveal the microstructure. Keller reagent was a solution mixture of 1% hydrofluoric acid, 1.5% hydrochloric acid, 2.5% nitric acid and balanced of distilled water. [69-73] The specimens are now observed for microstructure using radical metallurgical microscope fitted with digital camera.

Figure 4.2 Photographic view of Grinding and Polishing Machine

4.3.1.2 SEM and EDAX analysis

In this analysis scanning electron microscope (SEM) was used for determining the morphological aspects of sample (shape, size of particles) of AA7075/10%wt.SiC composite sample, and energy dispersive X-ray analysis (EDAX) used to got information regarding the chemical composition of AA7075/10%wt.SiC composite sample[71]. The instrument is the same for both analyses therefore the information can be complementary. The photographic view of SEM analysis set up is shown in figure 4.3.

Figure 4.3 Photographic View of SEM Analysis Set-Up

4.3.1.3 X-ray Diffraction Analysis

X-ray diffractometer is commonly used to identify phases in materials by comparing their diffraction patterns with those from known reference. The intensity of the X-rd peak is obtained for a given phase depends on its proportion and size in the material. Bruker AXS D-8 advance diffracometer with Cuk α radiation and nickel filter at 20MPa and 35 KV at 25^0C room temperature. Photographic view of machine is shown in figure 4.4. The samples were scanned with a scanning speed of 1.5 kcps in 2 θ range of 10-100^0C at 2^0/min goniometer rotation and the intensities were recorded at a chart speed of 20 mm/min.

Figure 4.4 Photographic View of X-Ray Diffraction Machine

4.3.1.4 Thermal Analysis

Thermal analysis was performed in the temperature range of 22-1000^{0}C at heating rate of 25^{0}C/min on Perkin Elmer apparatus at IIT Roorkee, India. The photographic view of differential thermal analysis set-up is shown in figure 4.5. The AA7075/%wt.SiC composite samples were subjected to thermo Gravimetric Analysis, Derivative Thermo Gravimetric and Differential Thermal Analysis to find information regarding their thermal degradation characteristics. Heating rate 25^{0}C/min under air supply 200ml/min was employed as degradation rate and temperature difference. The temperature difference occurs due to endothermic and/or exothermic enthalpy transitions or reactions such as dehydration, dissociation or decomposition, oxidation or other chemical reactions. The reference material was alumina powder.

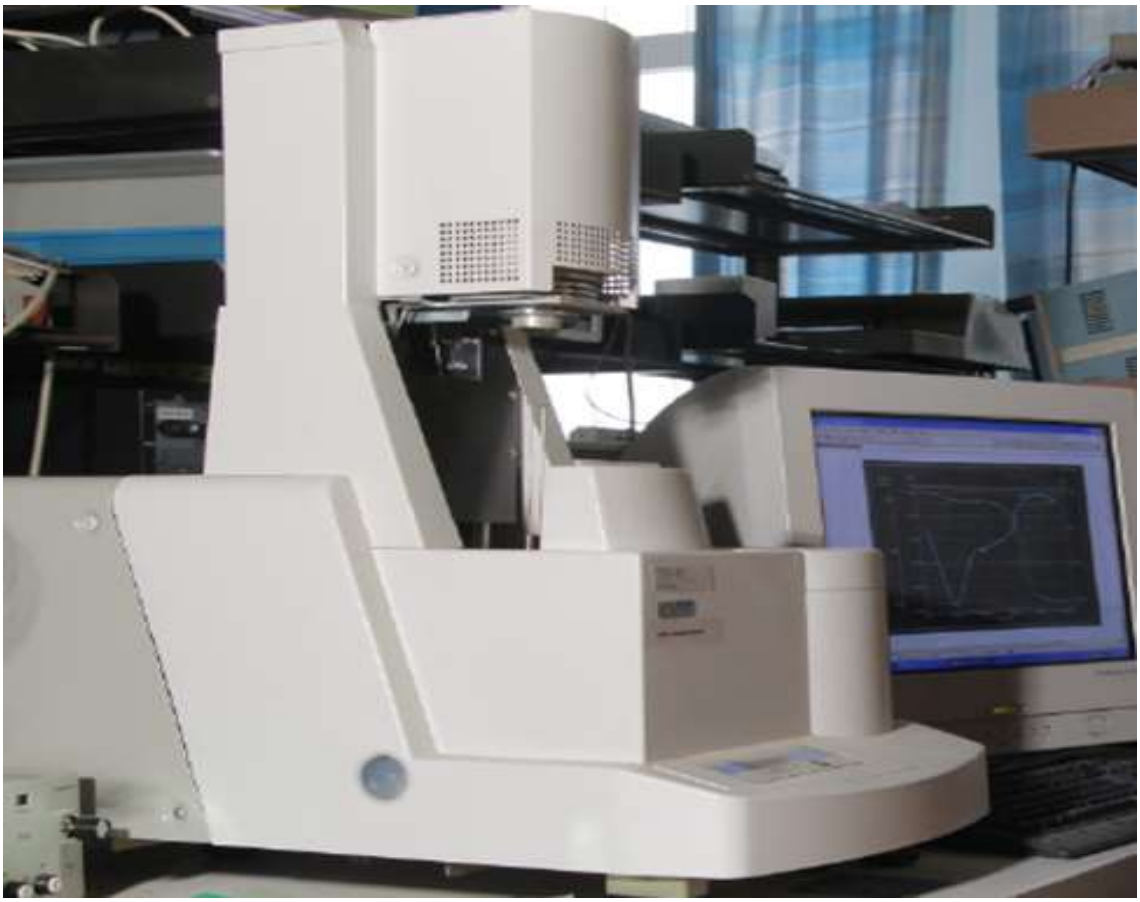

Figure 4.5 Photographic View of Differential Thermal Analysis Set-Up

4.3.1.5 SEM Fractography

SEM fractography is the high magnification examination of a fracture surface investigation. Close examination of the topography and fracture features can help to determine the fracture mode as well as determine the fracture origin and crack direction. The Scanning Electron Microscope is very important in the proper evaluation and classification of a fracture surface. SEM fractography is an excellent method of analyzing failures.The fractographs are taken using LEO 435 VP Scanning Electron Microscope (SEM) operating at 15kv. The SEM fractography of all the fractured tensile specimens of AA7075/10%wt.SiC of fabricated composite were carried out.

4.3.1.6 Mechanical Behavior

The mechanical behavior of composites consist of tensile testing, impact testing and micro hardness which are described below.

4.3.1.6.1 Tensile Testing

Three specimens from sample of newly fabricated composite were prepared according to ASTM E08 standard. Test are performed on tensometer model KIPL-PC 2000 at JMI, New Delhi, India, which is shown in figure 4.6 The tensile testing was carried with a strain rate referred in terms of speed, being 0.8mm/min.

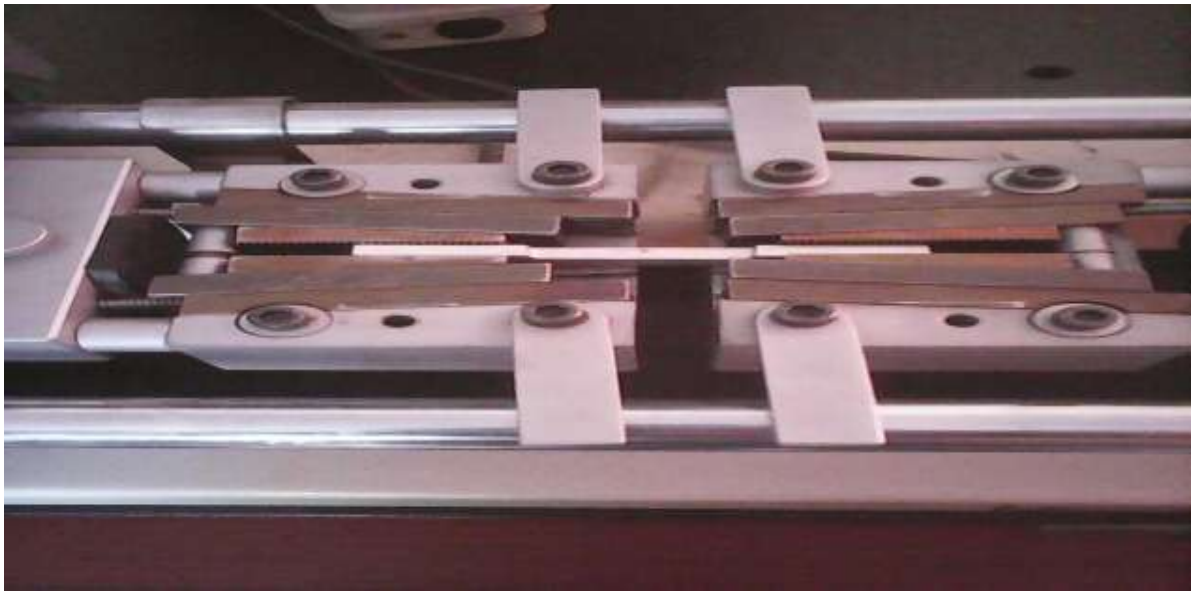

Figure 4.6 Photographic View of Tensometer

4.3.1.6.2 Charpy Impact Test

For impact test, the specimens were prepared as per ASTM standard E23. Three specimen samples were prepared for each test. The photographic view of the impact testing machine is shown by the figure 4.7.

Figure 4.7 Photographic view of Charpy Impact Testing machine

4.3.1.6.3 Micro Hardness

The micro hardness of the composite was measured on a Vickers microhardness tester. The specimens are prepared mechanically according to ASTM standard. Hardness testing of composite is done on VLPAK 2000 Hardness testing system (make mitutoyo, Japan) which is shown in figure 4.8.

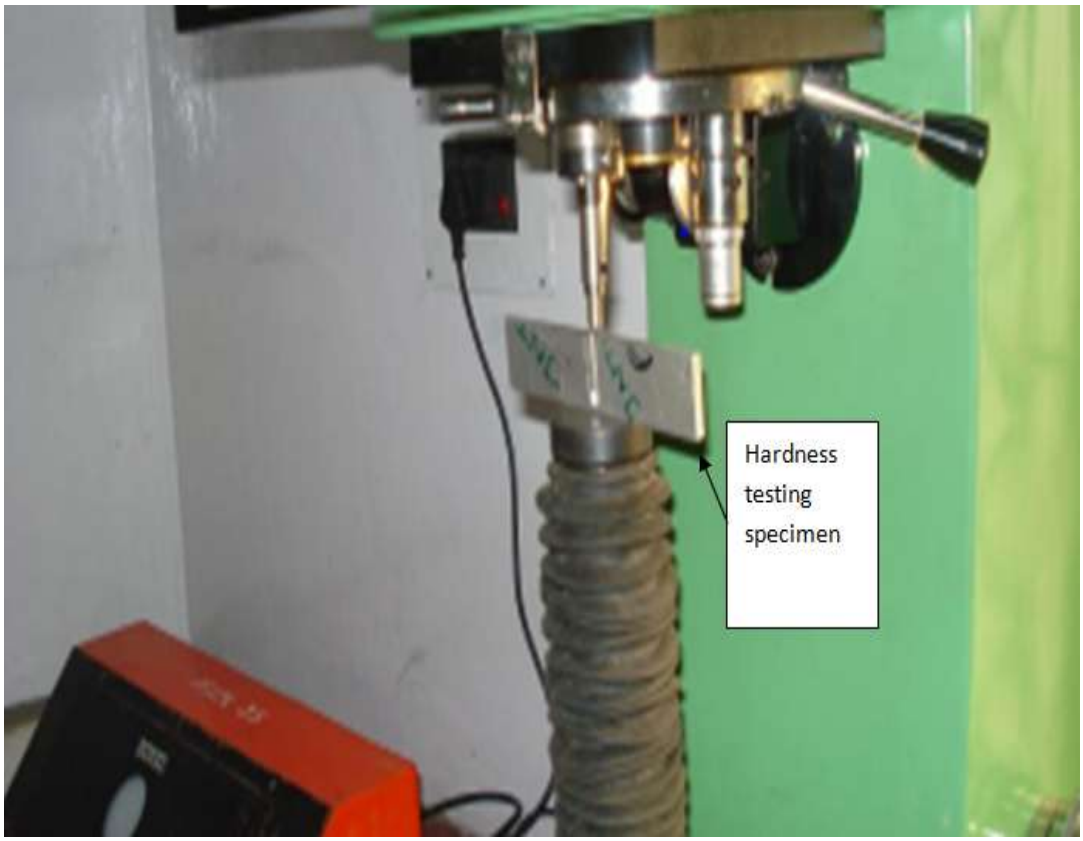

Figure 4.8 Photographic view of Vicker Hardness Testing System

4.4 CAUSE AND EFFECT DIAGRAM OF FRICTION STIR WELDING

To identify the effect of FSW process parameters on the quality of friction stir welding joint are presented by cause and effect diagram which is shown in figure 4.9.

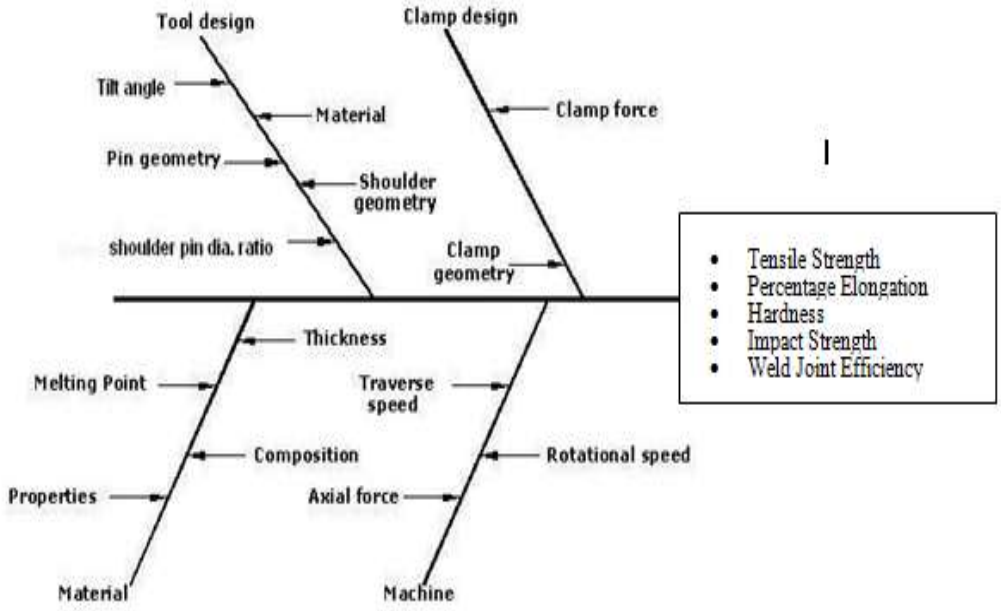

Figure 4.9 Cause and Effect Diagram of Friction Stir Welding

4.5 SELECTION OF PROCESS PARAMETERS AND THEIR RANGES OF FRICTION STIR WELDING PROCESS

Pilot experiments are performed to identify the ranges of process parameters for friction stir welding process. In this process, one process parameter varies from lower value to higher value and rest parameters remain constant at mid value and find the tensile strength and hardness [73-76]. Six process parameters were selected from cause and effect diagram for the pilot experiments which are given below. Results are plotted in figure 4.10 to figure 4.21.

4.5.1 Tool Rotation Speed

Tool rotation speed is varied from 1100 to 1900 rpm. The values of the other parameters are kept constant and their values are given as welding speed is 1.3 mm/sec, axial force is 7kn, tool geometry hexagonal, tilt angle is 2^0 and tool pin diameter is 8mm. Tool rotation speed versus response characteristics graphically represented by the figure 4.10 and figure 4.16. Figures show that tensile strength hardness increases with increase the tool rotation speed upto 1700rpm. After that it decreases.

4.5.2 Welding Speed

Welding speed is varied from 0.3 to 1.13 mm/sec. The values of the other parameters are kept constant and their values are given as rotational speed is 1500 rpm, axial force is 7kn and tool geometry hexagonal, tilt angle is 2^0, tool pin diameter is 8mm. Welding speed may vary according to the machine capability and control parameters of machine. It can be observed that a higher welding speed decreases the frictional heat input to the work material, which creates poor plastic flow of the metal and causes some defects in the welded joint. According to the figure 4.11 and figure 4.17 the response of FSW joints was low at the lowest value (0.3 mm/s) of welding speed and highest value (1.8 mm/s). The response was increased with increase in welding speed till 1.8 mm/sec.

4.5.3 Axial Force

Axial Force is varied from 3 to 11kn. The values of the other parameters are kept constant and their values are given as tool rotational speed is 1500rpm, welding speed is 1.3 mm/sec, tool geometry hexagonal, tilt angle is 2^0 and tool pin diameter is 8mm.The tensile strength was increased with increase in axial load up to a 9 kn. Further, increase in axial load decreased the responses of the joint which is explained by figure 4.12 and figure 4.18. During the FSW process, the rotation of tool produces a large amount of heat input which brings the metal to become very hot and plastic state. The axial force is more responsible for the plunge depth of the tool pin into the work piece.

4.5.4 Tool Geometry

It is observed that tool geometry (tool pin profile) varies. The values of the other parameters are kept constant and their values are given as tool rotational speed is 1500rpm, welding speed is 1.3 mm/sec, axial force 7kn, tilt angle is 2^0, and tool pin diameter is 8mm. Tool geometry is also responsible to produces material stir quality during welding. Since, the tool has different types of edges, the point of each edge acts as an individual cutting tool that causes deformation in the material. Effect of tool geometry on response is explained by the figure 4.13 and figure 4.19. In both the figure clearly represent that tool pin profile square, hexagonal and octagonal represent maximum variation in response that's why we select square, hexagonal and octagonal pin profile in our experiments.

4.5.5 Tilt Angle

Tilt angle is varied from 0 to 4^0. The values of the other parameters are kept constant and their values are given as tool rotational speed is 1500rpm, welding speed is 1.3 mm/sec, axial force 7kn, tool geometry is hexagonal, and tool pin diameter is 8mm. The tensile strength was slightly increased with increase in tilt angle up to 4^o, which is explained by figure 4.14 and figure 4.20. During the FSW process, the effect of tilt angle is very lesser than other process parameters. In both the figure clearly represent that tilt angle shows the linear result that's why we eliminate the tilt select square, hexagonal and octagonal pin profile in our experiments.

4.5.6 Tool Diameter

Tool diameter is varied from 4 to 12mm. The values of the other parameters are kept constant and their values are given as tool rotational speed is 1500 rpm, welding speed is 1.3 mm/sec, axial force 7 kn, tool geometry is hexagonal, and tool pin 2^0. The tensile strength was slightly increased with increase in Tool diameter up to 12mm, which is explained by figure 4.15 and figure 4.21. During the FSW process, the effect of tool diameter is very lesser than other process parameters.

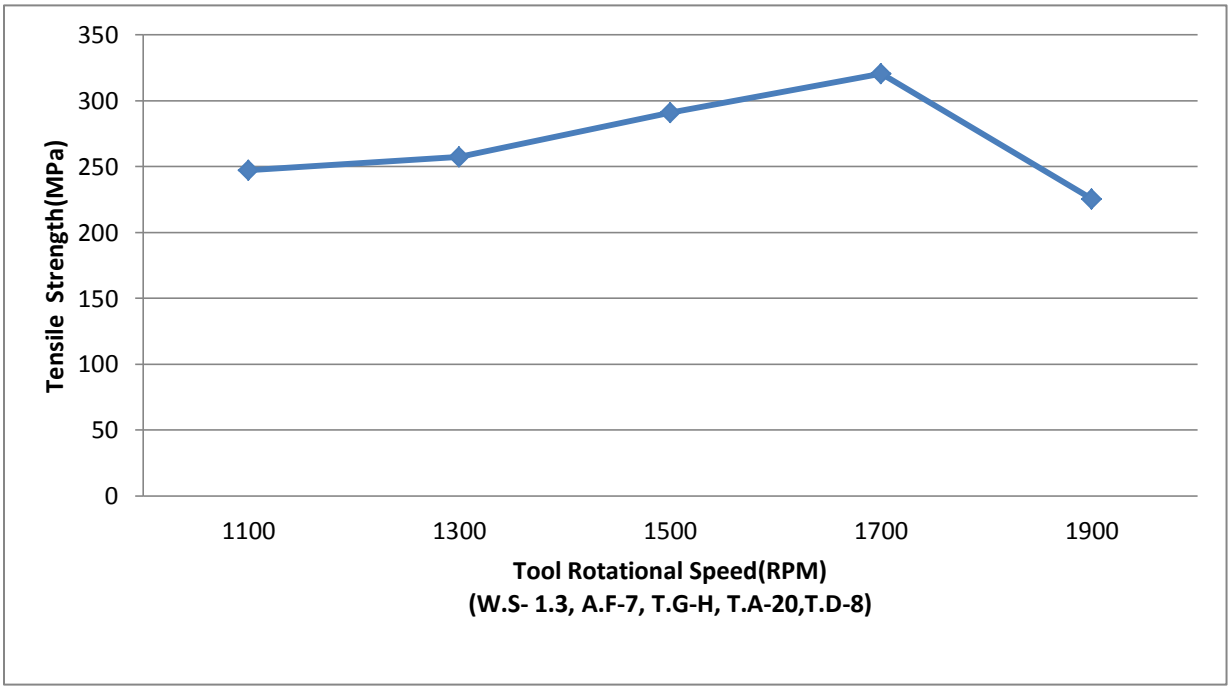

Figure 4.10 Scatter plot of tensile strength vs. tool rotation speed

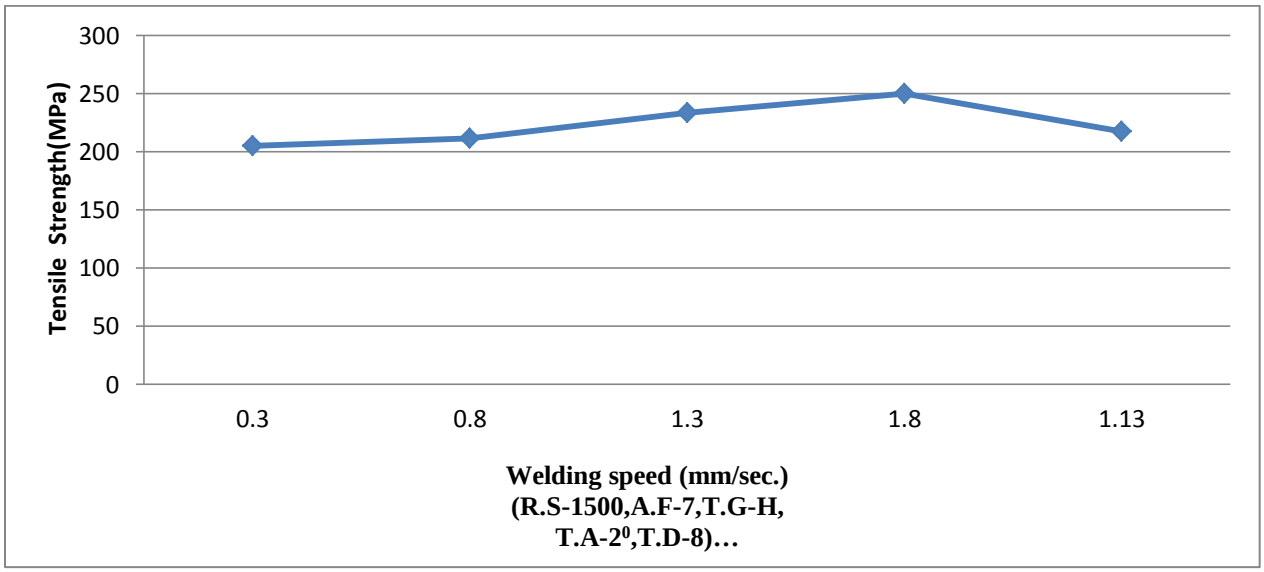

Figure 4.11 Scatter plot of tensile strength vs. welding speed

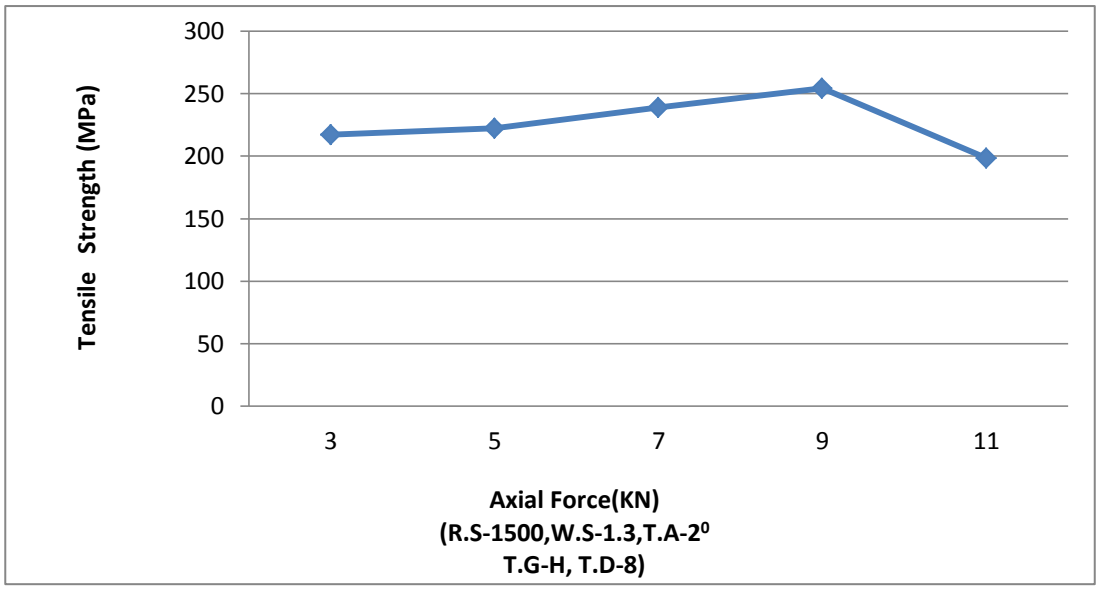

Figure 4.12 Scatter plot of tensile strength vs. axial force

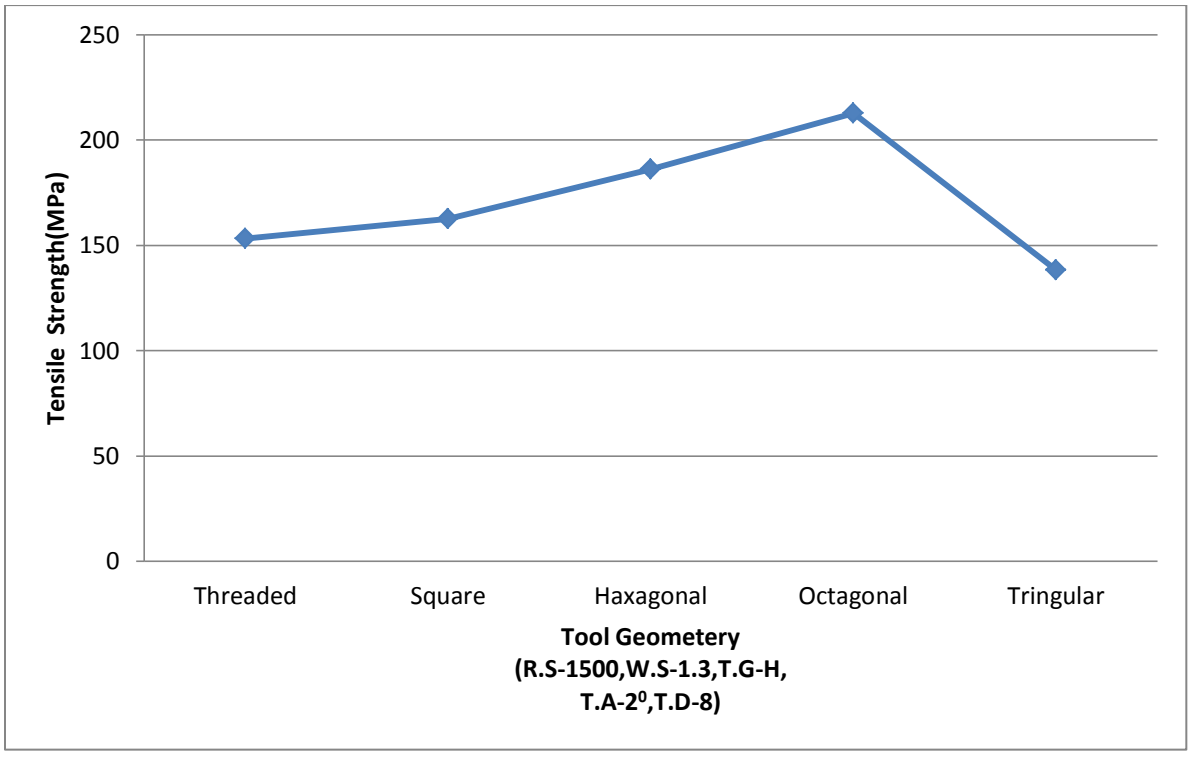

Figure 4.13 Scatter plot of tensile strength vs. tool geometry

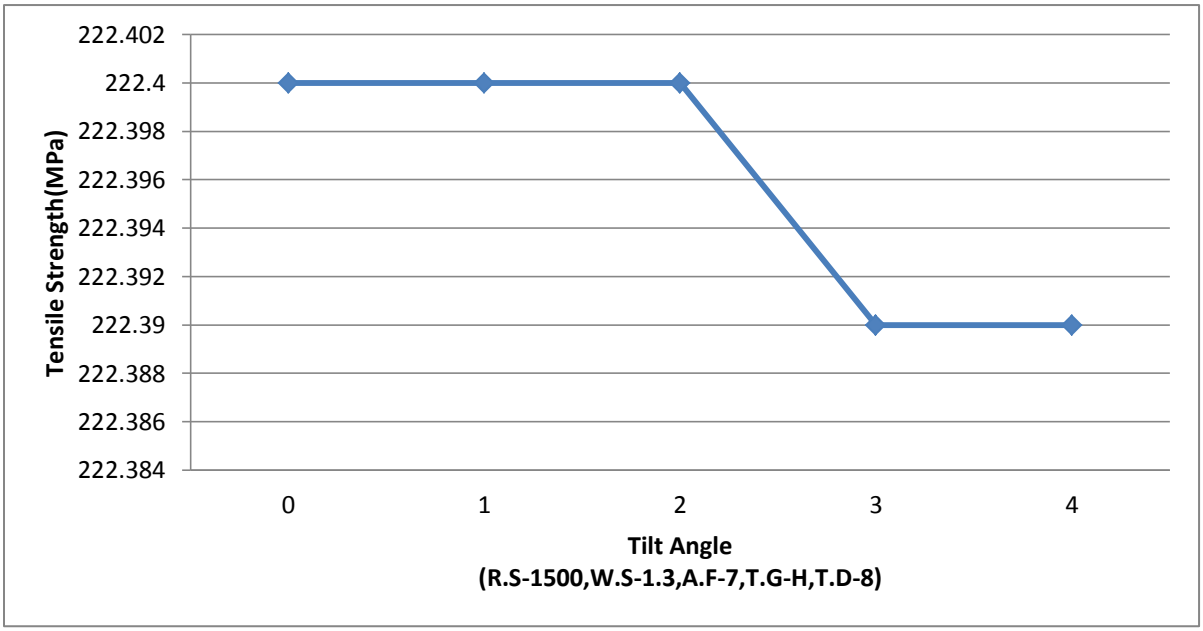

Figure 4.14 Scatter plot of tensile strength vs. tilt angle

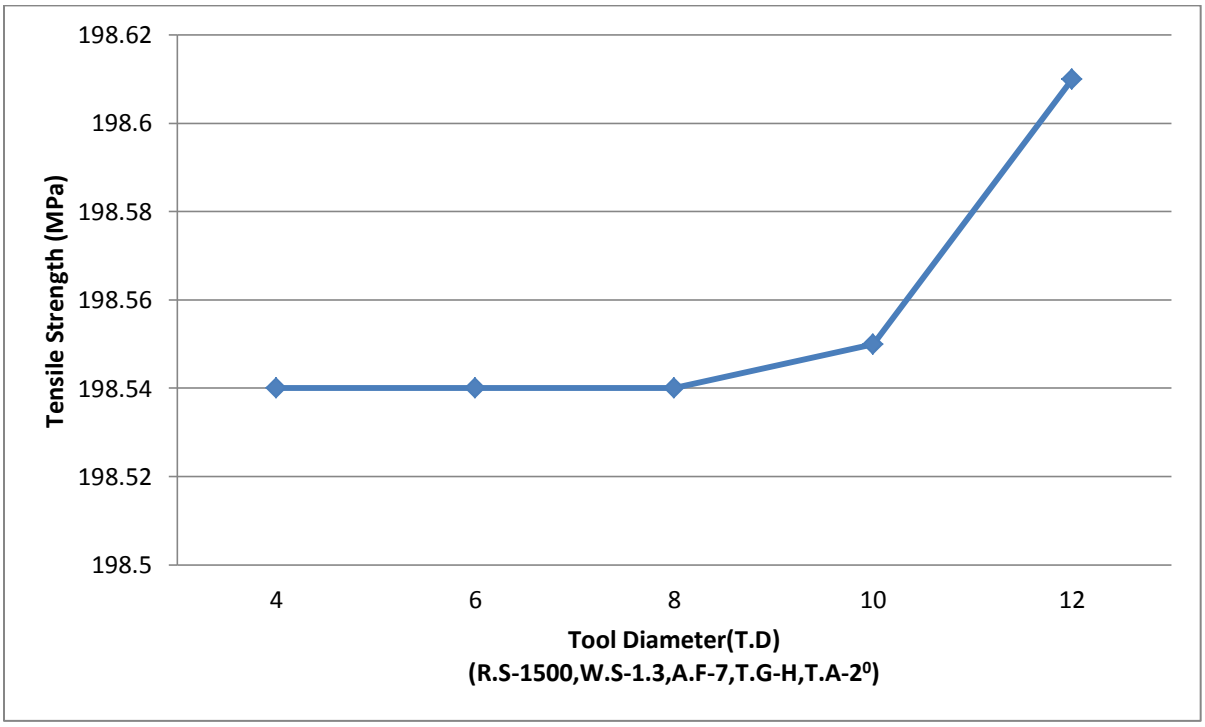

Figure 4.15 Scatter plot of tensile strength vs. tool diameter

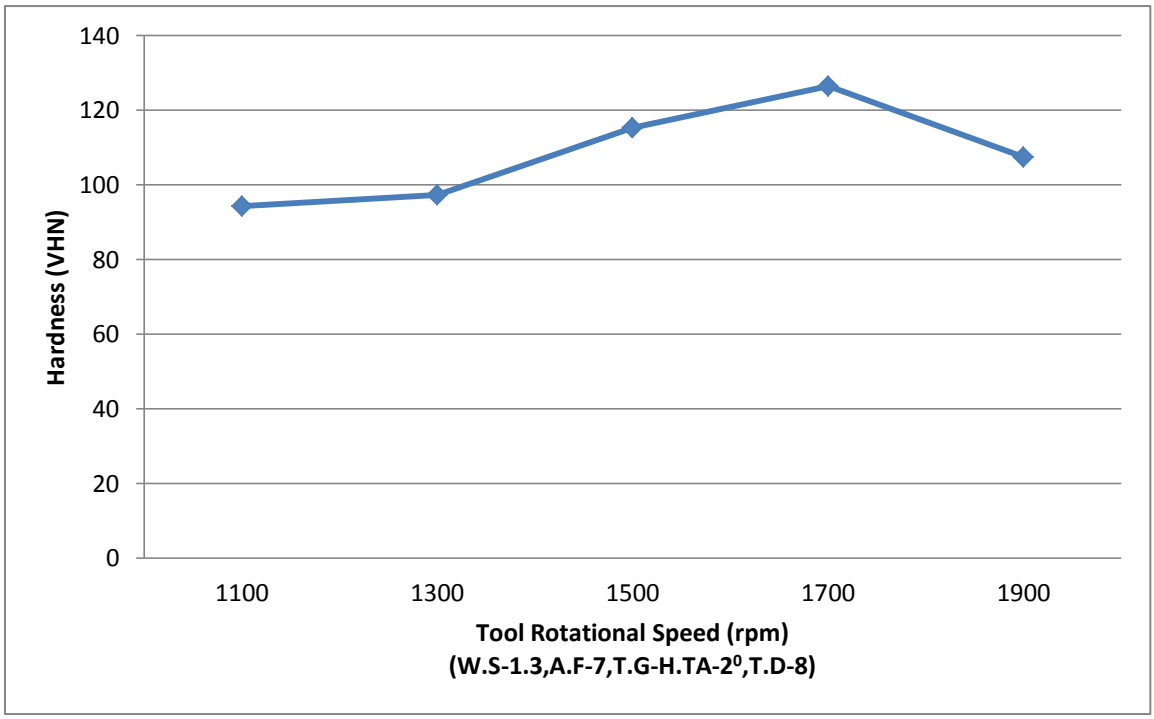

Figure 4.16 Scatter plot of hardness vs. tool rotation speed

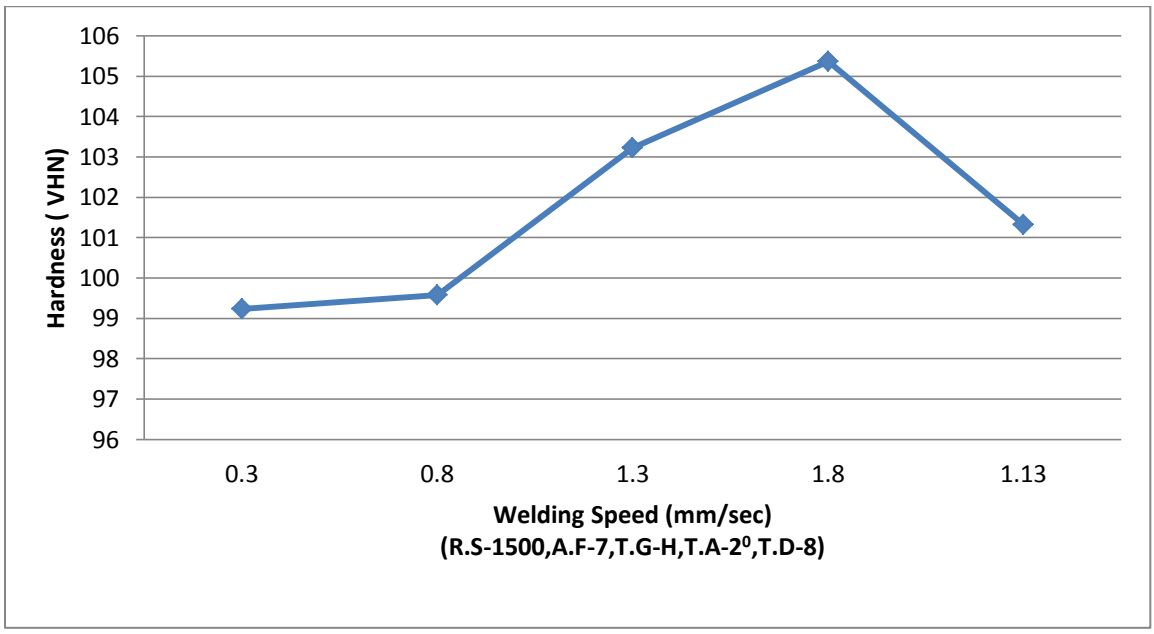

Figure 4.17 Scatter plot of hardness vs. welding speed

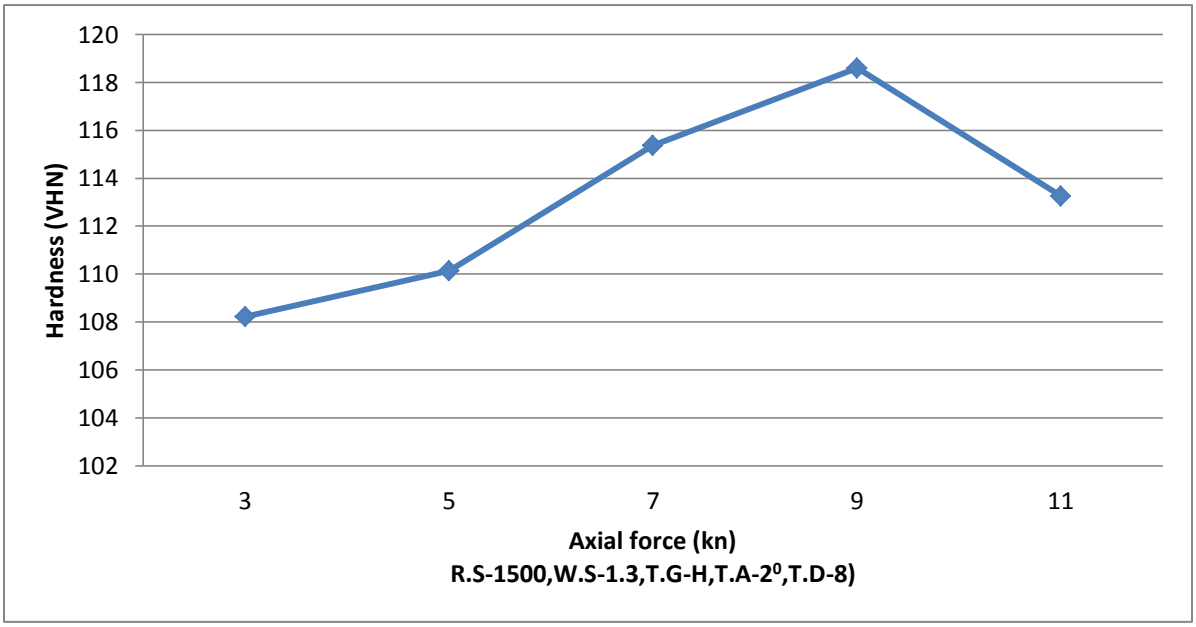

Figure 4.18 Scatter plot of hardness vs. Axial force

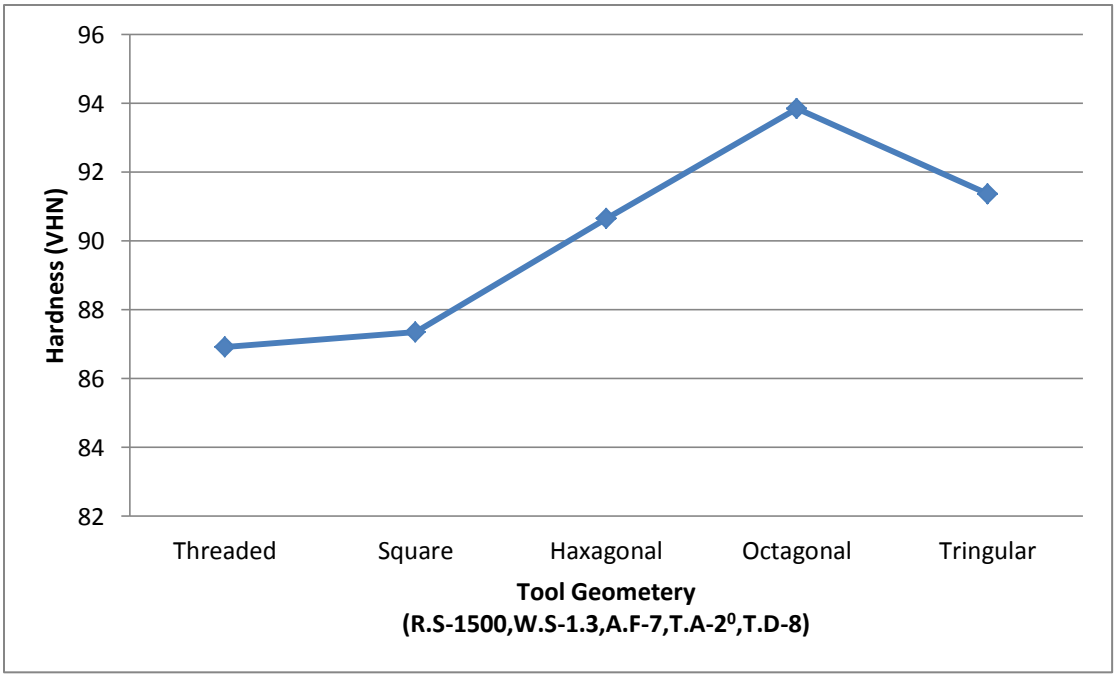

Figure 4.19 Scatter plot of hardness vs. tool geometry

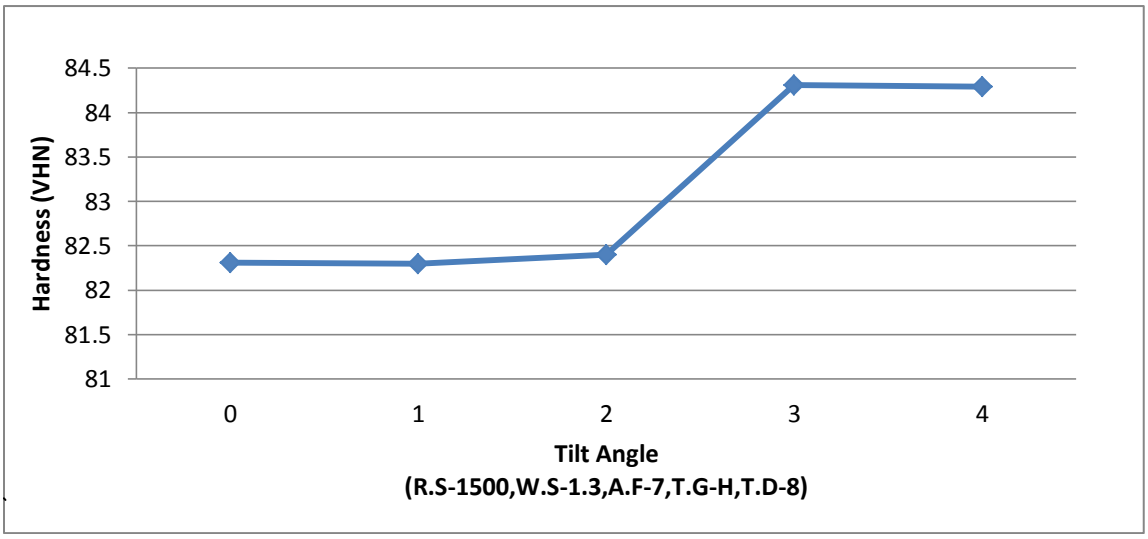

Figure 4.20 Scatter plot of hardness vs. tilt angle

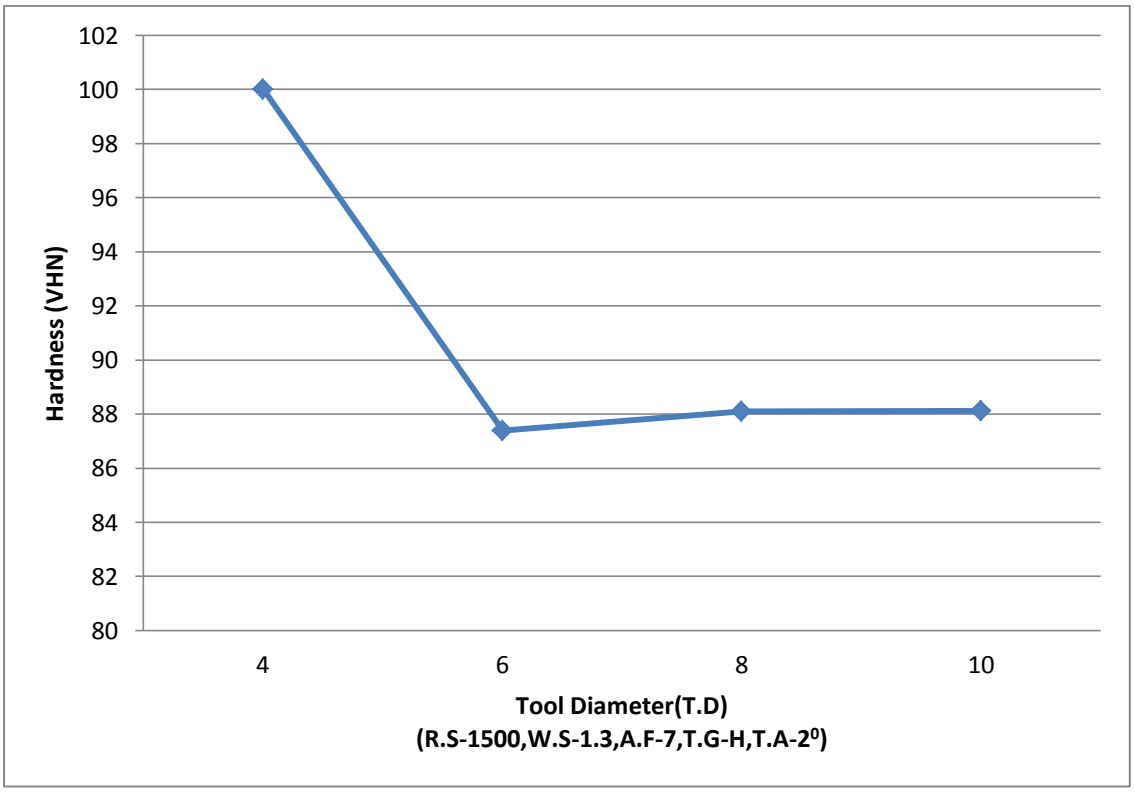

Figure 4.21 Scatter plot of hardness vs. tool diameter

Based on the above pilot experiments, four input process parameters (tool rotational speed, welding speed, axial force and tool geometery) and their ranges were chosen. These selected process parameters and their ranges are shown in table 4.1.

Table 4.1 Selected process parameters and their ranges based on pilot experiments

Symbol	Process parameters	Level 1	Level 2	Level 3
A	Tool rotation speed(rpm)	1300	1500	1700
B	Welding speed(mm/sec.)	0.8	1.3	1.8
C	Axial force(kn)	5	7	9
D	Tool geometery	S	H	O

CHAPTER-5

OPTIMIZATION TECHNIQUE

5.1 DESIGN OF EXPERIMENT

A scientific approach is necessary to perform the experiments in a plan way. So that appropriate data will be collected and analyzed by statistical methods resulting in valid and objective conclusions. There are two aspects of an experimental problem: the design of experiments and the statistical analysis of the data. These two points are closely related since the method of analysis depends directly on the design of experiments employed [75-78]. The advantages of design of experiments are as follows:

- Number of trials are significantly reduced
- Important decision process parameters which control and improve the performance of the product of the process can be identified.
- Optimal setting of the process parameters can be found out.
- Qualitative estimation of parameters can be made
- Experimental error can be estimated.

In the present work, the Taguchi's method has been used to plan the experiments and subsequent analysis of the data collection.

5.1.1Taguchi Approach

Taguchi approach is an efficient problem solving tool which can improve the performance of the product. Taguchi recommends a three-stage process: system design, parameter design and tolerance design [118]. Taguchi's parameter design approach is used to study the effect of process parameters on various responses of Friction Stir Welding process.

5.1.2 Experimental Design Strategy

Taguchi suggests two different routes to carry out the complete analysis. First, the standard approach, where the results of a single run or average of repetitive runs are processed through main effect and ANOVA analysis (Raw data analysis).The second approach which Taguchi strongly recommends for multiple runs is to use signal-to-noise

ratio (S/N) for the same steps in the analysis. The S/N ratio is a concurrent quality metric linked to the loss function [118]. By maximizing the S/N ratio, the loss associated can be minimized. The S/N ratio determines the most robust set of operating conditions from variation within the result. The S/N ratio is treated as a response of the experiment. In the present investigation, the raw data analysis and S/N data analysis have been performed. The effects of selected FSW process parameters on the selected quality characteristics have been investigated through the plots of the main effects based on raw data. The optimum condition for each of the quality characteristics have been established through S/N data analysis by raw data analysis.

5.1.3 Signal to Noise Ratio

Taguchi method uses a statistical measure of performance called signal-to-noise (S/N) ratio to analyze the results. In its simplest form, the S/N ratio is the ratio of the mean response (signal) to the standard deviation (noise). S/N ratio is gained by minimizing the loss function and defined in three different conditions: lower-the-better, larger-the-better, and nominal-the-better. In this work, the S/N ratio was chosen according to the criterion 'the larger-the-better', in order to maximize the response. The S/N ratio of the larger the better expressed as follows [118]

$$S/N = -10 \log \frac{1}{n} \left(\sum_{i=1}^{n} 1/yi^2\right)$$

Where, n is the number of repetitions of the experiments

y_i is the average measured value of experimental data

5.1.4 Steps in Experimental Design and Analysis

The important steps in the Taguchi experimental design and analysis are discussed in the subsequent research work.

5.1.4.1 Selection of Orthogonal Array (OA)

For selecting a particular OA to be used as matrix for conducting the experiments, the following two points must be considered [118].

1. How many number of parameter and interactions required

2. How many number of levels for parameters required

The total degree of freedom (DOF) of an experiment is a direct function of total number of trials. If the number of levels of a parameter increases, the DOF of the parameter also increases because the DOF of a parameter is the number of levels minus one. Thus, increasing the number of level for a parameter increases the total degree of freedom in the experiment which in turn increases the total number of trials. In this work, four process parameters and three levels are selected. Each three level parameter has 2 degrees of freedom (DOF= Number of levels-1) the total DOF required for four parameters each at three levels is i.e 8 (4x(3-1)). As per Taguchi's method, the total DOF of selected OA must be greater than or equal to the total DOF require for experiments. Taguchi recommended minimizing the size of the experiments [80-84].

- Two level arrays: L4, L8, L12, L16, L32
- Three level arrays: L9, L18, L27 So, L_{27} OA was selected for this work.

5.1.4.2 Data Analysis

A number of methods have been suggested by taguchi for analyzing the data: observation method, ranking method, column effect method, ANOVA, S/N ANOVA, plot of average response curve, interaction graphs etc [118]. However, in the present investigation the following methods have been used:

- Plot of average response curves
- ANOVA for raw data
- ANOVA for S/N data
- S/N Response graphs
- Interaction graphs
- Residual graphs

Plot of average response at each level of a parameter indicates the trend. It is a pictorial representation of the effect of parameter on the response. The change in the response characteristic with the change in levels of a parameter can easily be visualized from these curves. The S/N ratio is treated as a response of the experiment, which is a measure of the variation within a trial when noise factors are present. A standard

ANOVA can be conducted on S/N ratio which will identify the significant parameters (means and variation). Interaction graphs are used to select the best combination of interactive parameter [118]. Residual plots are used to check the accuracy.

5.1.4.3 Analysis of Variance (ANOVA)

After performing the statistical S/N analysis, ANOVA needs to be employed for determining the relative importance of various factors. Analysis of Variance (ANOVA) test was performed to identify the parameters that are statistically significant. ANOVA is also applied to the results of the experiments to determine the percentage contribution of each parameter against a stated level of confidence [118]. The effects of the FSW parameters on the selected response were investigated through the main effects plots. The optimum level for each FSW parameter was established through ANOVA. The purpose of the statistical ANOVA is to determine the most influential design parameter that significantly affects the mechanical properties for the friction stir welded joints. Also, ANOVA is used to investigate the relationship between the response and selected process parameters. The problem to be solved in this study was to examine the possible differences in the mechanical properties (tensile strength, hardness, and welded joint efficiency) of friction stir welded joints, which result from different combinations of the selected process parameters. ANOVA test is used to investigate the significance of the process parameters which affect the responses of friction stir welding joints. In addition, the F-test named after Fisher can also be used to determine which process has a significant effect on the responses. Usually, the change of the process parameter has a significant effect on the quality characteristics, when F is large. The results of ANOVA indicates that the considered process parameters are highly significant factors affecting the responses of friction stir welding joints in the order of rotational speed, welding speed, axial force and tool pin geometry. [85-86] The Minitab software 17 was used to study the statistical analysis for the obtained results.

5.1.4.4 Determination of Confidence Interval

The estimate of mean is only a point estimate based on the average of result obtained from the experiment. Statistically this provides a 50% chance of the true average being greater than mean. It is therefore the value of a statistical parameter as a range with in which it is likely to fall, for a given level of confidence. The following two types of confidence interval are suggested by Taguchi in regards to estimated mean of the optimal treatment condition [118].

1. Around the estimated average of a treatment condition predicted from the experiment. This type of confidence interval is designated as CI_{POP} (confidence interval for the population).
2. Around the estimation average of a treatment condition used in a confirmation experiment to verify predictions. This type of confidence interval is designated as CI_{CE} (confidence interval for a sample group).

   The difference between CI_{POP} and CI_{CE} is that CI_{POP} is for the entire population i.e all parts ever made under the specified conditions and CI_{CE} is for only a sample group made under the specified conditions. Because of the smaller size (in confirmation experiments) relative to entire population CI_{CE} must slightly be wider.

5.1.4.5 Confirmation Experiments

The confirmation experiment is a final step in verifying the conclusion from the previous round of experimentation. The optimum condition is set for the significant parameters and a selected number of tests are run under the specified conditions. The average of confirmation experiment results is compared with the anticipated average based on the parameters and levels tested. The confirmation experiments are a crucial step and are highly recommended to verify the experimental conclusion [118].

5.2 CONDUCT OF EXPERIMENTS FOR RESPONSE CHARACTERISTICS

According to the Taguchi's orthogonal array (L_{27}) experimens with four process parameters(A,B,C&D) and three ranges(1,2 &3) were condected shown in table 5.1.

Table 5.1 Taguchi's orthogonal array(L_{27})

Experimental Run	Process Parameters and ranges			
	A	B	C	D
1	1	1	1	1
2	1	1	2	2
3	1	1	3	3
4	1	2	1	2
5	1	2	2	3
6	1	2	3	1
7	1	3	1	3
8	1	3	2	1
9	1	3	3	2
10	2	1	1	1
11	2	1	2	2
12	2	1	3	3
13	2	2	1	2
14	2	2	2	3
15	2	2	3	1
16	2	3	1	3
17	2	3	2	1
18	2	3	3	2
19	3	1	1	1
20	3	1	2	2
21	3	1	3	3
22	3	2	1	2
23	3	2	2	3
24	3	2	3	1
25	3	3	1	3
26	3	3	2	1
27	3	3	3	2

5.2.1 Responses

According to the Taguchi's orthogonal array (L_{27}), 27 experiments were performed and measured the responses,which are shown in table 5.2

Table 5.2 Measured responses of friction stir welding pocess

S.NO	Tool Rotational Speed	Welding Speed	Axial Force	Tool Geometry	Tensile Strength (Mpa)	Percentage Elongation	Micro Hardness(VHN)	Joint efficiency (%)
1	1300	0.8	5	S	221.11	3.481	90.55	68.88
2	1300	0.8	7	H	249.14	3.799	100.9	77.61
3	1300	0.8	9	O	235	3.62	95.17	73.21
4	1300	1.3	5	H	251.32	3.753	101.78	78.29
5	1300	1.3	7	O	269.1	3.961	108.98	83.83
6	1300	1.3	9	S	243.41	3.704	98.58	75.83
7	1300	1.8	5	O	216	3.341	90.25	67.29
8	1300	1.8	7	S	237.62	3.745	96.23	74.02
9	1300	1.8	9	H	229.16	3.562	93.81	71.39
10	1500	0.8	5	H	234.14	3.599	94.82	72.94
11	1500	0.8	7	O	267	3.94	108.13	83.18
12	1500	0.8	9	S	247.14	3.741	100.09	76.99
13	1500	1.3	5	O	288	4.12	116.64	89.72
14	1500	1.3	7	S	311	4.481	125.95	96.88
15	1500	1.3	9	H	297.1	4.241	120.32	92.55
16	1500	1.8	5	S	283.15	4.102	114.67	88.21
17	1500	1.8	7	H	292.24	4.198	118.35	91.04
18	1500	1.8	9	O	285.16	4.122	115.49	88.83
19	1700	0.8	5	O	241.11	3.581	100.65	75.11
20	1700	0.8	7	S	279.75	4.105	113.29	87.15
21	1700	0.8	9	H	249.4	3.764	101	77.69
22	1700	1.3	5	S	268.13	3.951	108.59	83.53
23	1700	1.3	7	H	284.11	4.258	115.06	88.51
24	1700	1.3	9	O	261.25	3.883	105.8	81.39
25	1700	1.8	5	H	243	3.689	100.85	75.7
26	1700	1.8	7	O	260	3.87	105.3	81
27	1700	1.8	9	S	249.43	3.764	101.02	77.7

5.3 MULTI RESPONSE OPTIMIZATION TECHNIQUE

5.3.1 Planning for Optimizing Multi Response Characteristics

In this work, optimization of multi response characteristics is used for friction stir welded AA7075/10%SiC composites. The response characteristics are Tensile Strength and Hardness. In order to optimize multi response characteristics, grey based Taguchi method is used. The step wise procedure of multi response optimization is shown in figure 5.1

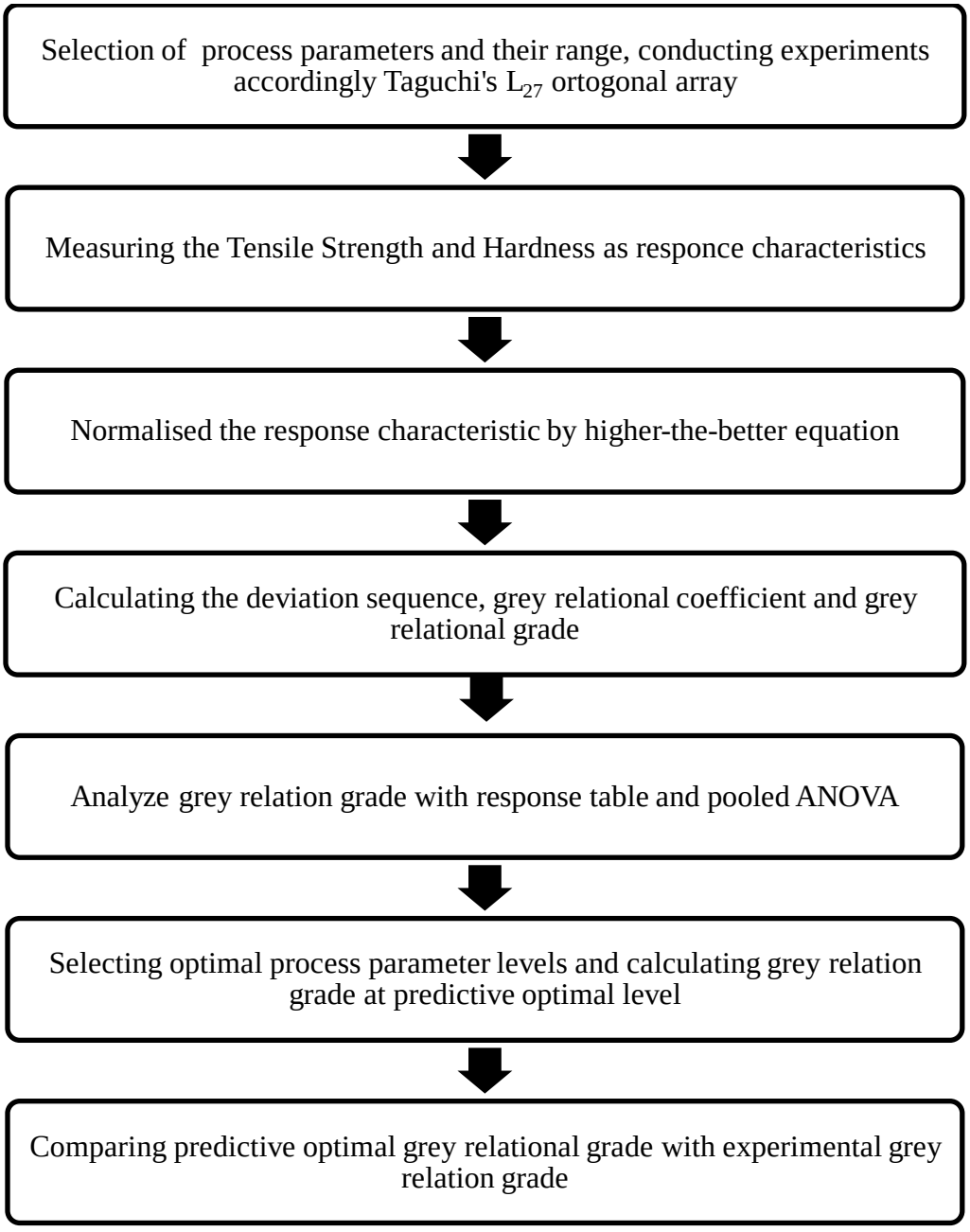

Figure 5.1 Step wise procedure of grey relation analysis.

5.3.2 Grey Relational Analysis (GRA)

Grey relational analysis (GRA) is a part of the grey theory which was developed by Deng. The technique is used for solving multiple response problems. This technique combined the whole range of response characteristic values into one single value. GRA made a multi-decision problem into a single decision problem. Taguchi method works for optimization of a single performance characteristic. In this work, GRA is used to optimize welding parameters for tensile strength and hardness.

CHAPTER-6

RESULTS AND DISCUSSION

6.1 CHARACTERIZATION OF AA7075/10%wt.SiC COMPOSITE

The standard specimens were prepared from AA7075/10%wt.SiC. The various composite to identify the microstructure through optical microscope analysis. Also analyzed the presence of elements, phase through SEM and EDAX analysis, XRD analysis, DTA analysis and SEM fractography analysis.

6.1.1 Microstructure

Optical microstructures were checked with the help of microscope with attached to computer, at 100x shown by figure 6.1. and at 400x shown by figure 6.2.The optical microstructure of AA7075/10%wt.SiC metal matrix composite samples are shown in figure 6.1. The images clearly show the distribution of SiC particles in AA7075 are uniformly distributed. Figure 6.2 indicates, the macroscopic distribution of the SiC particles is more uniform and particle clustering is limited. There is no porosity in these structures. Hence, these composites have good mechanical properties and are suitable for welding experiments.

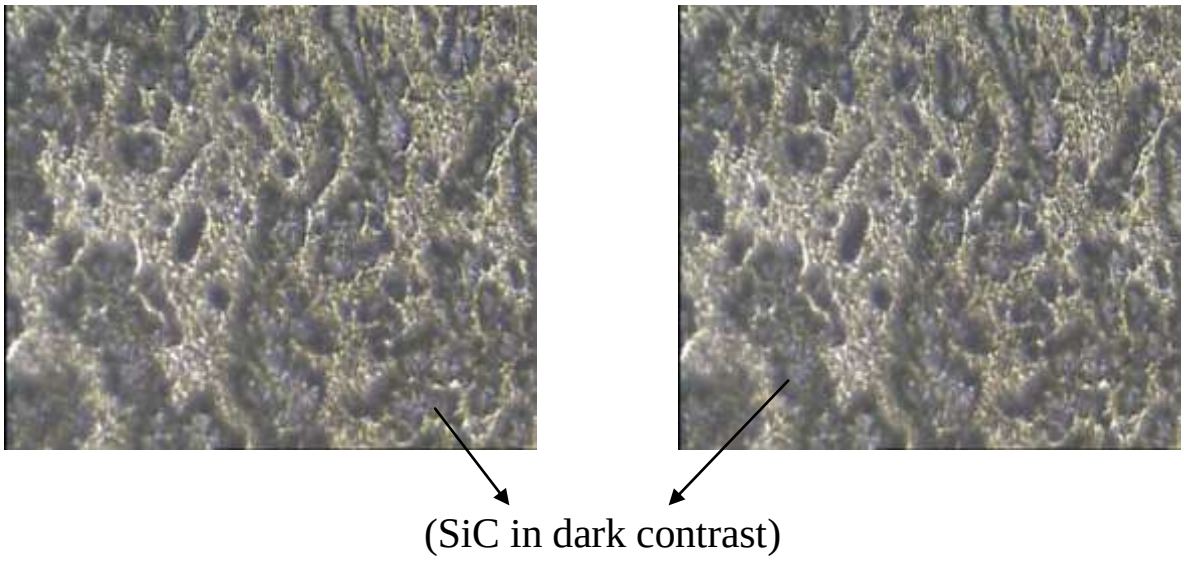

Figure 6.1 Optical microstructure of AA7075/10wt% SiC composite at 100X magnification

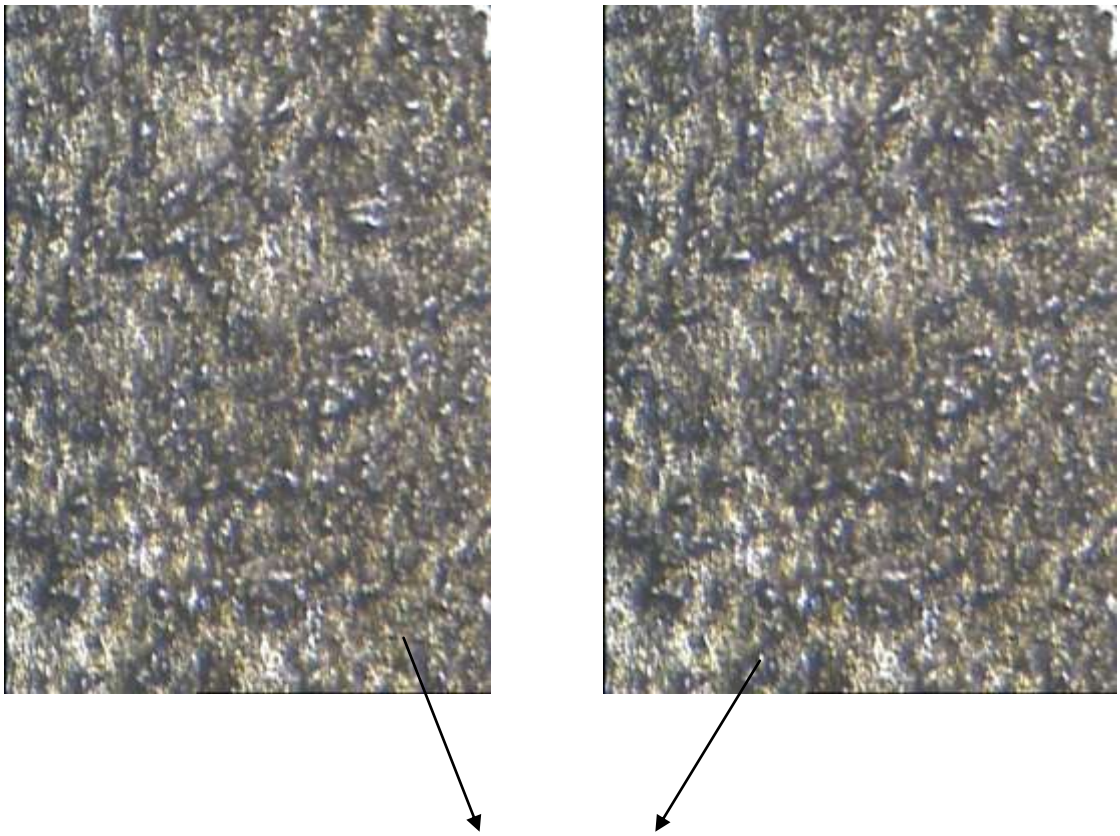

Figure 6.2 Optical microstructure of AA7075/10wt% SiC composite at 400X magnification

6.1.2 Scanning Electron Microscopy (SEM) and Energy Dispersive X-ray Analysis (EDAX) analysis

Figure 6.3 and figure 6.4 showed the SEM analysis and EDAX analysis of AA7075/10%wt.SiC composite respectively. According to both figures of AA7075/10%wt.SiC composite. SiC clearly shows the uniform distribution of SiC reinforcement. Result of EDAX revealed that the main constituents like Mg, Si, Zn and Cu are present in the major quantity. No new component had been formed in EDAX analysis of AA7075/10%wt./SiC composites. No adverse reaction has been observed in EDAX analysis of AA7075/10%wt.SiC composite.

Table 6.1 Weight and atomic % AA7075/SiC

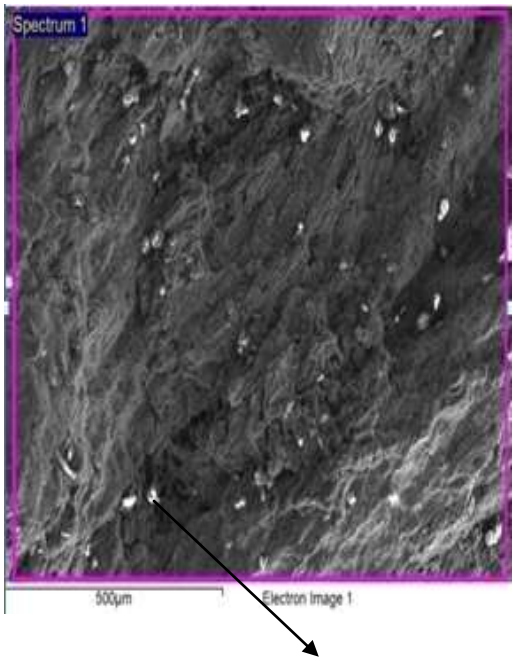

Element	Weight%	Atomic%
C K	9.77	11.95
O K	6.61	8.17
Mg K	2.41	2.00
Al K	65.01	62.17
Si k	09.45	11.75
Fe k	0.71	0.50
Cu k	1.12	0.87
Zn k	4.92	1.49
Total	100	

Figure 6.3 SEM of AA7075/10 %wt.SiC

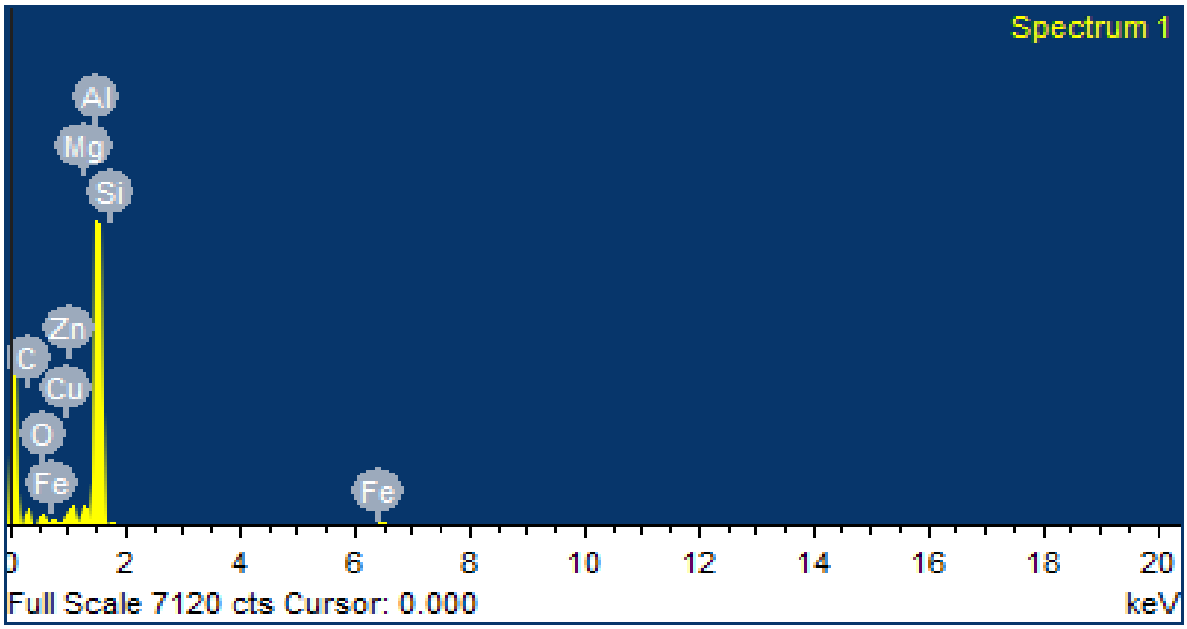

Figure 6.4 EDAX profile of AA7075/10% wt SiC

6.1.3 X-ray Diffraction Analysis

X-ray diffraction (XRD) measurements were performed using a Bruker ASX D-8 X-ray diffractometer. It is shown in figure 6.3 X-ray diffraction was carried out at a scanning rate of 0.01º 2θ/sec using Cu k (α) radiation. The source voltage and current were maintained at 40 KV and 40MA respectively. Peaks obtained in the diagram were analyzed. XRD patterns of the AA7075/10%wt.SiC are shown in Figure 6.5. The XRD pattern confirmed the presence of Al matrix and SiC particulate in the composite. Figure 6.3indicates that elements are properly distributed in AA7075/10%wt./SiC (20–40 μm) composites. Also, no adverse reactions have been observed in AA7075/10 %wt./SiC(20–40 μm) composites.

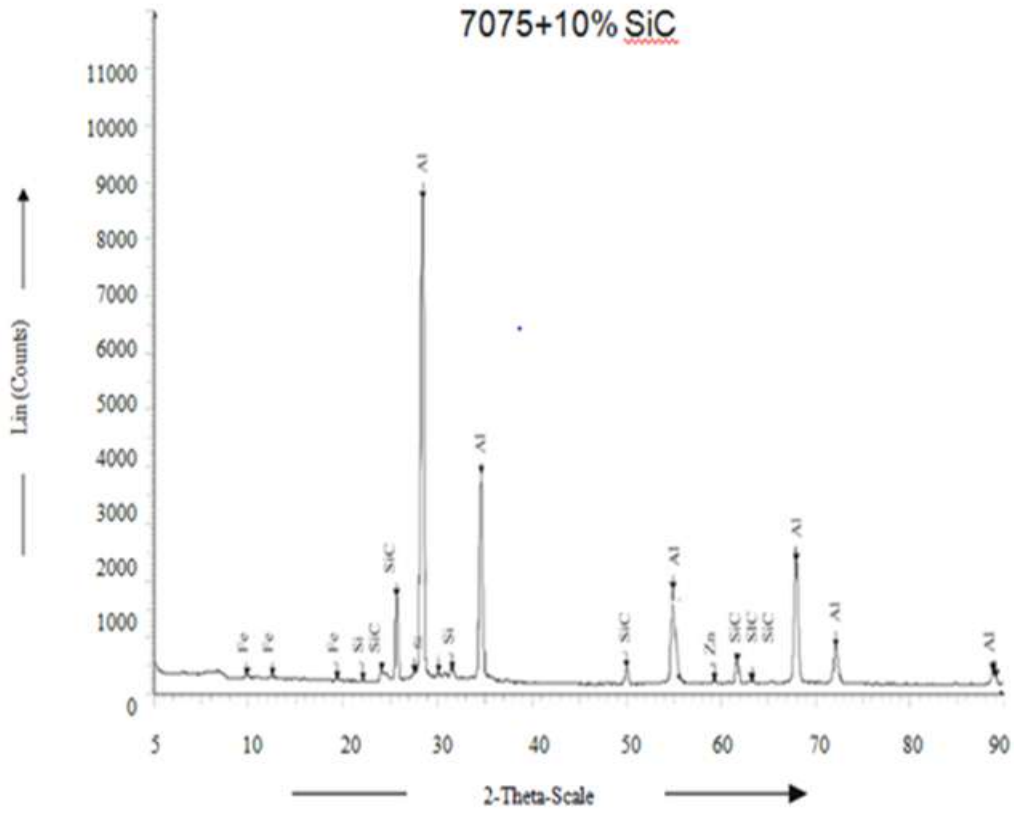

Figure 6.5 X-ray diffraction curves of AA7075/10wt%SiC Composite

6.1.4 Thermal Analysis

The TG, DTG and DTA curves are shown in figure 6.6 T.G curve performed in the temperature range of 22^0C– 850^0C.The sample was analyzed through TG, differential thermo gravimetric (DTG) and DTA to find their thermal degradation characteristics. The heating rate of 10^0C/min and atmosphere of air was employed for the degradation rate and temperature differences. According to the figure 6.6 TG, DTG and DTA curves are clearly shown. The DTA curve shows a depression that comes down from the baseline. It indicates that there is an endothermic reaction. This occurred at 642^0C. The value of enthalpy change is 282 mJ/mg on DTA curve. In DTG curve, percentage of mass decreases from 99.2^0C to 99.9^0C.It is observed around 0.7% due to the presence of moisture. After that mass of the composite increases with increases the temperature from 400^0C to 826^0C.It is around 2.3% due to the nitridation of zinc as a constitute of SiC composite by nitrogen gas.

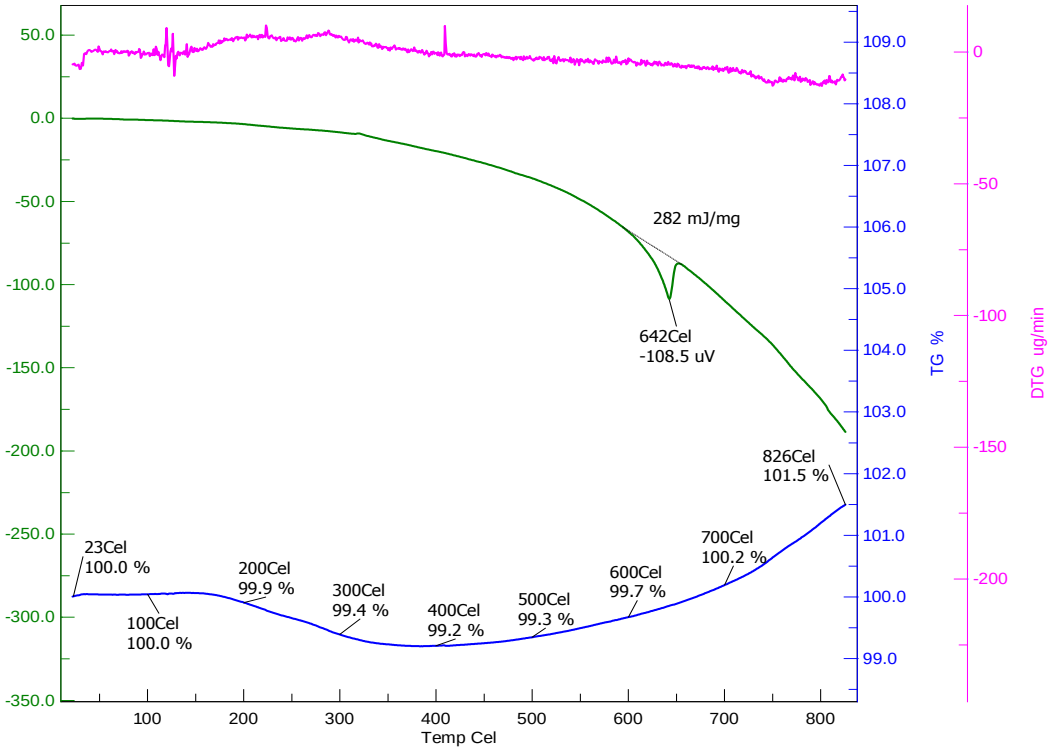

Figure 6.6 TG, DTG and DTA curv of AA7075/10% wt.SiC Composite

6.1.5 SEM Fractography

The SEM fractography of fractured tensile specimens of AA7075/10%wt.SiC composite of fabricated welded joints were carried out. The figure 6.7 shows SEM fractography of AA7075/10%wt.SiC composite. The fractured surface represents dimpled structure which is a typical characteristic of tensile overload fracture. Fractography indicate that there had been strong bonding between the reinforcement particulate and the matrix material. The strong interfacial bond between reinforcement particles and the matrix results in improvement of tensile strength. Homogeneous distribution of reinforcement in matrix is essential for optimum mechanical properties [37].

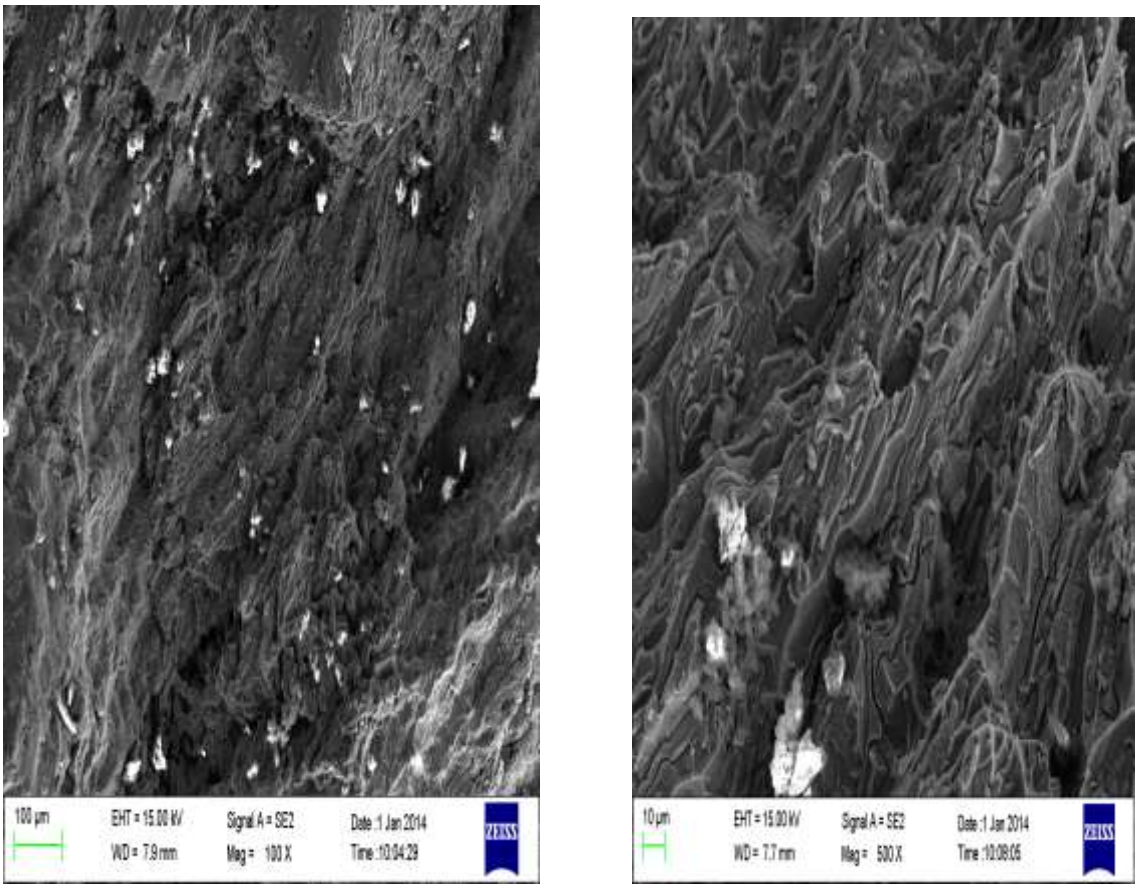

Figure 6.7 SEM fractography of AA7075/10%wt.SiC

6.2 Results of Welding Response Characteristics

6.2.1 Signal to noise ratio(S/N ratio)

Tensile strength, hardness and weld joint efficiency are the main response considered in this work. In order to describe the effect of process parameters on responses, the means and S/N ratio for every process parameter can be calculated. The signals are the indicators of the effect on mean (average) responses and the noises are measures of the effect on the deviations from the sensitiveness of the experiment to the noise factors. The S/N ratio was chosen according to the criterion 'the larger-the-better', in order to maximize the response. The S/N ratio of the larger expressed as follows.

$S/N = -10 \log \frac{1}{n} \left(\sum_{i=1}^{n} 1/yi^2\right)$

where, n is the number of repetitions of the experiments

yi is the average measured value of experimental data.

6.2.2 Analysis of Tensile Strength

The tensile strength data were analyzed to decide the effect of friction stir welding process parameters. The experimental results were then transformed into means and signal to noise ratio which are given in table 6.2. The analysis of mean for each of experiments will give the better combination of process parameters levels that confirm that higher tensile strength achieved. The mean response refers to the average value of performance characteristics for each parameter at different levels. The mean response of raw data and S/N ratio of tensile strength for each parameter at level 1,2,3 were calculated and are shown in table 6.3 and table 6.4 respectively.

Table 6.2.Tensile Strength and S/N ratio results of Friction Stir Welding

S.NO	Tool Rotational Speed (rpm)	Welding Speed (mm/sec.)	Axial Force (kn)	Tool Geometry	Tensile Strength ((MPa)	S/N Ratio
1	1300	0.8	5	S	221.11	46.89
2	1300	0.8	7	H	249.14	47.93
3	1300	0.8	9	O	235.00	47.42
4	1300	1.3	5	H	251.32	48.00
5	1300	1.3	7	O	269.10	48.6
6	1300	1.3	9	S	243.41	47.73
7	1300	1.8	5	O	216.00	46.69
8	1300	1.8	7	S	237.62	47.52
9	1300	1.8	9	H	229.16	47.20
10	1500	0.8	5	H	234.14	47.39
11	1500	0.8	7	O	267.00	48.53
12	1500	0.8	9	S	247.14	47.86
13	1500	1.3	5	O	288.00	49.19
14	1500	1.3	7	S	311.00	49.86
15	1500	1.3	9	H	297.10	49.46
16	1500	1.8	5	S	283.15	49.04
17	1500	1.8	7	H	292.24	49.31
18	1500	1.8	9	O	285.16	49.10
19	1700	0.8	5	O	241.11	47.64
20	1700	0.8	7	S	279.75	48.94
21	1700	0.8	9	H	249.40	47.94
22	1700	1.3	5	S	268.13	48.57
23	1700	1.3	7	H	284.11	49.07
24	1700	1.3	9	O	261.25	48.34
25	1700	1.8	5	H	243	47.71
26	1700	1.8	7	O	260	48.30
27	1700	1.8	9	S	249.43	47.94

Table 6.3 Response Table for Means

Process parameters	Level	Rotational Speed	Welding Speed	Axial Force	Tool Geometry
Average value of tensile strength	L1	239.10	247.10	249.60	260.10
	L2	278.30	274.80	272.20	258.80
	L3	259.60	255.10	255.20	258.10
Main effects	Max.-Min.	39.20	27.70	22.70	2
	Rank	1	2	3	4

Table 6.4 Response Table for S/N ratio

Process parameters	Level	Rotational Speed	Welding Speed	Axial Force	Tool Geometry
Average value of tensile strength	L1	47.55	47.84	47.90	48.26
	L2	48.86	48.76	48.67	48.22
	L3	48.27	48.09	48.11	48.20
	Max.-Min.	1.31	0.92	0.77	0.06
	Rank	1	2	3	4

The response table 6.3 and table 6.4 data is clearly graphically presented by figure 6.8 and figure 6.9 respectively. These graphs were plotted with the help of statistical software Minitab 17. These graphs indicates that the tensile strength was maximum when rotational speed, welding speed, axial force are at level 2, and tool geometry at level 1, i.e. rotational speed 1500 rpm, welding speed 1.3 mm/sec and axial force 7 KN .

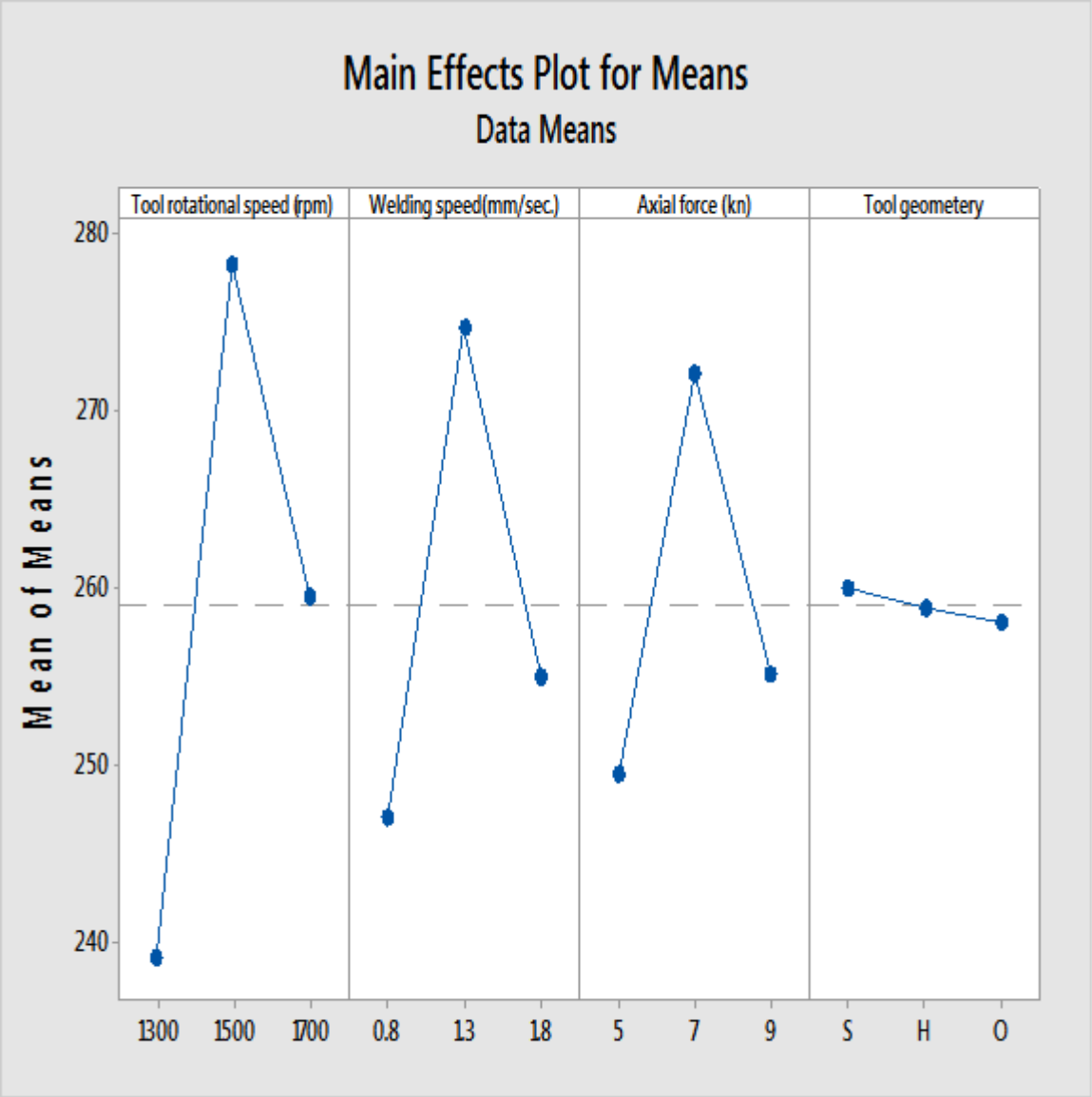

Figure 6.8 Effects of Process Parameters on Tensile strength (Main effects)

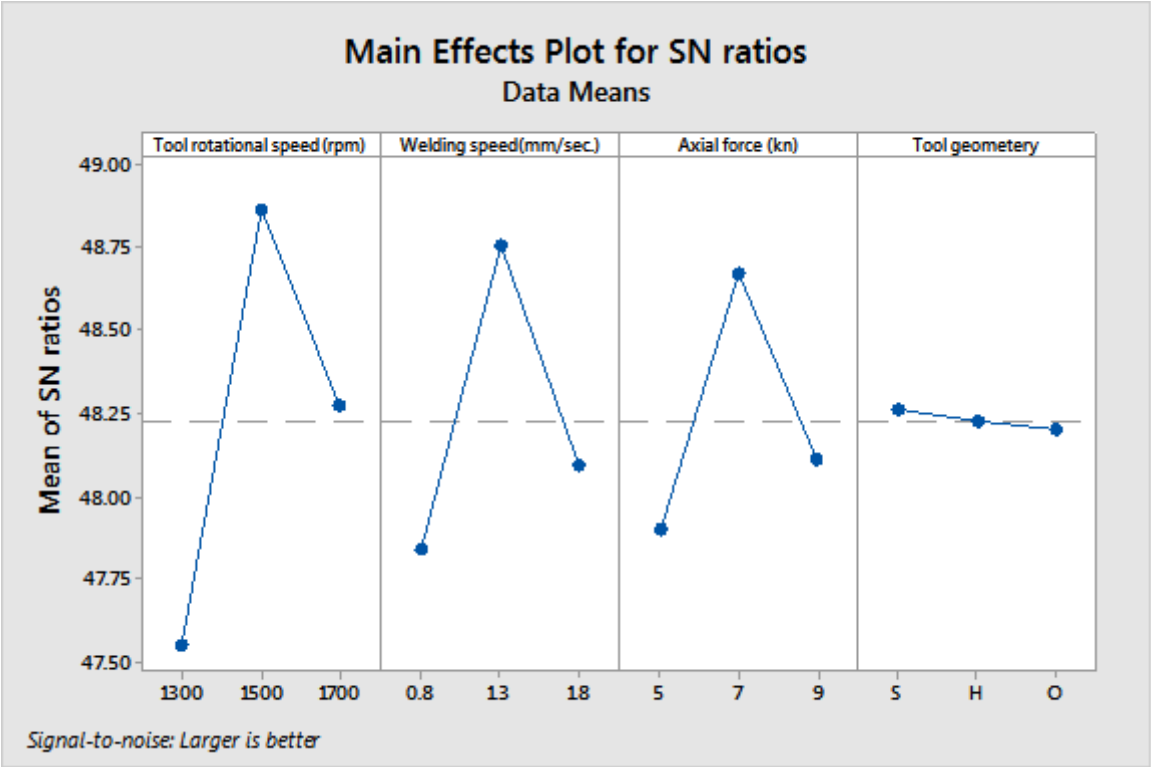

Figure 6.9 Effects of Process Parameters on Tensile strength S/N (ratio)

6. 2.2.1 Effect of Rotational Speed on Tensile Strength

Figure 6.8 and figure 6.9 represent the effect of tool rotational speed on Tensile strength of friction stir welded AA7075/10%wt.SiC composite joints. The highest tensile strength was achieved at the rotational speed of 1500 rpm. At a lower rotational speed (1300 rpm) and higher rotational speed (1700 r/min), the tensile strength of joint was poor. When the rotational speed was increased from 1300 r/min, the tensile strength also increased and reached a maximum at 1500 rpm. If the rotational speed was increased above 1500 rpm, the tensile strength of the joint was decreased. A lower tool rotational speed (1300 rpm) produced a lower heating condition as well as poor stirring action by the tool pin and improper consolidation of work material by the tool shoulder. Hence, a lower tensile strength was obtained. The increase in rotational speed increased the heat input per unit length of the joint, which causes a greater uniform grain refinement resulting in enhanced the tensile strength. A very significant increase in the rotational

speed (i.e. more than 1500 rpm) may produce an excessive release of stirred material on the top surfaces, which resulted in the formation of micro voids into the stirred zone. The rise in temperature as well as lower cooling rate and coarsening of grains at more than desired temperature may also reduce the tensile properties at high rotational speed.

6.2.2.2 Effect of Welding Speed on Tensile Strength

Figure 6.8 and figure 6.9 present the effect of welding speed on tensile strength of friction stir welded AA7075/10%wt.SiC composite joints. The tensile strength of FSW joint was low at the lower welding speed of 0.8 rpm. The tensile strength was increased with increase in welding speed until the maximum of 1.3 mm/s. Further, increase in welding speed reduced the tensile strength of FSW joint. It can be observed that a higher welding speed decreases the frictional heat input to the work material, which creates poor plastic flow of the metal and causes some voids like defects in the welded joint. This restricts grain growth and causes reduction in the width of the weld. Hence, poor tensile strength is obtained.

6.2.2.3 Effect of Axial Force on Tensile Strength

Figure 6.8 and figure 6.9 analyzed the effect of axial force on Tensile Strength of friction stir welded AA7075/10%wt.SiC composite joints. The lowest strength was obtained at axial load of 5 kN and 9 kN. The Tensile Strength of composite joint was increased with increase in axial load up to a maximum load of 7 KN. Further, increase in axial load decreased the tensile strength of the joint. During the FSW process, the rotation of tool produces a large amount of heat input which brings the metal to become very hot and plastic state. The axial force is more responsible for the plunge depth of the tool pin into the work piece. The joining of materials depends on the extrusion process by axial force and the rotation of tool pin which propel the plasticized material. At a lower axial force (5 KN), the lowest frictional heat is generated which is not sufficient to generate a adequate plastic state. At a higher axial force (9 KN) the plunge depth of the tool into the work piece is higher which drastically decreases the strength [75]. The joint fabricated with an axial force (7 KN) produced a finer grain structure with uniform distribution of reinforcement particle in the stir zone and resulted higher Tensile Strength.

6.2.2.4 Effect of Tool Pin Profile on Tensile Strength

Figure 6.8 and figure 6.9 represent the different values of tensile strength for different types of tool pin profile. It is observed that the square type tool pin profile gives the maximum value of tensile strength. The square type of tool pin profile generates good material stir quality during welding. Since, the tool has four edges, the point of each edge acts as an individual cutting tool that causes maximum deformation in the material. Hence, good surface finish and defect free joints are formed. Hexagonal and octagonal type tool pin profile produce insufficient mixing because tool pin is incapable of deforming appropriate material during rotation.

6.2.2.5 Analysis of Variance (ANOVA)

The ANOVA results for tensile strength of means and S/N ratio are given in table 6.5 and table 6.6 respectively. The purpose of ANOVA is to investigate the effect of process parameters on the tensile strength. ANOVA analysis was carried out for a level of significance of 5%, i.e. for 95% level of confidence. If the calculated F-ratio is more than the tabulated value i.e. 5.14 for parameter and 4.53 for interactions at confidence level, then the effect is significant. Percentage contribution represents the significant contribution on response. The Rotational Speed has maximum contribution (44.42 %) followed by Welding Speed (23.57%) and Axial force (16.04%). It can be seen from table 6.5 that Rotational speed and welding speed interaction has only significant effect of 14.09% contribution.

Table 6.5 Pooled ANOVA for Means (Tensile Strength)

Source	DOF	Seq SS	Adj SS	Adj MS	F Ratio	P	% PC
Rotational Speed	2	6930	6929.99	3464.98	140.9	0.00	44.42
Welding Speed	2	3668.8	3668.8	1834.41	74.6	0.00	23.57
Axial Force	2	2504	2503.99	1251.99	50.91	0.00	16.04
Tool Geometry	2	18.6	18.6	9.28	0.38	0.701	
Rotational Speed*Welding Speed	4	2124.5	2124.5	531.12	21.6	0.001	14.09
Rotational Speed* Axial Force	4	48.4	48.41	12.1	0.49	0.743	
Welding Speed* Axial Force	4	369.7	369.72	92.43	3.76	0.073	
Residual Error	6	147.5	147.55	24.59			1.87
Total	26	15811.5					100

Table 6.6 Pooled ANOVA for S/N ratios (Tensile Strength)

Source	DOF	Seq SS	Adj SS	Adj MS	F Ratio	P	% PC
Rotational Speed	2	7.7023	7.70234	3.85117	128.48	0.000	44.22
Welding Speed	2	4.0548	4.05477	2.02739	67.64	0.000	23.44
Axial Force	2	2.8523	2.85229	1.42615	47.58	0.000	16.59
Tool Geometry	2	0.0152	0.01517	0.00759	0.25	0.784	
Rotational Speed*Welding Speed	4	2.2855	2.28549	0.57137	19.06	0.001	13.70
Rotational Speed* Axial Force	4	0.0625	0.06253	0.01563	0.52	0.725	
Welding Speed* Axial Force	4	0.4679	0.46788	0.11697	3.9	0.068	
Residual Error	6	0.1798	0.17984	0.02997			2.04
Total	26	17.603					100

S = 0.1731 R-Sq = 99.0% R-Sq(adj) = 95.6%

DF:Degree of freedom, Seq SS: Sequential sum of squares, Adj SS: Adjusted sum of square, Adj MS: Adjusted mean square, F:Fisher ratio, P:Probability that exceeds the 95% confidence level, SS': Pure sum of squares, PC: Percentage of Contribution.

6.2.2.6 Interaction Plot for Tensile Strength

Figure 6.10 and figure 6.11 disclose pattern of line segments crossing each another or slight variation in the interaction plot paths, there is no actual 'disorder interaction' between rotational speed and welding speed or between rotational and axial force and profile plot paths crossed due to random variation. From the study of Table 6.5, it is apparent that potential of the model, R^2 is greater than 0.90. Normal probability plot of residuals as shown in figure 6.12 and figure 6.13, shows no drastic deviation with the normality. This result confirms the basic assumption used in analysis (errors are normally distributed).

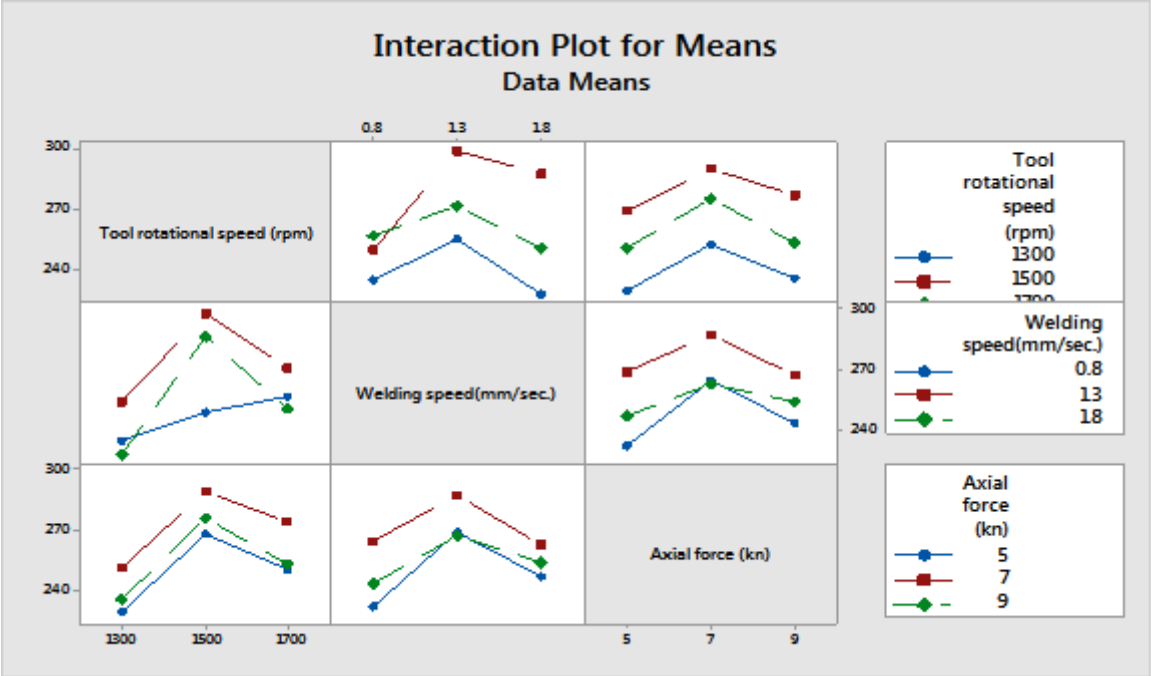

Figure 6.10 Interaction plot for tensile strength (Means)

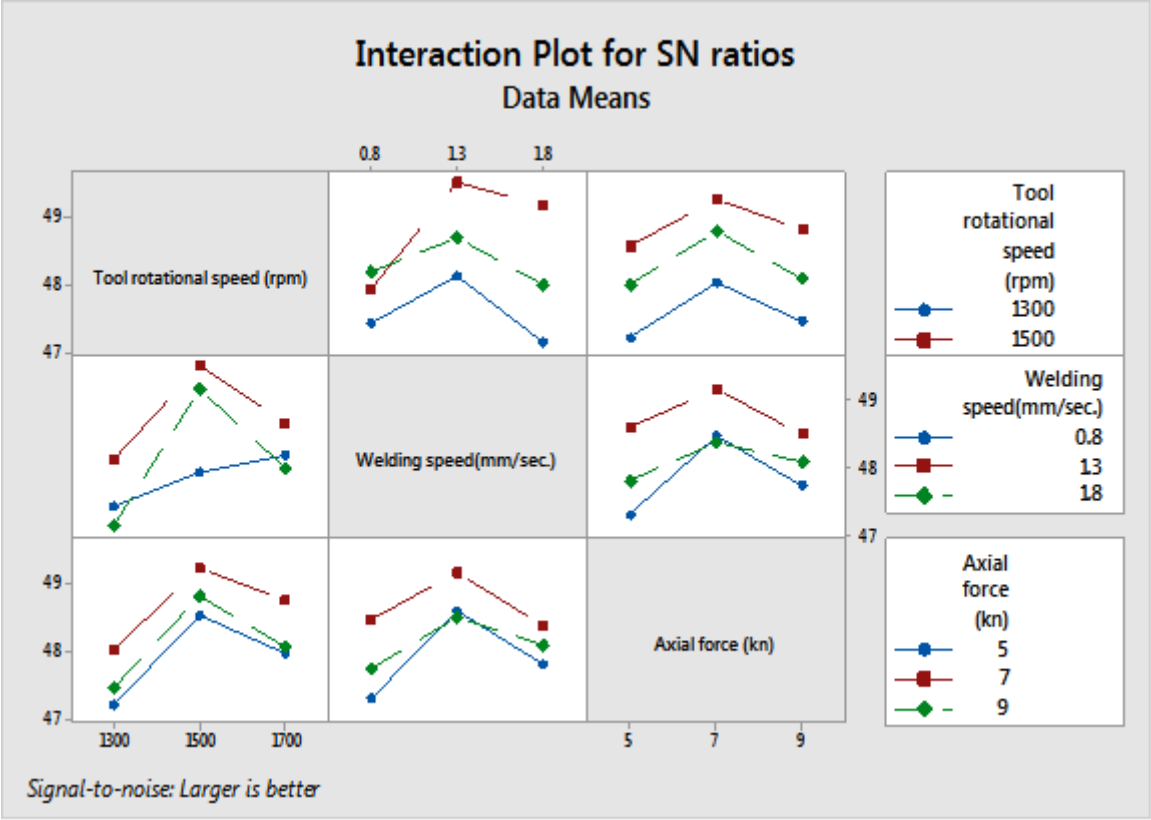

Figure 6.11 Interaction plot for tensile strength(S/N ratio)

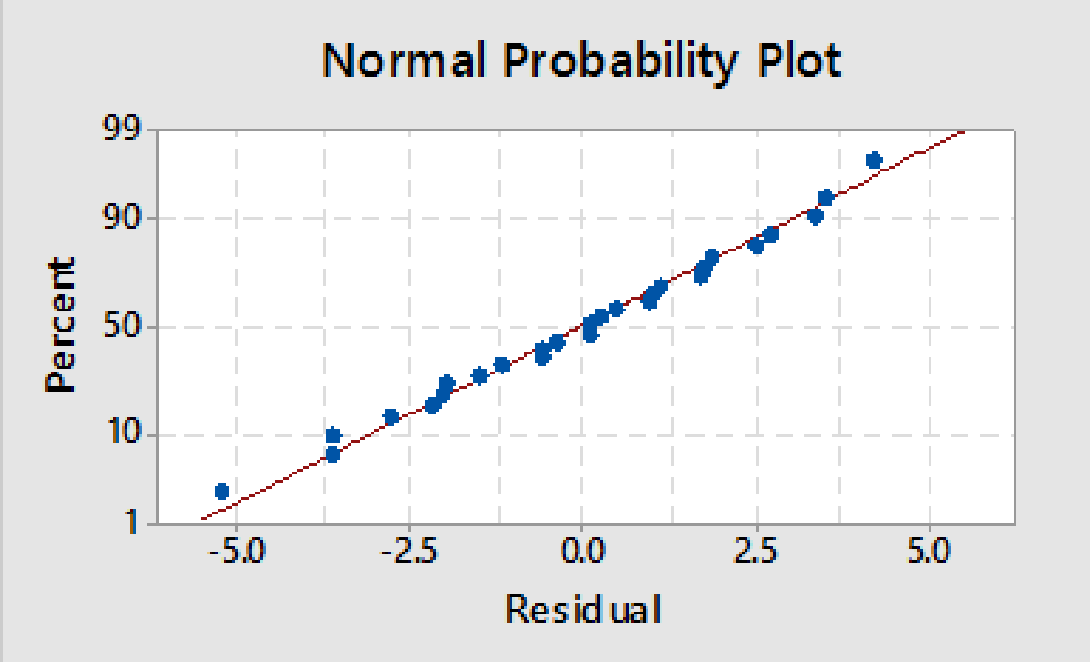

Figure 6.12 Normal probability plot of the residuals for tensile strength(Means)

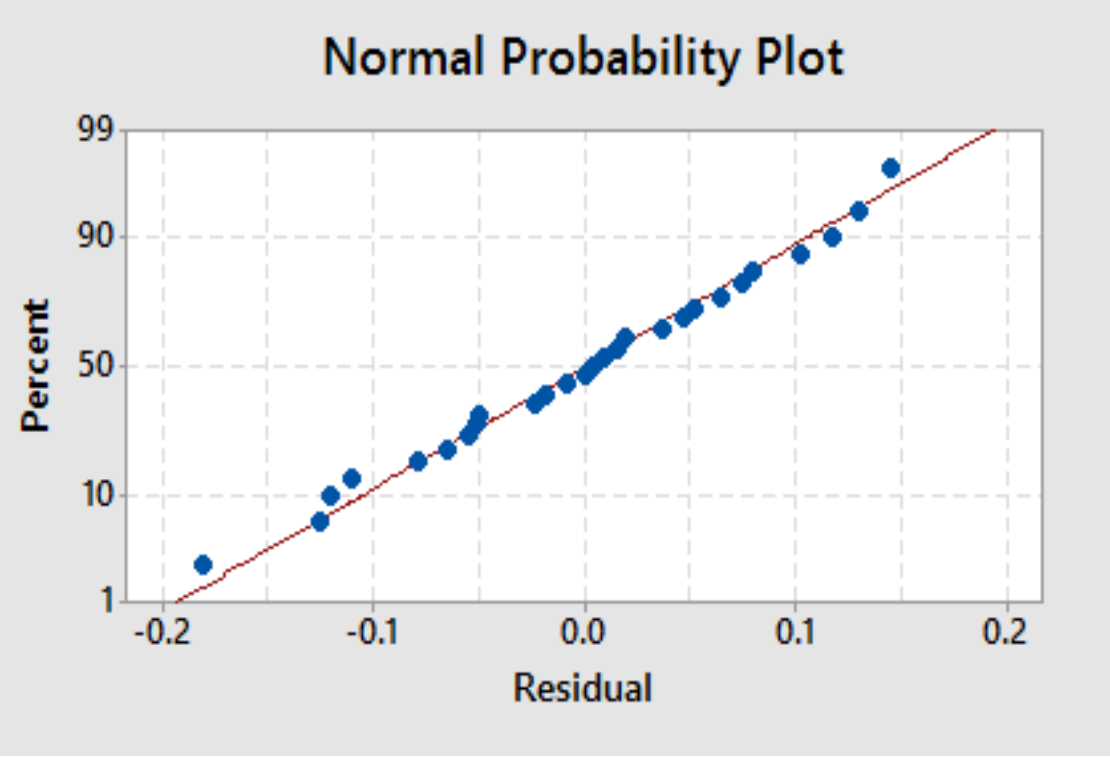

Figure 6.13 Normal probability plot of the residuals for tensile strength (S/N ratio)

6.2.2.7 Estimation of Optimum Performance Characteristic of Tensile Strength

As per Taguchi methodology, response table was used to calculate average tensile strength for each input process parameter at different levels. The calculated tensile strength for welding parameters at levels 1–3 is reported in Table 6.2. Larger tensile strength value corresponds to high quality performance. Therefore, optimal welding process parameters are corresponding to large value of tensile strength. Therefore, the combination of tool rotation at level 2, welding speed at level 2 and Axial force at level 2 tool geometry at level 1 which are showed in Table 6.7. Therefore, $A_2B_2C_2D_1$ with tool rotation speed of 1500 rpm, welding speed of 1.3 mm/sec, Axial force 7 kN and tool geometry of square are the optimum combination of process parameters for response optimization in welding of composites.

Table 6.7 Response table for Tensile Strength

Welding parameter	Level 1	Level 2	Level 3	Max-Min
Tool Rotation	237.98	**278.32**	259.57	40.34
Welding Speed	245.97	**274.93**	255.08	28.96
Axial force	249.55	**272.21**	255.22	22.66
Tool Geometry	**260.08**	258.84	258.06	2.02
Overall mean 258.99				

The confirmation experiments were conducted at the selected optimum levels ($A_2B_2C_2D_1$) to verify the quality characteristics for welding of AA7075/10%SiC composite using high speed steel tools. After the optimal level has been selected, one could predict the using the following equation [118].

$$\mu_{predicted} = \mu_m + \sum_{i=1}^{n}(\mu_o - \mu_m) \qquad (1)$$

Where, μ_m is the mean response, μ_o is the mean response at optimal level. Here, *n* is the number of factor that affects the response. It is very essential to perform a confirmatory experiment in the parameter design, particularly when less numbers of data are utilized for optimal. The confirmation experiment is used to verify the improvement in the quality characteristics [118].

$\mu_{predicted} = A_2+B_2+C_2-2T$

Where

T = overall mean = 258.99 MPa

Where, the values of A_2, B_2 and C_2 are taken from the Table 6.7.

A_2= Second level of tool rotational speed = 278.32 MPa

B_2 = Second level of welding speed = 274.93 MPa

C_2 = Second level of Axial force = 272.21MPa

Substituting the values of various terms in the above equation,

$\mu_{predicted\ mean\ grade} = 278.32+274.93+272.21 – 2*258.99$

$\mu_{predicted\ mean\ grade} = 307.48MPa$

The 95% confidence interval of confirmation experiment (Cl_{CE}) was calculated by following equation [89]:

$$Cl_{CE} = \sqrt{F_{\propto}(1, f_e)V_e\left[\frac{1}{n_{eff}} + \frac{1}{R}\right]} \qquad (2)$$

Where, V_e is the error variance, F_α (1, f_e) is the F-ratio at a confidence level of (1-α) against DOF, 1 and error degree of freedom f_e . α is confidence level [118].

$$n_{eff=} \frac{N}{1 + [Total\ DOF\ associated\ in\ the\ estimate\ of\ mean]}$$

Where, N is the total number of results = 81 and R is the sample size for confirmation experiment = 3.

$$n_{eff} = \frac{81}{1 + [2 + 2 + 2]}$$

$$n_{eff} = 11.571$$

Error variance V_e = 24.59

f_e= error, DOF= 6

F (1, 6) = 5.14 (Tabulated F-ratio) [118].

So, CL_{CE} = ±7.28

Predicted optimum range for confirmation experiment is:

Predicted T.S + CI_{CE}> Predicted T.S > Predicted T.S - CI_{CE}

307.48+7.28 > Predicted T.S > 307.48 -7.28

314.76 > Predicted T.S > 300.20

6.2.2.8 Verification of Optimal Parameters through Confirmation Test

Three confirmation experiments were conducted at the optimum level ($A_2B_2C_2D_1$) which is shown in table 6.8. From this table, the estimated error between predicted mean values and experimental average values are 1.10% for tensile strength. The average mean value of the tensile strength of welded joints is found within the confidence interval as reported in Table 6.8.

Table 6.8.Comparision of optimal predicted value and confirmation experiment result

Responses	Optimum welding Parameters		Confidence interval
	Predicted	Experimental	
Tensile strength(MPa)	307.48	304.40	314.76 > Predicted T.S > 300.20

The tensile strength of welded joints are lower than the base material. This is due to the welded joint formed as the combination of many thin layers in the direction of the joint thickness. It is fact that the different layers of plasticized metal have different mechanical properties because the cooling patterns of the layers are different. The upper layer is directly exposed in air, so its cooling rate is faster than the intermediate layers. The heat generations at different process parameters are not proper for different joints, which affects the weld quality.

6.2.3 Analysis of Percentage Elongation

The percentage elongation data were analyzed to determine the effect of friction stir welding process parameters. The experimental results were then transformed into means and signal to noise ratio which are given in table 6.9. The analysis of mean for each of experiments will give the better combination of process parameters levels that confirm that higher tensile strength achieved. The mean response refers to the average value of performance characteristics for each parameter at different levels. The mean response of raw data and S/N ratio of tensile strength for each parameter at level 1,2,3 were calculated and are shown in table 6.10 and table 6.11 respectively.

Table 6.9 Percentage Elongation and S/N ratio results of Friction Stir Welding

S.NO	Tool Rotational Speed(rpm)	Welding Speed(mm/sec.)	Axial Force(kn)	Tool Geometry	Percentage Elongation	S/N ratio(P.E)
1	1300	0.8	5	S	3.481	10.83
2	1300	0.8	7	H	3.799	11.59
3	1300	0.8	9	O	3.620	11.17
4	1300	1.3	5	H	3.753	11.49
5	1300	1.3	7	O	3.961	11.96
6	1300	1.3	9	S	3.704	11.37
7	1300	1.8	5	O	3.341	10.48
8	1300	1.8	7	S	3.745	11.47
9	1300	1.8	9	H	3.562	11.03
10	1500	0.8	5	H	3.599	11.12
11	1500	0.8	7	O	3.940	11.91
12	1500	0.8	9	S	3.741	11.46
13	1500	1.3	5	O	4.120	12.3
14	1500	1.3	7	S	4.481	13.03
15	1500	1.3	9	H	4.241	12.55
16	1500	1.8	5	S	4.102	12.26
17	1500	1.8	7	H	4.198	12.46
18	1500	1.8	9	O	4.122	12.3
19	1700	0.8	5	O	3.581	11.08
20	1700	0.8	7	S	4.105	12.27
21	1700	0.8	9	H	3.764	11.51
22	1700	1.3	5	S	3.951	11.93
23	1700	1.3	7	H	4.258	12.58
24	1700	1.3	9	O	3.883	11.78
25	1700	1.8	5	H	3.689	11.34
26	1700	1.8	7	O	3.870	11.75
27	1700	1.8	9	S	3.764	11.51

Table 6.10 Response Table for Means

Level	Rotational Speed	Welding Speed	Axial Force	Tool Geometry
1	3.663	3.737	3.735	3.897
2	4.06	4.039	4.04	3.874
3	3.874	3.821	3.822	3.826
Delta	0.398	0.302	0.304	0.071
Rank	1	3	2	4

Table 6.11 Response Table for S/N Ratio

Level	Rotational Speed	Welding Speed	Axial Force	Tool Geometry
1	11.27	11.44	11.43	11.79
2	12.15	12.11	12.11	11.74
3	11.75	11.62	11.63	11.64
Delta	0.89	0.67	0.69	0.16
Rank	1	3	2	4

The response table 6.10 and table 6.11 data is clearly graphically presented by figure 6.14 and figure 6.15 respectively. These graphs were plotted with the help of statistical software minitab 17. These graphs indicates that the tensile strength was maximum when rotational speed, welding speed, axial force are at level 2, and tool geometry at level 1, i.e. rotational speed 1500rpm, welding speed1.3mm/sec and axial force 7KN .

Figure 6.14 Effect of process parameters on percentage elongation (Main effects)

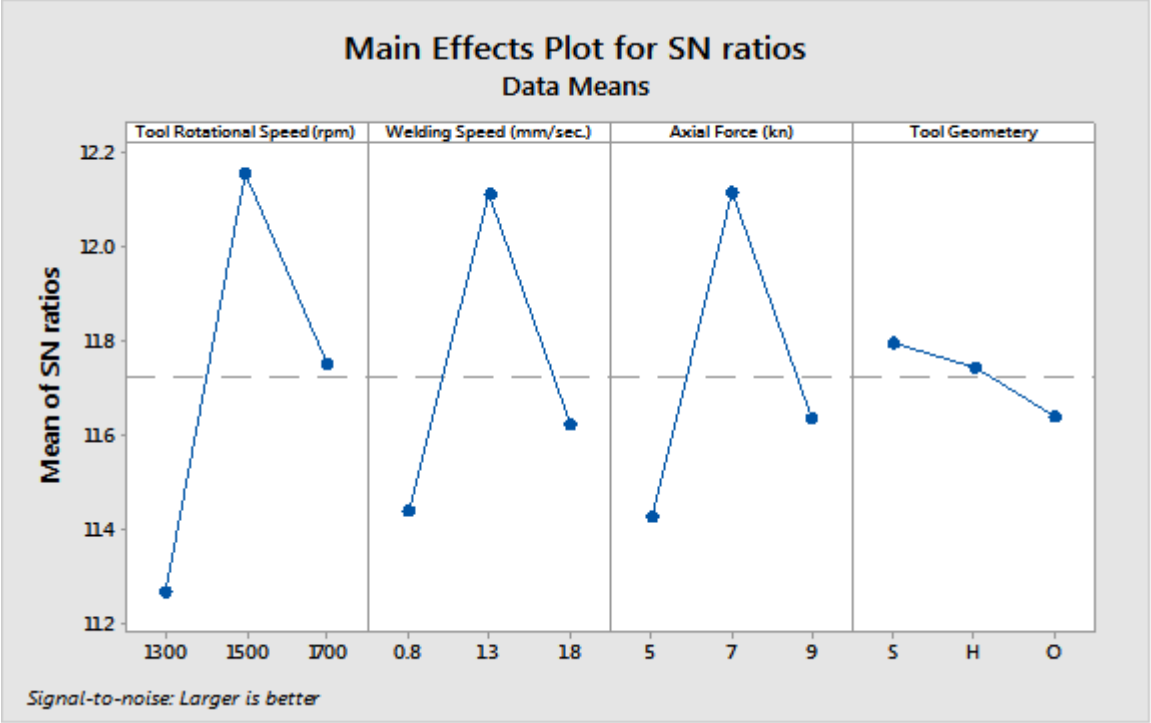

Figure 6.15 Effect of process parameters on percentage elongation (S/N Ratio)

6.2.3.1 Effect of Tool Rotation Speed on Percentage Elongation

Figure 6.14 and figure 6.15 shows the effect of rotational speed on percentage elongation. Above figure shows the different values of percentage elongation at different rotational speed. To generate a proper weld joint, moderate heat input is required. On such moderate heat input, the material will show minimal change in its mechanical properties as well as a defect free weld joint will be generated. This moderate heat input is achieved at 1500 r/min. At this speed, the grain structure of the material recrystallized and becomes fine and equalized. Therefore better percentage elongation achieved. At 700 rpm, insufficient heat is produced resulting the improper mixing of plasticized metal. Therefore, it leads to weld defects like flaws, gaps in the weld zone [36].While at 1700 rpm excess heat is produced cause lower percentage elongation achieved.

6.2.3.2 Effect of Welding Speed on Percentage Elongation

Figure 6.14 and figure 6.15 shows the effect of welding speed on percentage elongation of friction stir welded composite joint. The percentage elongation of FSW joint was low at the lower welding speed of 0.8 mm/s. The percentage elongation value was increased with increase in welding speed until the maximum of 1.3 mm/s. Further increase in welding speed decreased the percentage elongation of FSW joint.

6.2.3.3 Effect of Axial Force on Percentage Elongation

Figure 6.14 and figure 6.15 shows the effect of axial force on percentage elongation of friction stir welded composite joints. The lowest elongation was obtained at axial load of 5 kN and 9 kN. The percentage elongation of composite joint was increased with increase in axial load up to a maximum load of 7 kN. Further increase in axial load decreased the tensile elongation of the joint. During the FSW process, the rotation of tool produces a large amount of heat input which brings the metal to become very hot and plastic state. The axial force is more responsible for the plunge depth of the tool pin into the work piece [37].

6.2.3.4 Effect of Tool Pin Profile on Percentage Elongation

Figure 6.14 and 6.15 shows the different values of percentage elongation for different types of tool pin profile. It is observed that the square type tool pin profile gives the maximum value of percentage elongation The square type of tool pin profile produces good material stir quality during welding. Since, the tool has four edges, the point of each edge acts as an individual cutting tool that causes maximum deformation in the material. Hence, good surface finish and defect free joints are formed. Hexagonal and octagonal type tool pin profile produce insufficient mixing because tool pin is incapable of deforming appropriate material during rotation.

6.2.3.5 Analysis of Variance (ANOVA)

The ANOVA results for tensile strength of means and S/N ratio are given in table 6.12 and table 6.13 respectively. The purpose of ANOVA is to investigate the effect of process parameters on the tensile strength. ANOVA analysis was carried out for a level of significance of 5%, i.e. for 95% level of confidence. If the calculated F-ratio is more than the tabulated value i.e. 5.14 for parameter and 4.53 for interactions at confidence level, then the effect is significant. Percentage contribution represents the significant contribution on response. The Rotational Speed has maximum contribution (38.09 %) followed by Welding Speed (23.59%) and Axial force (23.82%). It can be seen from table 6.5 that Rotational speed and welding speed interaction has only significant effect of 12.08% contribution.

Table 6.12. Pooled ANOVA for means (Percentage Elongation)

Source	DOF	Seq SS	Adj SS	Adj MS	F Ratio	P	PC %
Rotational Speed	2	0.71201	0.71201	0.356006	94.07	0.000	38.09
Welding Speed	2	0.43804	0.43804	0.219021	57.87	0.000	23.59
Axial Force	2	0.4426	0.4426	0.221298	58.48	0.000	23.82
Tool Geometry	2	0.02343	0.02343	0.11714	3.1	0.119	
Rotational Speed* Axial Force	4	0.21321	0.21321	0.053302	14.08	0.003	12.08
Rotational Speed* Axial Force	4	0.00889	0.00889	0.00223	0.58	0.684	
Welding Speed* Axial Force	4	0.04152	0.04152	0.01038	2.74	0.13	
Residual Error	6	0.02271	0.02271	0.003784			2.40
Total	26	1.9024					100

S = 0.06166 R-Sq = 98.8% R-Sq(adj) = 94.8%

Table 6.13 Pooled ANOVA for S/N ratios (Percentage Elongation)

Source	DOF	Seq SS	Adj SS	Adj MS	F Ratio	P	PC %
Rotational Speed	2	3.55817	3.55817	1.77909	82.07	0.000	38.01
Welding Speed	2	2.16386	2.16386	1.08193	49.91	0.000	23.29
Axial Force	2	2.23898	2.23898	1.11949	51.65	0.000	24.08
Tool Geometry	2	0.11423	0.11423	0.05711	2.63	0.151	
Rotational Speed*Welding Speed	4	1.03617	1.03617	0.25904	11.95	0.005	11.85
Rotational Speed*Axial Force	4	0.05370	0.05370	0.01343	0.62	0.665	
Welding Speed* Axial Force	4	0.21576	0.21576	0.5394	2.49	0.153	
Residual Error	6	.13006	.13006	0.02168			2.74
Total	26	9.51093					100

6.2.3.6 Interaction Plot for Percentage Elongation

Figure 6.16 and figure 6.17 disclose pattern of line segments crossing each another or slight variation in the interaction plot paths, there is no actual 'disorder interaction' between rotational speed and welding speed or between rotational and axial force and profile plot paths crossed due to random variation. From the study of Table 6.5, it is apparent that potential of the model, R^2 is greater than 0.90. Normal probability plot of residuals as shown in figure 6.18 and figure 6.19, shows no drastic deviation with the normality. This result confirms the basic assumption used in analysis (errors are normally distributed).

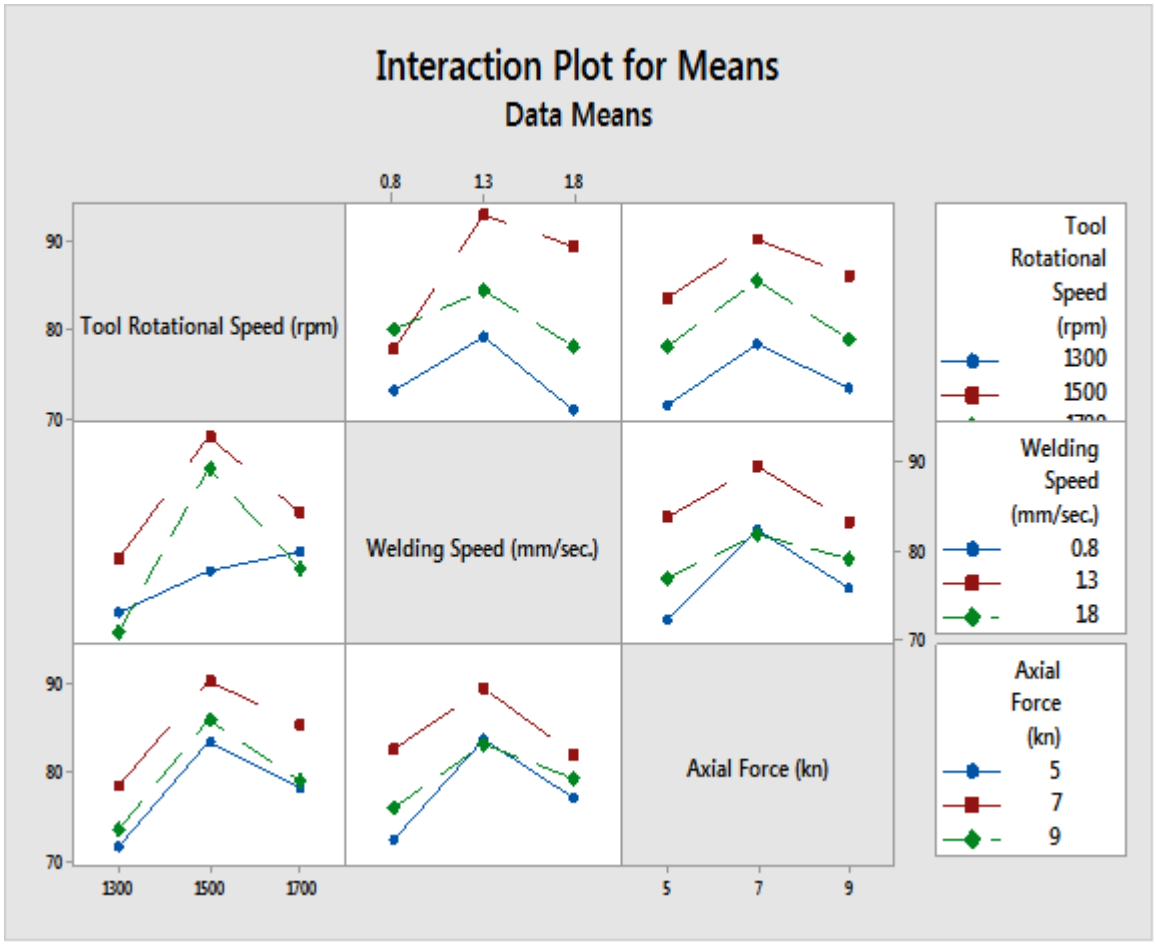

Figure 6.16 Interaction plot for Percentage Elongation (means)

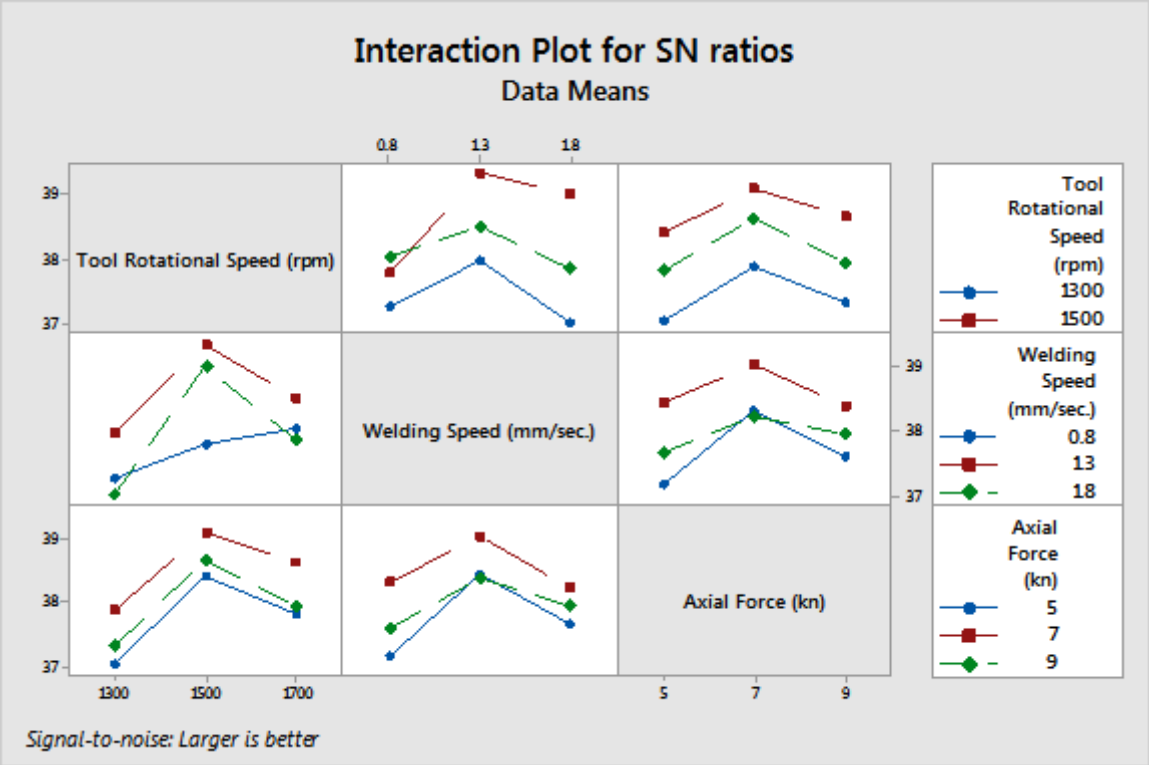

Figure 6.17 Interactions plots for Percentage Elongation (S/N Ratio)

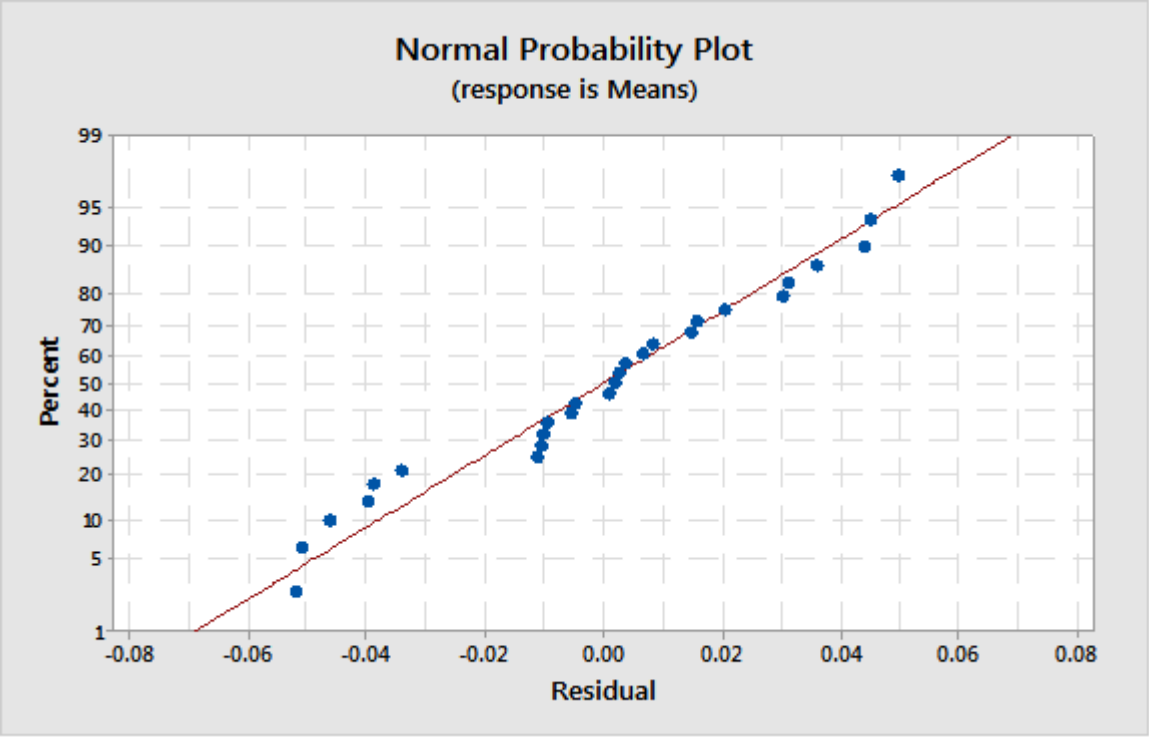

Figure 6.18 Normal probability plot residuals (Means)

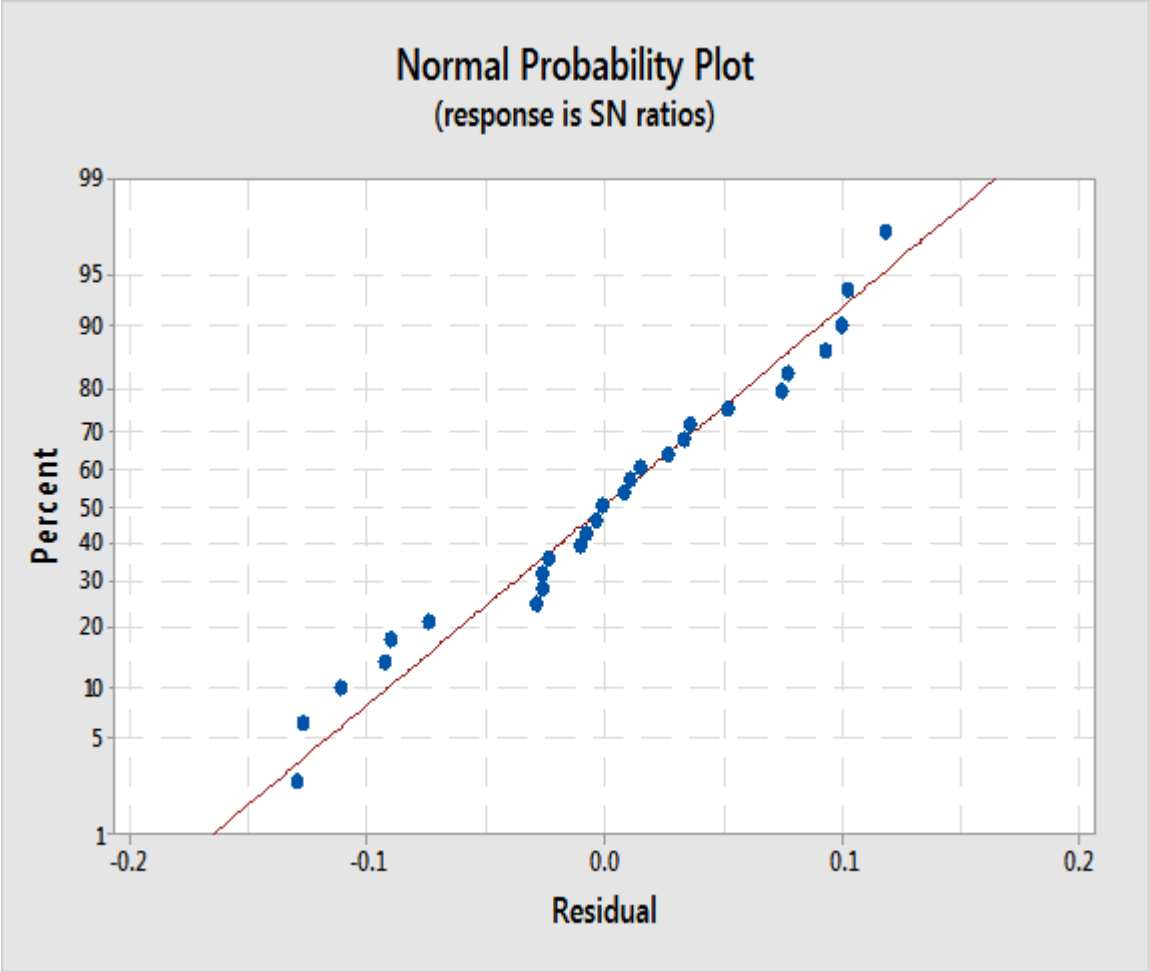

Figure 6.19 Normal probability plot residuals(S/N ratio)

6.2.3.7 Estimation of Optimum Performance Characteristic for Percentage Elongation

As per Taguchi methodology, response table was used to calculate percentage elongation for each input process parameter at different levels. The calculated percentage elongation for welding parameters at levels 1–3 is reported in Table 6.9. The combination of tool rotation at level 2,welding speed at level 2 and Axial force at level 2 tool geometry at level 1 which is shows in table 6.14. Therefore $A_2B_2C_2D_1$ with tool rotation speed of 1500 rpm, welding speed of 1.3 mm/sec, Axial force 7 kN and tool geometry of square are the optimum combination of process parameters for response optimization in welding of composites.

Table 6.14 Response table for Percentage Elongation

Welding parameter	Level 1	Level 2	Level 3	Max-Min
Tool Rotation	3.6628	**4.0603**	3.8738	.3975
Welding Speed	3.7366	**4.0391**	3.8213	.3025
Axial force	3.7351	**4.0396**	3.823	.3045
Tool Geometry	**3.8971**	3.8736	3.8264	.0707
Overall mean 3.8657				

The confirmation experiments were conducted at the selected optimum levels ($A_2B_2C_2D_1$) to verify the quality characteristics for drilling of AA7075/10%SiC composite using high speed steel tools. After the optimal level has been selected, one could predict the using the following equation [118]:

$$\mu_{predicted} = \mu_m + \sum_{i=1}^{n}(\mu_o - \mu_m)$$

Where, μ_m is the mean response, μ_o is the mean response at optimal level. Here, *n* is the number of factor that affects the response. It is very essential to perform a confirmatory experiment in the parameter design, particularly when less numbers of data are utilized for optimal. The confirmation experiment is used to verify the improvement in the quality characteristics. [118]

$\mu_{predicted} = A_2+B_2+C_2-2T$

Where

T = overall mean = 3.8657

Where, the values of A_2, B_2 and C_2 from table 6.14

A_2= Second level of tool rotational speed = 4.0603

B_2 = Second level of welding speed = 4.0391

C_2 = Second level of axial force = 4.0396

Substituting the values of various terms in the above equation,

$\mu_{predicted}$ = 4.0603+4.0391+4.0396 – 2*3.8657

$\mu_{predicted}$ = 4.3448

The 95% confidence interval of confirmation experiment (Cl_{CE}) was calculated by following equation [118]:

$$Cl_{CE} = \sqrt{F_{\propto}(1, f_e)V_e\left[\frac{1}{n_{eff}} + \frac{1}{R}\right]} \qquad (2)$$

Where, V_e is the error variance, F_{α} (1, f_e) is the F-ratio at a confidence level of (1-α) against DOF, 1 and error degree of freedom f_e. α is confidence level [118].

$$n_{eff} = \frac{N}{1 + [Total\ DOF\ associated\ in\ the\ estimate\ of\ mean]}$$

Where, N is the total number of results = 81 and R is the sample size for confirmation experiment = 3.

$$n_{eff} = \frac{81}{1 + [2 + 2 + 2]}$$

$$n_{eff} = 11.571$$

Error variance V_e = .00378

f_e= error DOF= 6

F (1, 6) = 5.14 (Tabulated F-ratio) [118].

So, CL_{CE} = ± .0903

Predicted optimum range for confirmation experiment is:

Predicted P.E + CI_{CE}> Predicted P.E > Predicted P.E - CI_{CE}

4.3448+.0903 > Predicted P.E > 4.3448 -.0903

4.4351 > Predicted P.E > 4.2545

6.2.3.8 Verification of Optimal Parameters Through Confirmation Test

Three confirmation experiments were conducted at the optimum level ($A_2B_2C_2D_1$) which are shown in table 6.15.The estimated error between predicted mean values and experimental average values are 1.31% for percentage of tensile elongation. The average mean value of percentage of elongation of welded joints is found within the confidence interval as reported in Table 6.15.

Table 6.15 Comparison of optimal predicted value and confirmation experiment result

Responses	Optimum welding Parameters		Confidence interval
	Predicted	Experimental	
Percentage of elongation	4.3448	4.2892	4.4351 > Predicted P.E > 4.2545

The percentage of tensile elongation of welded joints is lower than the base materials. This is due to the welded joint formed as the combination of many thin layers in the direction of the joint thickness. It is fact that the different layers of plasticized metal have different mechanical properties because the cooling patterns of the layers are different. The upper layer is directly exposed in air, so its cooling rate is faster than the intermediate layers. The heat generations at different process parameters are not proper for different joints, which affects the weld quality.

6.2.4 Analysis of Hardness

The hardness result shown in table 6.16. The mean response of raw data and S/N ratio of tensile strength for each parameter at level 1,2,3 were calculated and are given in table 6.17 and table 6.18 respectively.

Table 6.16. Hardness results of FSW joints

S.NO	Tool Rotational	Welding	Axial	Tool	Hardness (H.V)	S/N ratio
1	1300	0.8	5	S	90.55	39.1374
2	1300	0.8	7	H	100.9	40.0776
3	1300	0.8	9	O	95.17	39.5701
4	1300	1.3	5	H	101.78	40.1533
5	1300	1.3	7	O	108.98	40.747
6	1300	1.3	9	S	98.58	39.8755
7	1300	1.8	5	O	90.25	39.1089
8	1300	1.8	7	S	96.23	39.6664
9	1300	1.8	9	H	93.81	39.4446
10	1500	0.8	5	H	94.82	39.5383
11	1500	0.8	7	O	108.13	40.679
12	1500	0.8	9	S	100.09	40.0076
13	1500	1.3	5	O	116.64	41.3366
14	1500	1.3	7	S	125.95	42.004
15	1500	1.3	9	H	120.32	41.6068
16	1500	1.8	5	S	114.67	41.1891
17	1500	1.8	7	H	118.35	41.4636
18	1500	1.8	9	O	115.49	41.2505
19	1700	0.8	5	O	100.65	40.0559
20	1700	0.8	7	S	113.29	41.0842
21	1700	0.8	9	H	101.00	40.0867
22	1700	1.3	5	S	108.59	40.7157
23	1700	1.3	7	H	115.06	41.2185
24	1700	1.3	9	O	105.8	40.4899
25	1700	1.8	5	H	100.85	40.0735
26	1700	1.8	7	O	105.3	40.4482
27	1700	1.8	9	S	101.02	40.0877

Table 6.17 Response Table for Means

Process parameters	Level	Rotational Speed	Welding Speed	Axial Force	Tool Geometry
Average value of hardness	L1	97.36	100.51	102.09	105.44
	L2	112.72	111.30	110.24	105.21
	L3	105.73	104.00	103.47	105.16
	Max.- min.	15.36	10.79	8.16	0.28
	Rank	1	2	3	4

Table 6.18 Response Table for S/N Ratio

Process parameters	Level	Rotational Speed	Welding Speed	Axial Force	Tool Geometry
Average value of hardness	L1	39.75	40.03	40.15	40.42
	L2	41.01	40.91	40.82	40.41
	L3	40.47	40.30	40.27	40.41
	Max.- min.	1.25	0.88	0.68	0.01
	Rank	1	2	3	4

The response table 6.17 and table 6.18 data is clearly graphically presented by figure 6.20 and figure 6.21 respectively. These graphs were plotted with the help of statistical software minitab 17. These graphs indicates that the hardness was maximum when rotational speed, welding speed, axial force are at level 2, and tool geometry at level 1, i.e. rotational speed 1500rpm, welding speed1.3 mm/sec and axial force 7 KN.

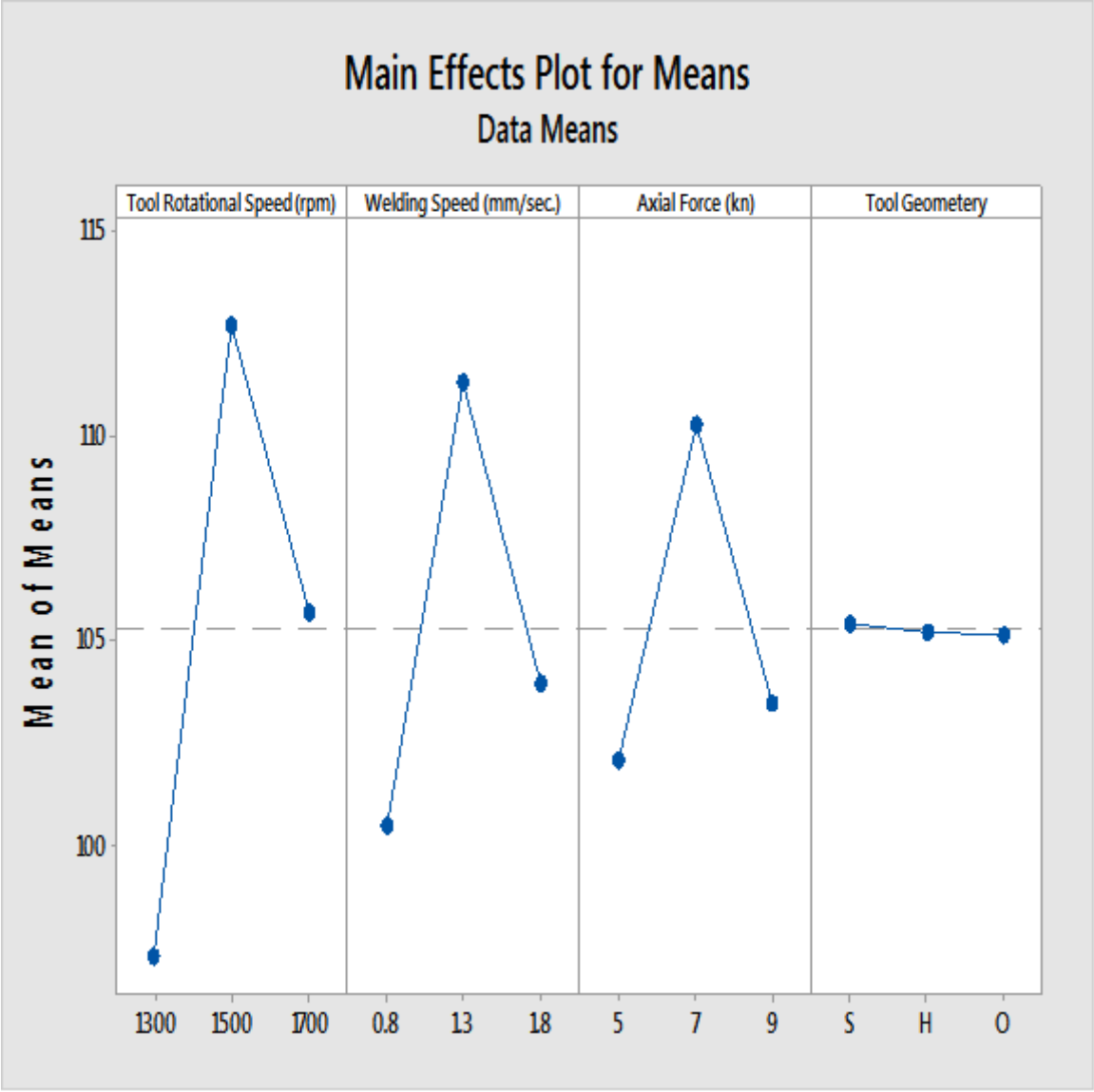

Figure 6.20 Effects of Process Parameters of Hardness (Means)

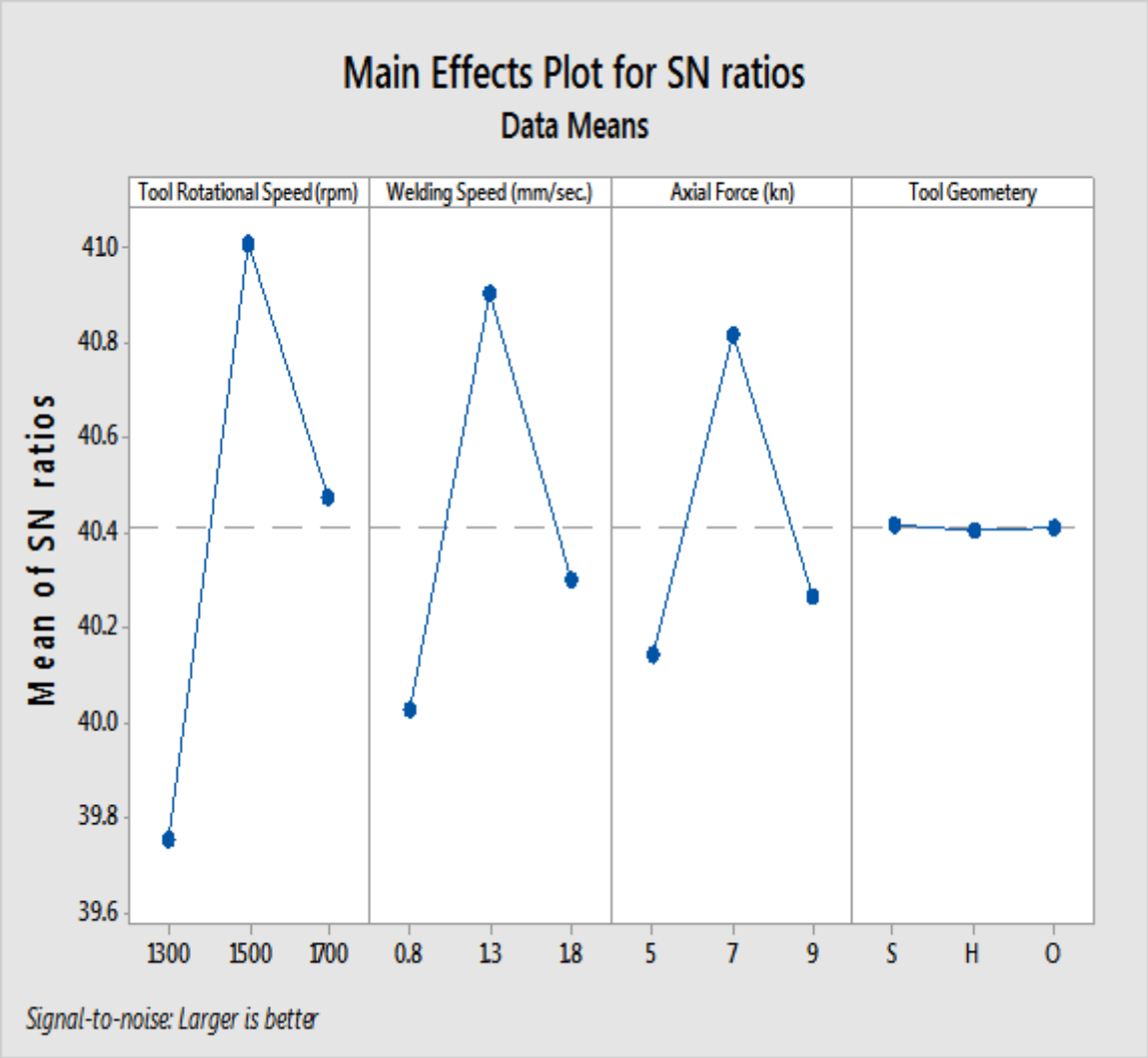

Figure 6.21 Effects of Process Parameters of Hardness (S/N ratio)

6.2.4.1 Effect of Rotational Speed on Hardness

Figure 6.20 and figure 6.21 shows the effect of tool rotational speed on hardness of friction stir welded AA7075/10%wt. composite welded joints. To generate a proper weld joint, moderate heat input is required. On such moderate heat input, the material will show minimal change in its mechanical properties as well as a defect free weld joint will be generated. This moderate heat input is achieved at 1500 rpm. At this speed, the grain structure of the material recrystallized and becomes fine and equalized. At 1300 rpm, insufficient heat is produced resulting the improper mixing of plasticized metal. Therefore, it leads to weld defects like flaws, gaps in the weld zone [77]. While at 1700

r/min excess heat is produced, which causes turbulence in the plasticized material that further leads to tunnel defect at weld nugget.

6.2.4.2 Effect of Welding Speed on Hardness

Figure 6.20 and figure 6.21 shows the effect of welding speed on hardness of friction stir welded composite joint. The hardness of FSW joint was low at the lower welding speed of 0.8 mm/s. The hardness value was increased with increase in welding speed until the maximum of 1.3 mm/s. Further increase in welding speed decreased the hardness of friction stir welding joints. It can be observed that a higher welding speed decreases the frictional heat input to the work material.

6.2.4.3 Effect of Axial Force on Hardness

Figure 6.20 and figure 6.21 shows the effect of axial force on hardness of friction stir welded composite joints. The lowest hardness was obtained at axial load of 5 KN and 9 KN. The hardness of composite joint was increased with increase in axial load up to a maximum load of 7 KN. Further increase in axial load decreased the hardness of the joint. During the friction stir welding process, the rotation of tool produces a large amount of heat input which brings the metal to become very hot and plastic state.

6.2.4.4 Effect of Tool Pin Geometry on Hardness

Figure 6.20 and figure 6.21 shows the different values of hardness for different types of tool pin geometry. It is observed that the square type tool pin profile gives the maximum value of tensile hardness. The square type of tool pin geometry produces good material stir quality during welding. Since, the tool has four edges, the point of each edge acts as an individual cutting, that causes maximum deformation in the material. Hence, good surface finish and defect free joints are formed. Hexagonal and octagonal type tool pin profile produce insufficient mixing because tool pin is incapable of deforming appropriate material during rotation.

6.2.4.5 Analysis of Variance (ANOVA)

The ANOVA results for hardness of means and S/N ratio are given in table 6.19 and 6.20 respectively. The purpose of ANOVA is to investigate the effect of process parameters and their influence on the hardness. ANOVA analysis was carried out for a level of significance of 5%, i.e. for 95% level of confidence. If the calculated F-ratio is more than the tabulated value i.e. 5.14 for parameter and 4.53 for interactions at confidence level, then the effect is significant. Table 6.19 Tables clearly shows that Rotational Speed has maximum contribution (45.22%) followed by Welding Speed (23.30%) and Axial force (14.74%). It can be seen from table 6.5 that rotational speed and welding speed interaction has only significant influence of 15.15% compared to other interactions.

Table 6.19 Pooled ANOVA for Means (Hardness)

	DOF	Seq SS	Adj SS	Adj MS	F Ratio	P	PC %
Rotational Speed	2	1064.14	1064.14	532.072	172.05	0.000	45.22
Welding Speed	2	545.65	545.65	272.823	88.22	0.000	23.30
Axial Force	2	342.81	342.81	171.407	55.43	0.000	14.74
Tool Geometry	2	0.41	0.41	0.206	0.07	0.936	
Tool Rotational Speed* Welding speed	4	346.19	346.19	86.549	27.99	0.001	15.15
Rotational Speed* Axial Force	4	14.02	14.02	3.504	1.13	0.424	
Welding Speed* Axial Force	4	55.76	55.76	13.939	4.51	0.051	
Residual Error	6	18.56	18.56	3.093			1.56
Total	26	2387.54					100

Table 6.20 Pooled ANOVA for SN ratios (Hardness)

Source	DOF	Seq SS	Adj SS	Adj MS	F Ratio	P	PC %
Rotational Speed	2	7.1382	7.1382	3.5691	158.08	0.000	45.36
Welding Speed	2	3.6342	3.6342	1.8171	80.48	0.000	23.23
Tilt Angle	2	2.3292	2.3292	1.1645	51.58	0.000	14.99
Tool Geometry	2	0.0007	0.0007	0.00034	0.01	0.985	
Rotational Speed*Welding Speed	4	2.2374	2.2374	0.55934	24.77	0.001	14.69
Rotational Speed*Axial Force	4	0.0949	0.0949	0.02373	1.05	0.455	
Welding Speed* Axial Force	4	0.4138	0.4138	0.10344	4.58	0.049	
Residual Error	6	.1355	.1355	0.02258			1.70
Total	26	15.9838					100

6.2.4.6 Interaction Plots for Hardness

Figure 6.22 and figure 6.23 disclose pattern of line segments crossing each another or slight variation in the interaction plot paths, there is no actual 'disorder interaction' between rotational speed and welding speed or between rotational and axial force and profile plot paths crossed due to random variation. From the study of Table 6.20, it is apparent that potential of the model, R^2 is greater than 0.90. Normal probability plot of residuals as shown in figure 6.24 and figure 6.25, shows no drastic deviation with the normality. This result confirms the basic assumption used in analysis (errors are normally distributed).

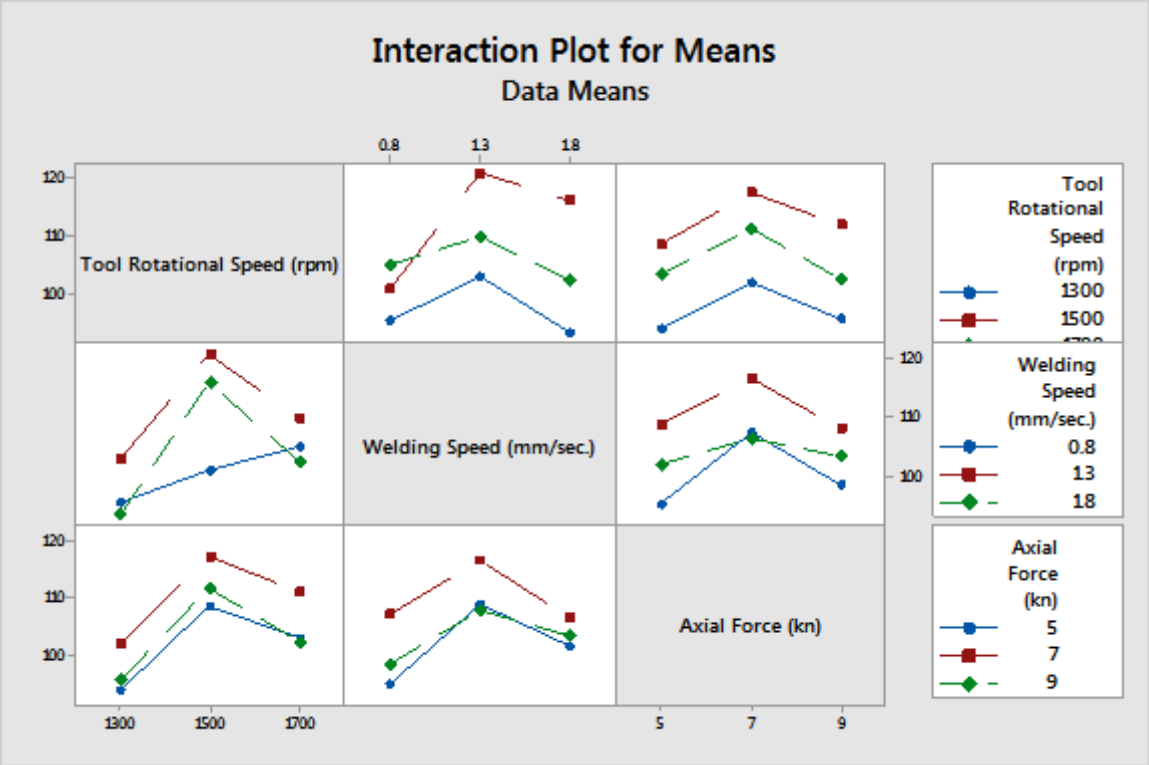

Figure 6.22 Interaction plot for hardness (Means)

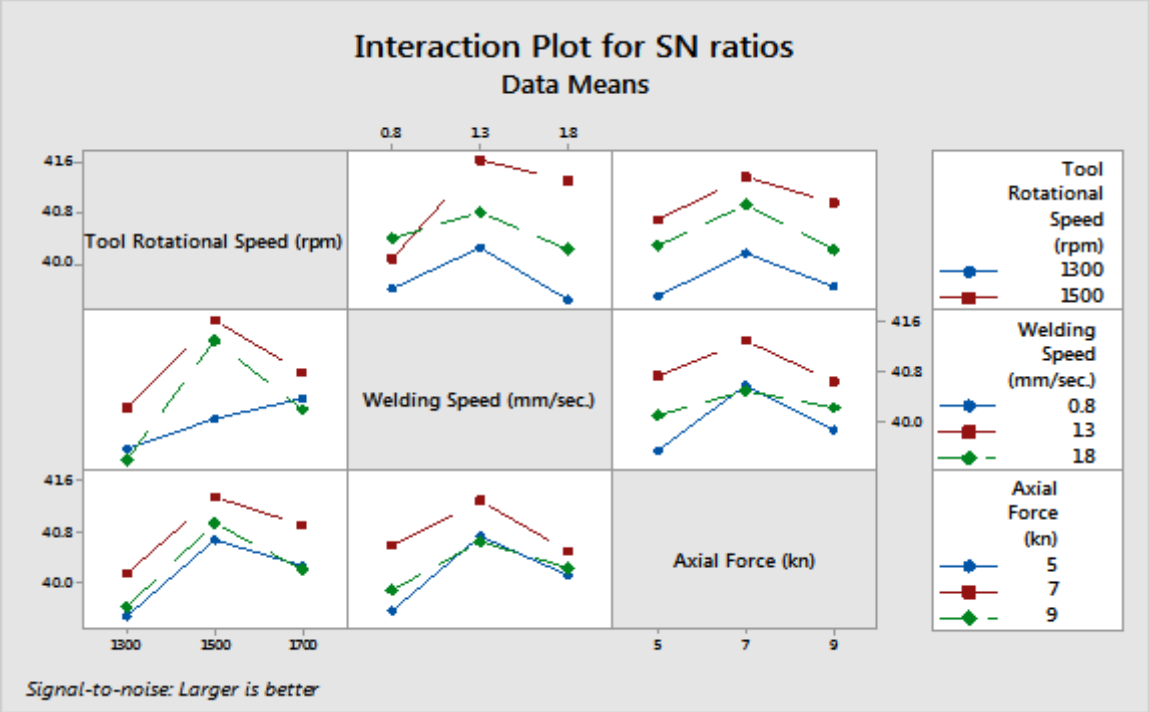

Figure 6.23 Interaction plot for hardness (S/N Ratio)

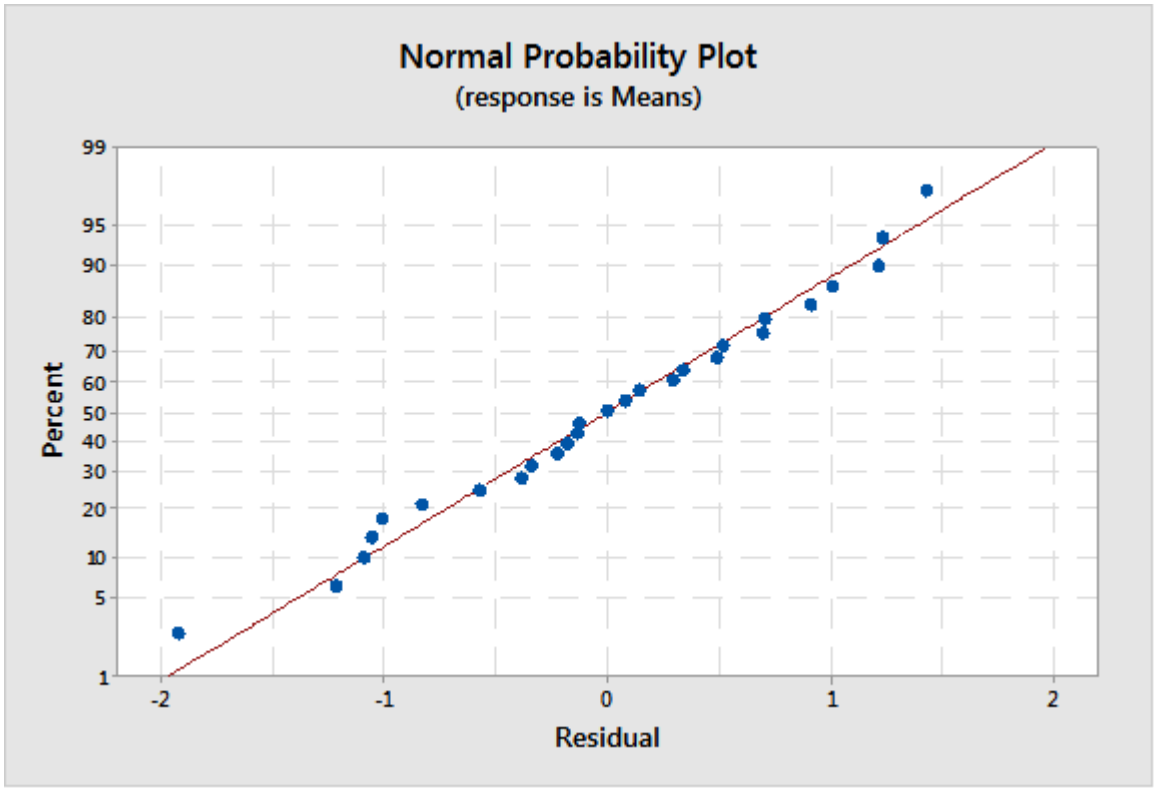

Figure 6.24 Normal probability plot of the residuals for hardness

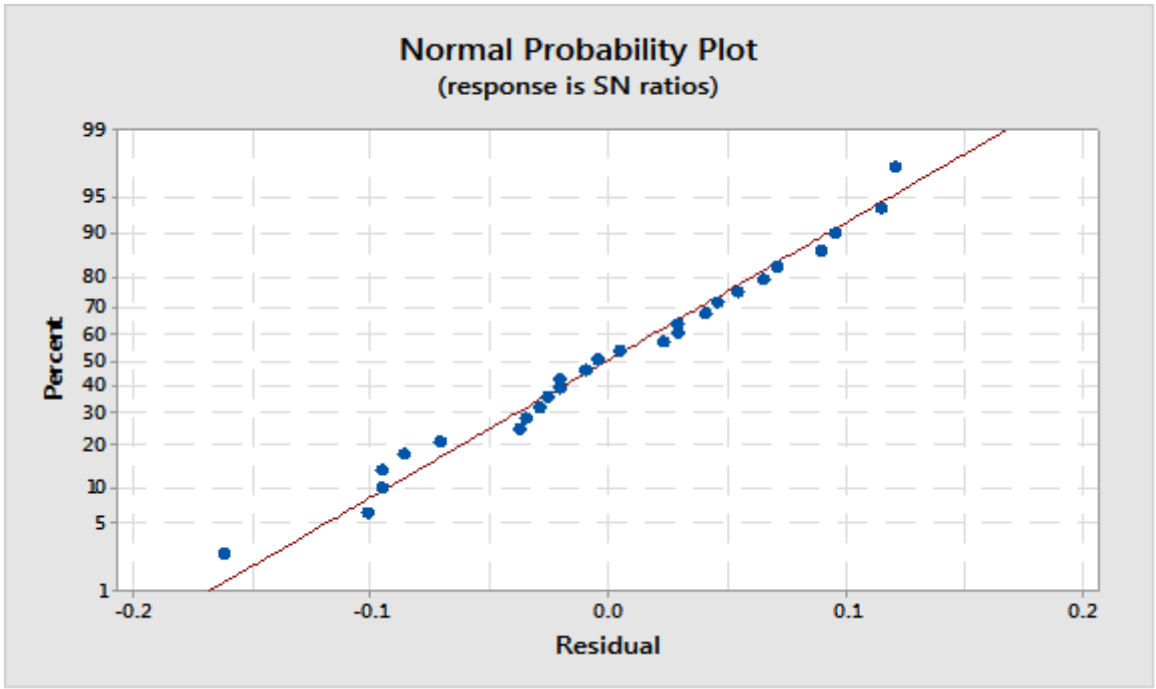

Figure 6.25 Normal probability plot of the residuals for hardness

6.2.4.7 Estimation of Optimum Performance Characteristic for Hardness

As per Taguchi methodology, response table was used to calculate average hardness for each input process parameter at different levels. The calculated hardness for welding parameters at levels 1–3 is reported in table 6.16. The combination of tool rotation at level 2,welding speed at level 2 and Axial force at level 2 tool geometry at level 1 which is shows in table 6.21. Therefore $A_2B_2C_2D_1$ with tool rotation speed of 1500 rpm, welding speed of 1.3 mm/sec, Axial force 7 kN and tool geometry of square are the optimum combination of process parameters for response optimization in welding of composites.

Table 6.21 - Response table for Hardness

Welding parameter	Level 1	Level 2	Level 3	Max-Min
Tool Rotation	97.3611	**112.7177**	105.6466	15.3566
Welding Speed	100.5111	**111.3000**	103.9966	10.7889
Axial force	102.0888	**110.2355**	103.4755	8.1467
Tool Geometry	**105.4411**	105.2100	105.1166	0.3245
Overall mean	105.2583			

The confirmation experiments were conducted at the selected optimum levels ($A_2B_2C_2D_1$) to verify the quality characteristics for friction stir welding of Al7075/10%SiC composite using high speed steel tools. After the optimal level has been selected, one could predict the using the following equation [118]:

$$\mu_{predicted} = \mu_m + \sum_{i=1}^{n}(\mu_o - \mu_m) \qquad (1)$$

Where, μ_m is the mean response, μ_o is the mean response at optimal level. Here, *n* is the number of factor that affects the response. It is very essential to perform a confirmatory experiment in the parameter design, particularly when less numbers of data are utilized for optimal. The confirmation experiment is used to verify the improvement in the quality characteristics.

$\mu_{predicted} = A_2+B_2+C_2-2T$

Where

T = overall mean = 105.2583

Where, the values of A_2, B_2 and C_2 are taken from the Table 6.21.

A_2= Second level of tool rotational speed = 112.7177

B_2 = Second level of welding speed = 111.300

C_2 = Second level of tilt angle = 110.2355

Substituting the values of various terms in the above equation,

$\mu_{predicted} = 112.7177+111.300+110.2355 – 2*105.2583$

$\mu_{predicted} = 123.736$

The 95% confidence interval of confirmation experiment (Cl_{CE}) was calculated by following equation [Ref 89]:

$$Cl_{CE} = \sqrt{F_{\propto}(1, f_e)V_e\left[\frac{1}{n_{eff}} + \frac{1}{R}\right]} \qquad (2)$$

Where, V_e is the error variance, F_α (1, f_e) is the F-ratio at a confidence level of (1-α) against DOF, 1 and error degree of freedom f_e . α is confidence level [118].

$$n_{eff} = \frac{N}{1 + [Total\ DOF\ associated\ in\ the\ estimate\ of\ mean]}$$

Where, N is the total number of results = 81 and R is the sample size for confirmation experiment = 3.

$$n_{eff} = \frac{81}{1 + [2 + 2 + 2]}$$

$$n_{eff} = 11.571$$

Error variance V_e = 3.093

f_e= error DOF= 6

F (1, 6) = 5.14 (Tabulated F-ratio) [118].

So, CL_{CE} = ± 2.58

Predicted optimum range for confirmation experiment is:

Predicted H.V + CI_{CE}> Predicted H.V > Predicted H.V - CI_{CE}

123.736+2.58 > Predicted H.V > 123.736 -2.58

126.316 > Predicted H.V > 121.156

6.2.4.8 Verification of Optimal Parameters through Confirmation Test

Three confirmation experiments were conducted at the optimum level ($A_2B_2C_2D_1$) which is shown in table 6.22. From this table, the estimated error between predicted mean values and experimental average values 1.17% for hardness. The average mean value of hardness of welded joints is found within the confidence interval as reported in Table 6.22

Table 6.22 Comparison of optimal predicted value and confirmation experiment result

Responses	Optimum welding Parameters		Confidence interval
	Predicted	Experimental	
Hardness	123.736	122.273	126.316 > Predicted H.V > 121.156

The hardness of welded joints are lower than the base materials. This is due to the welded joint formed as the combination of many thin layers in the direction of the joint thickness. It is fact that the different layers of plasticized metal have different mechanical properties because the cooling patterns of the layers are different. The upper layer is directly exposed in air, so its cooling rate is faster than the intermediate layers. The heat generations at different process parameters are not proper for different joints, which affects the weld quality.

6.2.5 Analysis of Welded Joint Efficiency (J.E)

The welded Joint Efficiency (J.E) data were analyzed to determine the effect of friction stir welding process parameters. The experimental results were then transformed into means and signal to noise ratio which are given in table 6.23. The analysis of mean for each of experiments will give the better combination of process parameters levels that confirm that higher welded joint efficiency (J.E) achieved. The mean response refers to the average value of performance characteristics for each parameter at different levels. The mean response of raw data and S/N ratio of welded joint efficiency for each

parameter at level 1,2,3 were calculated and are given in table 6.24 and table 6.25 respectively.

Table 6.23 Results of Welded Joint Efficiency (J.E) of FSW joints

S.NO	Tool Rotational Speed	Welding Speed	Axial Force	Tool Geometry	Joint Efficiency (J.E)	S/N ratio
1	1300	0.8	5	S	68.88	36.7621
2	1300	0.8	7	H	77.61	37.7988
3	1300	0.8	9	O	73.21	37.2913
4	1300	1.3	5	H	78.29	37.8744
5	1300	1.3	7	O	83.83	38.4682
6	1300	1.3	9	S	75.83	37.5967
7	1300	1.8	5	O	67.29	36.559
8	1300	1.8	7	S	74.02	37.3876
9	1300	1.8	9	H	71.39	37.0727
10	1500	0.8	5	H	72.94	37.2594
11	1500	0.8	7	O	83.18	38.4001
12	1500	0.8	9	S	76.99	37.7288
13	1500	1.3	5	O	89.72	39.0577
14	1500	1.3	7	S	96.88	39.7251
15	1500	1.3	9	H	92.55	39.328
16	1500	1.8	5	S	88.21	38.9102
17	1500	1.8	7	H	91.04	39.1847
18	1500	1.8	9	O	88.83	38.9717
19	1700	0.8	5	O	75.11	37.5142
20	1700	0.8	7	S	87.15	38.8053
21	1700	0.8	9	H	77.69	37.8078
22	1700	1.3	5	S	83.53	38.4368
23	1700	1.3	7	H	88.51	38.9396
24	1700	1.3	9	O	81.39	38.211
25	1700	1.8	5	H	75.7	37.582
26	1700	1.8	7	O	81	38.1694
27	1700	1.8	9	S	77.7	37.8089

The response table 6.24 and table 6.25 data is clearly graphically presented by figure 6.26 and figure 6.27 respectively. These graphs were plotted with the help of statistical software Minitab 17. These graphs indicates that the hardness was maximum when rotational speed, welding speed, axial force are at level 2, and tool geometry at level 1, i.e. rotational speed 1500rpm, welding speed1.3mm/sec, axial force 7kn and tool geometry is square.

Table 6.24 Response Table for Means

Level	Rotational Speed	Welding Speed	Axial Force	Tool Geometry
L1	239.1	247.1	249.6	260.1
L2	278.3	274.8	272.2	258.8
L3	259.6	255.1	255.2	258.1
Max.- Min.	39.2	27.7	22.7	2
Rank	1	2	3	4

Table 6.25 Response Table for S/N ratio

Level	Rotational Speed	Welding Speed	Axial Force	Tool Geometry
L1	47.55	47.84	47.9	48.26
L2	48.86	48.76	48.67	48.22
L3	48.27	48.09	48.11	48.2
Max.- Min.	1.31	0.92	0.77	0.06
Rank	1	2	3	4

Figure 6.26 Effects of Process Parameters on Joint Efficiency (Main effects)

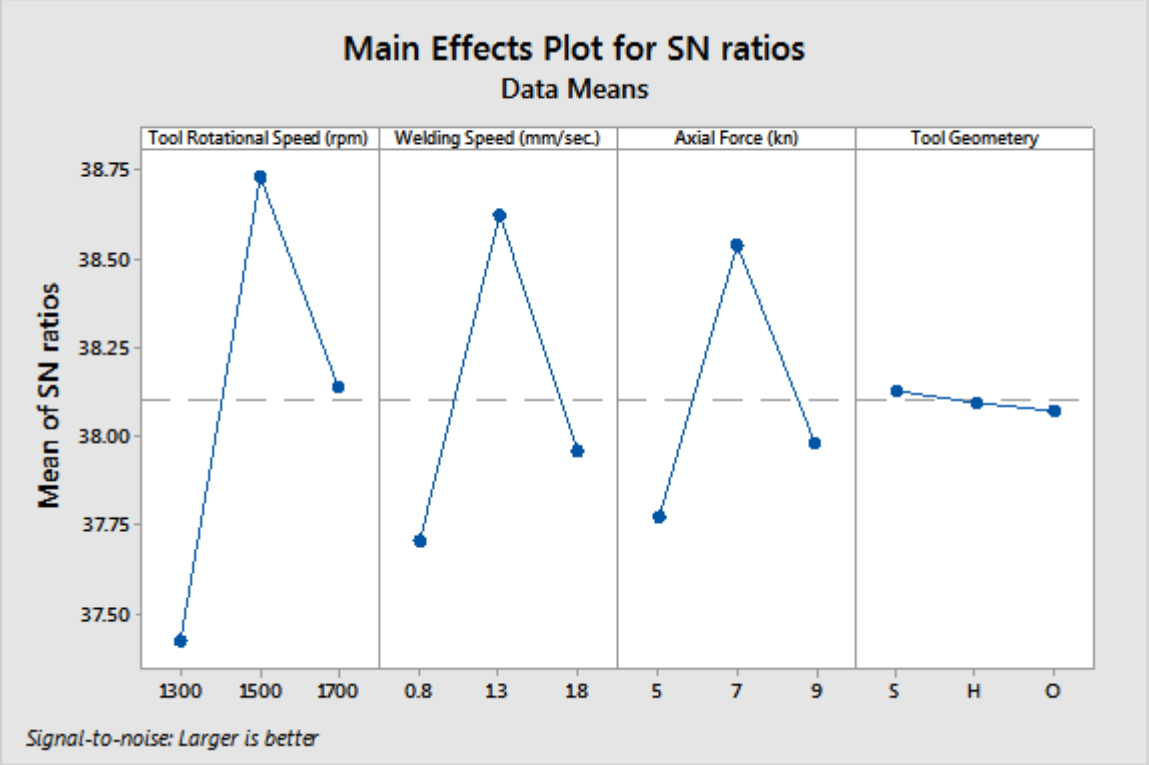

Figure 6.27 Effects of Process Parameters on joint efficiency (S/N ratio)

6.2.5.1 Effect of Rotational Speed on Joint Efficiency

Figure 6.26 and figure 6.27 shows the effect of tool rotational speed on joint efficiency of friction stir welded AA7075/10%wt.SiC composite joints. The maximum joint efficiency was obtained at the rotational speed of 1500 rpm. At a lower rotational speed (1300 rpm) and higher rotational speed (1700 rpm), the joint efficiency of joint was poor. When the rotational speed was increased from 1300 rpm, correspondingly the joint efficiency also increased and reached a maximum at 1500 rpm.

6.2.5.2 Effect of Welding Speed on Joint Efficiency

Figure 6.26 and figure 6.27 shows the effect of welding speed on joint efficiency of friction stir welded AA7075-10%wt.SiC composite joints. The joint efficiency of FSW joint was low at the lower welding speed of 0.8 mm/s. The joint efficiency was increased with increase in welding speed until the maximum of 1.3 mm/s. Further increase in welding speed decreased the joint efficiency of friction stir welded AA7075-10%wt.SiC composite joint.

6.2.5.3 Effect of Axial Force on Joint Efficiency

Figure 6.26 and figure 6.27 shows the effect of axial force on joint efficiency of friction stir welded AA7075/10%wt.SiC composite joints. The lowest strength was obtained at axial load of 5 kN and 9 kN. The joint efficiency of composite joint was increased with increase in axial load up to a maximum load of 7 kN. Further increase in axial load decreased the tensile strength of the joint.

6.2.5.4 Effect of Tool Pin Profile on Joint Efficiency

Figure 6.26 and figure 6.27 shows the different values of joint efficiency for different types of tool pin profile. It is observed that the square type tool pin profile gives the maximum value of joint efficiency. The square type of tool pin profile produces good material stir quality during welding. Since, the tool has four edges, the point of each edge acts as an individual cutting tool that causes maximum deformation in the material. Hence, good surface finish and defect free joints are formed. Hexagonal and octagonal type tool pin profile produce insufficient mixing because tool pin is incapable of deforming appropriate material during rotation.

6.2.5.5 Analysis of Variance (ANOVA)

The ANOVA results for Joint Efficiency of means and S/N ratio are given in table 6.26 and table 6.27 respectively. The purpose of ANOVA is to investigate the effect of process parameters and their influence on the tensile strength. ANOVA analysis was carried out for a level of significance of 5%, i.e. for 95% level of confidence. If the calculated F-ratio is more than the tabulated value i.e. 5.14 for parameter and 4.53 for interactions at confidence level, then the effect is significant. Percentage contribution gives the significant contribution on response. Tables clearly shows that Rotational Speed has maximum contribution (44.26%) followed by Welding Speed (23.57%) and Axial force (16.19%).

Table 6.26 Pooled ANOVA for Means (Joint Efficiency)

Source	DOF	Seq SS	Adj SS	Adj MS	F Ratio	P	% PC
Rotational Speed	2	672.54	672.54	336.272	140.9	0	44.26
Welding Speed	2	356.05	356.05	178.027	74.6	0	23.57
Axial Force	2	243.01	243.01	121.504	50.91	0	16.19
Tool Geometry	2	1.8	1.8	0.901	0.38	0.701	
Rotational Speed*Welding Speed	4	206.18	206.18	51.545	21.6	0.001	14.09
Rotational Speed* Axial Force	4	4.7	4.7	1.174	0.49	0.743	
Welding Speed* Axial Force	4	35.88	35.88	8.97	3.76	0.073	
Residual Error	6	14.32	14.32	2.387			1.87
Total	26	1534.49					100

Table 6.27- Pooled ANOVA for SN ratios (Joint Efficiency)

Source	DOF	Seq SS	Adj SS	Adj MS	F Ratio	P	% PC
Rotational Speed	2	7.7023	7.70234	3.85117	128.48	0	44.22
Welding Speed	2	4.0548	4.05477	2.02739	67.64	0	23.44
Axial Force	2	2.8523	2.85229	1.42615	47.58	0	16.59
Tool Geometry	2	0.0152	0.01517	0.00759	0.25	0.784	
Rotational Speed*Welding Speed	4	2.2855	2.28549	0.57137	19.06	0.001	13.70
Rotational Speed* Axial Force	4	0.0625	0.06253	0.01563	0.52	0.725	
Welding Speed* Axial Force	4	0.4679	0.46788	0.11697	3.9	0.068	
Residual Error	6	0.1798	0.17984	0.02997			2.04
Total	26	17.603					100

6.2.5.6 Interaction Plots for Joint Efficiency

Figure 6.28 and figure 6.29 disclose pattern of line segments crossing each another or slight variation in the interaction plot paths, there is no actual 'disorder interaction' between rotational speed and welding speed or between rotational and axial force and profile plot paths crossed due to random variation. From the study of Table 6.27, it is apparent that potential of the model, R^2 is greater than 0.90. Normal probability plot of residuals as shown in figure 6.30 and figure 6.31 shows no drastic deviation with the normality. This result confirms the basic assumption used in analysis (errors are normally distributed).

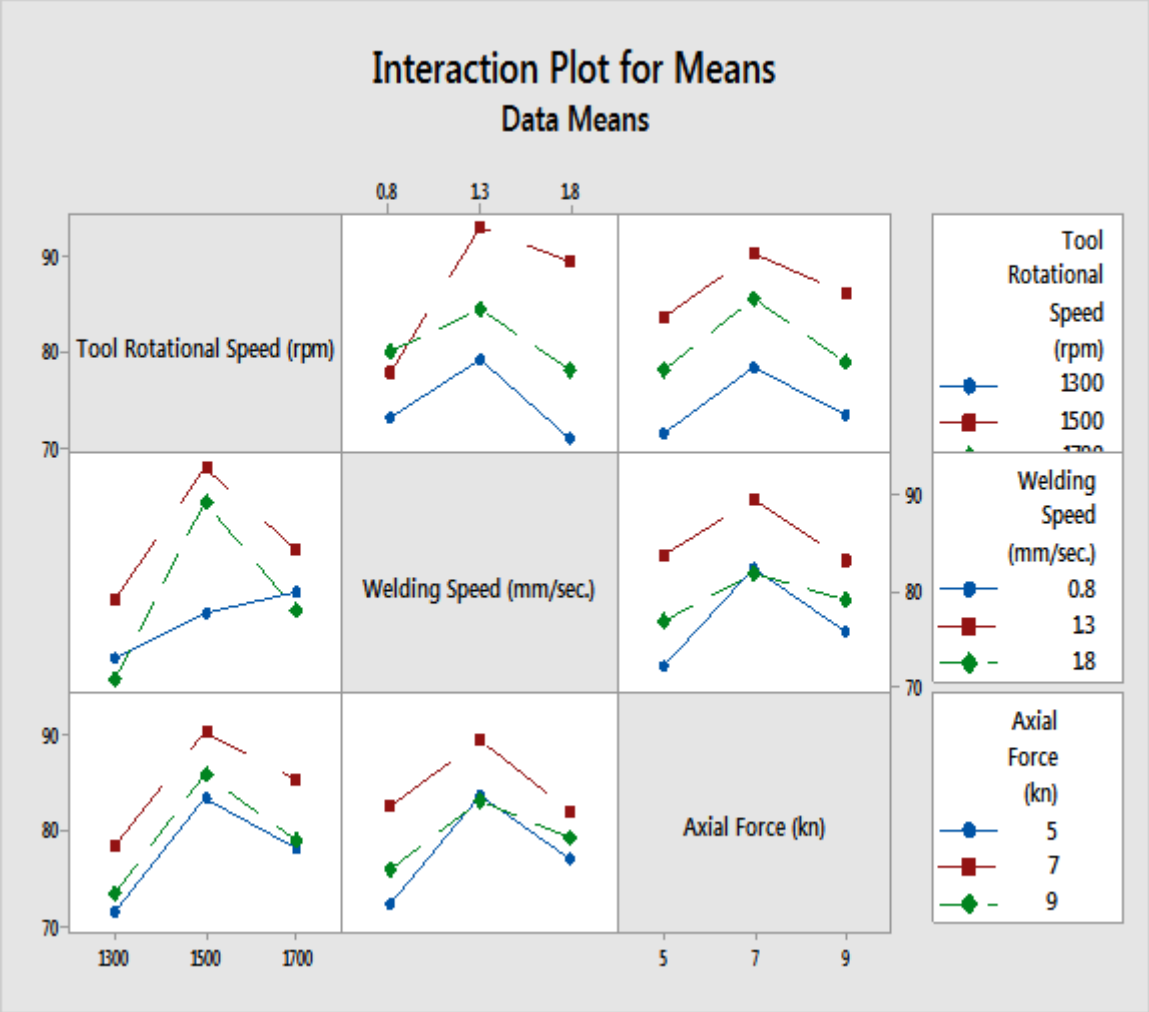

Figure 6.28 Interaction plot for Joint Efficiency (Means)

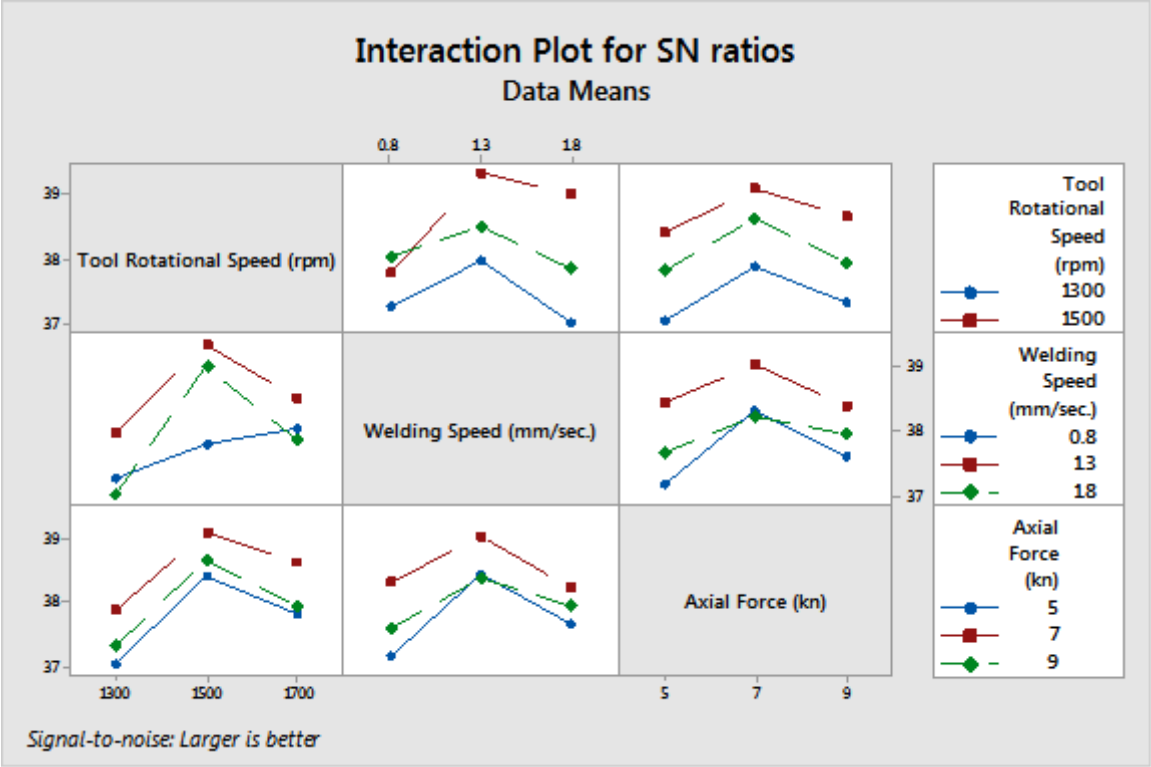

Figure 6.29 Interaction plot for Joint Efficiency (SN Ratio)

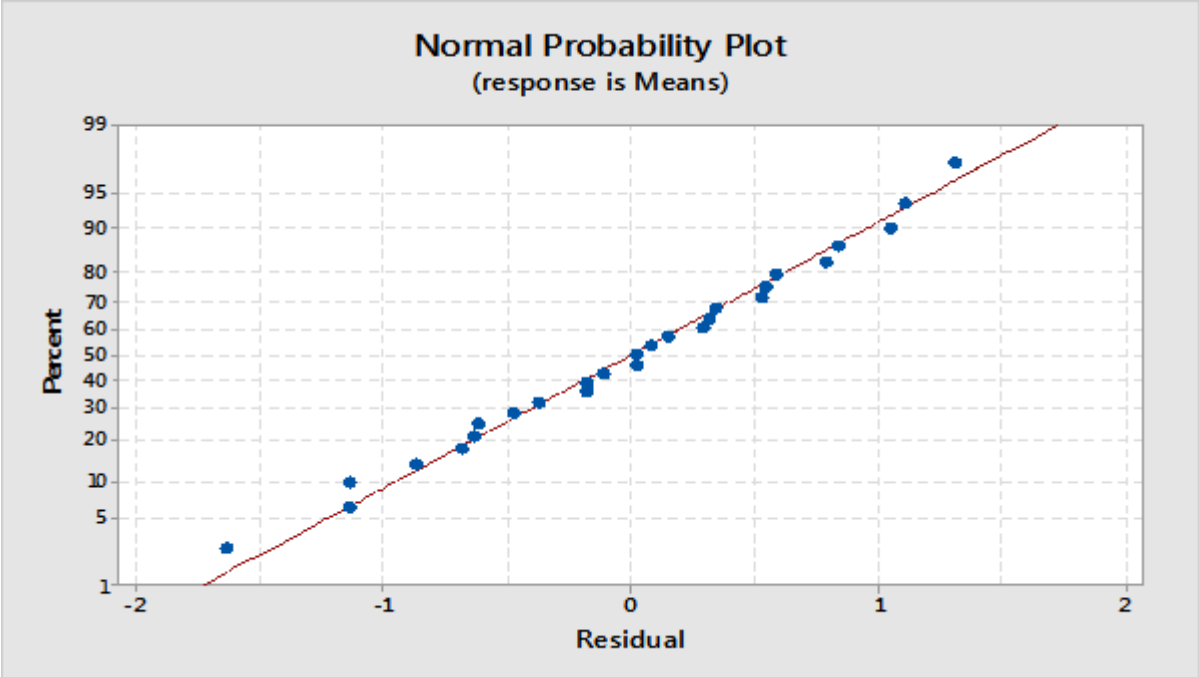

Figure 6.30 Normal probability plot of the residuals for Joint Efficiency

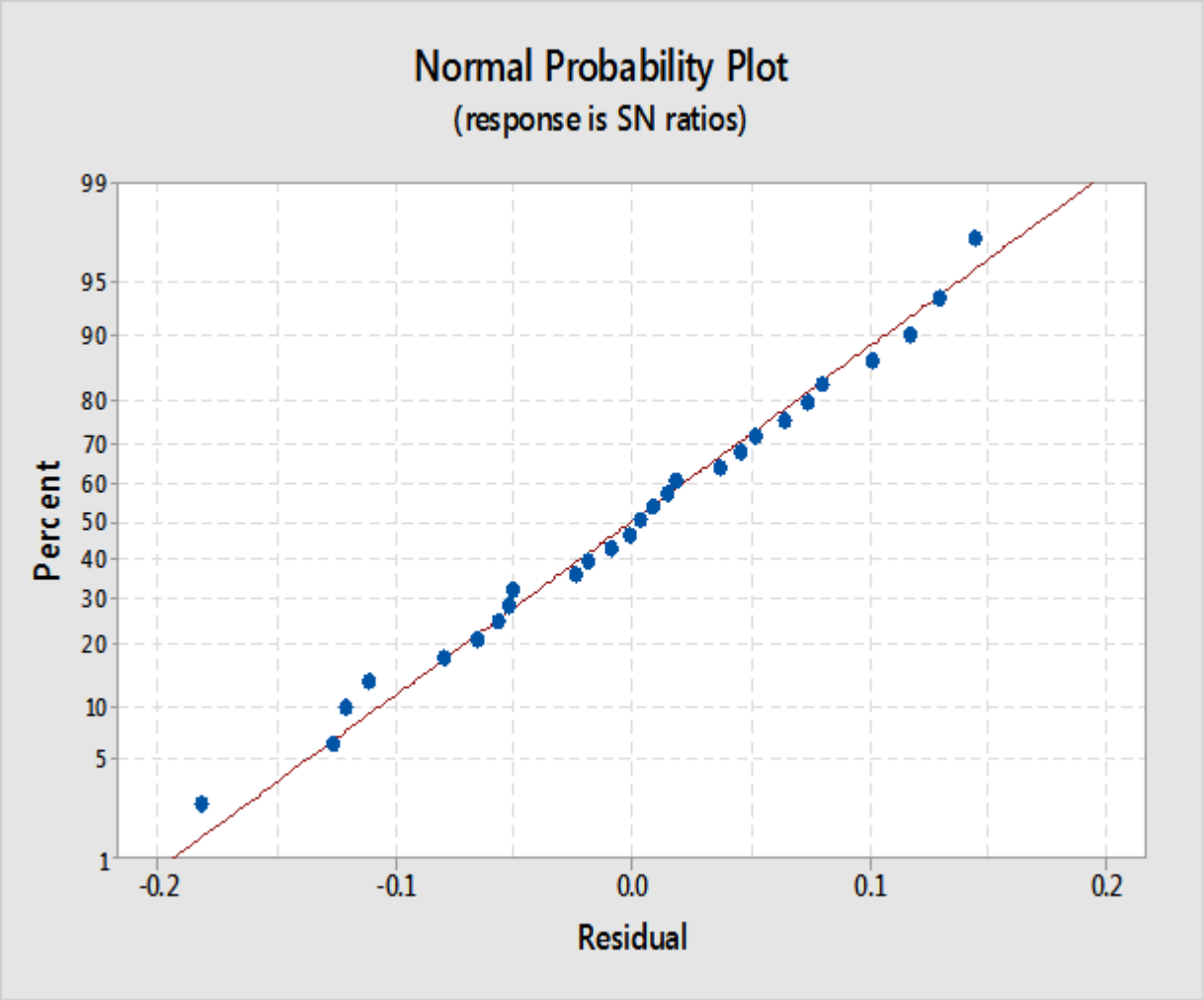

Figure 6.31 Normal probability plot of the residuals for Joint Efficiency

6.2.5.7 Estimation of Optimum Performance Characteristic for Joint Efficiency

As per Taguchi methodology, response table was used to calculate average Joint Efficiency for each input process parameter at different levels. The calculated Joint Efficiency for welding parameters at levels 1–3 is reported in Table 6.23. The combination of tool rotation at level 2,welding speed at level 2 and Axial force at level 2 tool geometry at level 1 which is shows in table 6.28. Therefore $A_2B_2C_2D_1$ with tool rotation speed of 1500 rpm, welding speed of 1.3 mm/sec, Axial force 7 kN and tool geometry of square are the optimum combination of process parameters for response optimization in welding of composites.

Table 6.28 Response table for Joint Efficiency (J.E)

Welding parameter	Level 1	Level 2	Level 3	Max-Min
Tool Rotation	74.4833	**86.7044**	80.8644	12.2211
Welding Speed	77.5288	**85.6144**	79.4644	8.0856
Axial force	77.74	**84.8022**	79.5088	7.0622
Tool Geometry	**81.0211**	80.6355	80.3955	
Overall mean	80.75			

The confirmation experiments were conducted at the selected optimum levels ($A_2B_2C_2D_1$) to verify the quality characteristics for friction stir welding of Al7075/10%SiC composite using high speed steel tools. After the optimal level has been selected, one could predict the using the following equation [118].

$$\mu_{predicted} = \mu_m + \sum_{i=1}^{n}(\mu_o - \mu_m)$$

Where, μ_m is the mean response, μ_o is the mean response at optimal level. Here, *n* is the number of factor that affects the response. It is very essential to perform a confirmatory experiment in the parameter design, particularly when less numbers of data are utilized for optimal. The confirmation experiment is used to verify the improvement in the quality characteristics [118].

$\mu_{\text{predicted mean grade}} = A_2+B_2+C_2-2T$

Where

T = overall mean = 80.75

Where, the values of A_2, B_2 and C_2 are taken from the Table 6.28

A_2= Second level of tool rotational speed = 86.7044

B_2 = Second level of welding speed = 85.6144

C_2 = Second level of axial force = 84.8022

Substituting the values of various terms in the above equation,

$\mu_{predicted\ mean\ grade}$ = 86.7044+85.6144+84.8022 – 2*80.75

$\mu_{predicted\ mean\ grade}$ = 95.621

The 95% confidence interval of confirmation experiment (Cl_{CE}) was calculated by following equation [118]:

$$Cl_{CE} = \sqrt{F_{\propto}(1, f_e)V_e\left[\frac{1}{n_{eff}} + \frac{1}{R}\right]}$$

Where, V_e is the error variance, F_{α} (1, f_e) is the F-ratio at a confidence level of (1-α) against DOF, 1 and error degree of freedom f_e . α is confidence level [38].

$$n_{eff} = \frac{N}{1 + [Total\ DOF\ associated\ in\ the\ estimate\ of\ mean]}$$

Where, N is the total number of results = 81 and R is the sample size for confirmation experiment = 3.

$$n_{eff} = \frac{81}{1 + [2 + 2 + 2]}$$

$$n_{eff} = 11.571$$

Error variance V_e = 2.387

f_e= error, DOF= 6

F (1, 6) = 5.14 (Tabulated F-ratio) [118].

So, CL_{CE} = ±2.26

Predicted optimum range for confirmation experiment is:

Predicted J.E+ CI_{CE}> Predicted J.E > Predicted J.E - CI_{CE}

95.621+2.26 > Predicted J.E > 95.621 -2.26

97.881 > Predicted J.E > 93.361

6.2.5.8 Verification of Optimal Parameters through Confirmation Test

Three confirmation experiments were conducted at the optimum level ($A_2B_2C_2D_1$), which are shown in table 6.29. From this table, the estimated error between predicted mean values and experimental average values are 1.82% joint efficiency. The average mean value of the joint efficiency of welded joints was found within the confidence interval as reported in Table 6.29.

Table 6.29.Responses of optimum levels of process parameters

Responses	Optimum welding Parameters		Confidence interval
	Predicted	Experimental	
Joint Efficiency	95.621	93.874	97.881 > Predicted J.E > 93.361

The Joint efficiency of welded joints are lower than the base materials. This is due to the welded joint formed as the combination of many thin layers in the direction of the joint thickness. It is fact that the different layers of plasticized metal have different mechanical properties because the cooling patterns of the layers are different. The upper layer is directly exposed in air, so its cooling rate is faster than the intermediate layers. The heat generations at different process parameters are not proper for different joints, which affects the weld quality.

6.3 MULTI RESPONSE OPTIMIZATION

In this work, optimization of multi response characteristics is used for AA7075/10%wt.SiC composite. The response characteristics are Tensile Strength and Hardness. In order to optimize multi response characteristics, grey based Taguchi method is used.

6.3.1 Analysis of Grey Relation Grade

Table 6.30 shows the experimental result of tensile strength and hardness of AA7075/10%wt.SiC composite.

Table 6.30 Multi responses results of Friction Stir Welding

S.NO	Tool Rotational Speed(rpm)	Welding Speed(mm/sec.)	Axial Force(kn)	Tool Geometry	Tensile Strength (MPa)	S/N Ratio	Hardness (H.V)	S/N ratio
1	1300	0.8	5	S	221.11	46.89	90.55	39.14
2	1300	0.8	7	H	249.14	47.93	100.9	40.08
3	1300	0.8	9	O	235	47.42	95.17	39.57
4	1300	1.3	5	H	251.32	48	101.78	40.15
5	1300	1.3	7	O	269.1	48.6	108.98	40.75
6	1300	1.3	9	S	243.41	47.73	98.58	39.88
7	1300	1.8	5	O	216	46.69	90.25	39.11
8	1300	1.8	7	S	237.62	47.52	96.23	39.67
9	1300	1.8	9	H	229.16	47.2	93.81	39.44
10	1500	0.8	5	H	234.14	47.39	94.82	39.54
11	1500	0.8	7	O	267	48.53	108.13	40.68
12	1500	0.8	9	S	247.14	47.86	100.09	40.01
13	1500	1.3	5	O	288	49.19	116.64	41.34
14	1500	1.3	7	S	311	49.86	125.95	42.00
15	1500	1.3	9	H	297.1	49.46	120.32	41.61
16	1500	1.8	5	S	283.15	49.04	114.67	41.19
17	1500	1.8	7	H	292.24	49.31	118.35	41.46
18	1500	1.8	9	O	285.16	49.1	115.49	41.25
19	1700	0.8	5	O	241.11	47.64	100.65	40.06
20	1700	0.8	7	S	279.75	48.94	113.29	41.08
21	1700	0.8	9	H	249.4	47.94	101	40.09
22	1700	1.3	5	S	268.13	48.57	108.59	40.72
23	1700	1.3	7	H	284.11	49.07	115.06	41.22
24	1700	1.3	9	O	261.25	48.34	105.8	40.49
25	1700	1.8	5	H	243	47.71	100.85	40.07
26	1700	1.8	7	O	260	48.3	105.3	40.45
27	1700	1.8	9	S	249.43	47.94	101.02	40.09

6.3.1.1 Data Pre-Processing

Data pre-processing is generally required when the range and units of the data has differed from the others. It is also used when the data range is too large, or when the data is scattered. Data pre-processing is a method of converting the original sequence to a

comparable sequence. Depending on the data, there are various methods of data pre-processing. In this work, to maximize the tensile strength and hardness "higher is better" characteristic is used [119].

The original sequence is normalized as follows:

$$x_i^*(k) = \frac{x_i^0(k) - min\, x_i^0(k)}{max\, x_i^0(k) - min\, x_i^0(k)} \quad \textbf{(1)}$$

Where $i = 1. . . . m$; $k = 1, . . . , n$. m is the number of experimental data items and n is the number of parameters. $x_i^0(k)$ denotes the original sequence, $x_i^*(k)$ the sequence after the data pre-processing, max $x_i^0(k)$ the largest value of $x_i^0(k)$, min $x_i^0(k)$ the smallest value of $x_i^0(k)$ and x^0 is the desired value.

The measured responses in table 6.30 normalized using equation 1. The normalized data for response were tabulated in table 6.31.

6.3.1.2 Grey Relational Deviation, Coefficient and Grey Relational Grade

In grey relational analysis, the measure of the relevancy between two sequences is defined as the grey relational grade. When only one sequence, *x*0 *(k)*, is available as the reference sequence, and all other sequences serve as comparison sequences, it is called a local grey relation measurement. After data preprocessing is carried out, the grey relation coefficient *ζi* (k) for the *k*th performance characteristics in the *i*th experiment can be expressed as [119]

$$\xi_i(k) = \frac{\Delta_{min} + \zeta\Delta_{max}}{\Delta_{0i}(k) + \zeta\Delta_{max}} \quad \textbf{(2)}$$

Where, Δ*oi* is the deviation sequence of the reference sequence and the comparability sequence.

Table 6.31Pre-processing (normalized) and deviation data

Trial Run	Tensile Strength (Mpa)		Hardness (VHN)	
	Normalized Sequence	Deviation Sequence	Normalized Sequence	Deviation Sequence
1	0.0538	0.9462	0.0084	0.9916
2	0.3488	0.6512	0.2983	0.7017
3	0.2000	0.8000	0.1378	0.8622
4	0.3718	0.6282	0.3230	0.6770
5	0.5589	0.4411	0.5246	0.4754
6	0.2885	0.7115	0.2333	0.7667
7	0.0000	1.0000	0.0000	1.0000
8	0.2276	0.7724	0.1675	0.8325
9	0.1385	0.8615	0.0997	0.9003
10	0.1909	0.8091	0.1280	0.8720
11	0.5368	0.4632	0.5008	0.4992
12	0.3278	0.6722	0.2756	0.7244
13	0.7579	0.2421	0.7392	0.2608
14	1.0000	0.0000	1.0000	0.0000
15	0.8537	0.1463	0.8423	0.1577
16	0.7068	0.2932	0.6840	0.3160
17	0.8025	0.1975	0.7871	0.2129
18	0.7280	0.2720	0.7070	0.2930
19	0.2643	0.7357	0.2913	0.7087
20	0.6711	0.3289	0.6454	0.3546
21	0.3516	0.6484	0.3011	0.6989
22	0.5487	0.4513	0.5137	0.4863
23	0.7169	0.2831	0.6950	0.3050
24	0.4763	0.5237	0.4356	0.5644
25	0.2842	0.7158	0.2969	0.7031
26	0.4632	0.5368	0.4216	0.5784
27	0.3519	0.6481	0.3017	0.6983

$$\Delta_{0i} = \|x_0^*(k) - x_i^*(k)\| \quad (3)$$

$$\Delta_{min} = \min_{\forall j \epsilon i} \min_{\forall k} \|x_0^*(k) - x_j^*(k)\| \quad (4)$$

$$\Delta_{max} = \max_{\forall j \epsilon i} \max_{\forall k} \|x_0^*(k) - x_j^*(k)\| \quad (5)$$

Where, $x_0^*(k)$ shows the reference sequence and $x_i^*(k)$ shows the comparable

sequence. ζ is distinguishing coefficient its value are adjusted as per the requirement. A value of ζ = 0.5 is used in this study. Using equation 3, the normalized data (table 6.31) is converted into deviation sequence. This calculated deviation data (Δ_{0i}) for tensile strength and hardness were tabulated in table 6.31. The normalized and deviation data in table 6.31 is converted into grey relational coefficient using equation 2. These calculated grey relational coefficients are tabulated in table 6.32.

Table 6.32 Grey relational coefficient and Grey relational grade

Trial Run	Grey Relation Coefficient		Grey Relation Grade
	Tensile Strength	Hardness	
1	0.3457	0.3352	0.3405
2	0.4343	0.4161	0.4252
3	0.3846	0.3671	0.3758
4	0.4432	0.4248	0.4340
5	0.5313	0.5126	0.5220
6	0.4127	0.3947	0.4037
7	0.3333	0.3333	0.3333
8	0.3930	0.3752	0.3841
9	0.3672	0.3571	0.3622
10	0.3820	0.3644	0.3732
11	0.5191	0.5004	0.5098
12	0.4265	0.4084	0.4175
13	0.6738	0.6572	0.6655
14	1.0000	1.0000	1.0000
15	0.7736	0.7602	0.7669
16	0.6304	0.6128	0.6216
17	0.7169	0.7014	0.7091
18	0.6477	0.6305	0.6391
19	0.4046	0.4137	0.4092
20	0.6032	0.5851	0.5941
21	0.4354	0.4171	0.4262
22	0.5256	0.5070	0.5163
23	0.6385	0.6211	0.6298
24	0.4884	0.4697	0.4791
25	0.4113	0.4156	0.4134
26	0.4822	0.4636	0.4729
27	0.4355	0.4173	0.4264

6.3.1.3 Response Table for grey relation grade

To find out the effect of each friction stir welding process parameter on the grey relational grade at different levels. This calculated response of each factor is tabulated in Table 6.33

Table 6.33 Response Table for grey relation grade

Process Parameters	Level 1	Level 2	Level 3	Max-Min
Rotational Speed	0.3979	**0.6336**	0.4853	0.2358
Welding Speed	0.4302	**0.6019**	0.4847	0.1718
Axial Force	0.4563	**0.5830**	0.4774	0.1267
Tool Geometry	**0.5227**	0.5045	0.4896	0.0330
Overall mean grade	0 .5055			

The larger grey relational grade corresponds to optimal process parameters. Therefore, optimal factor level is $A_2B_2C_2D_1$, i.e., the rotational speed at level 2(1500 rpm), welding speed at level 2 (1.3 mm/sec), Axial force at level 2 (7kn), and tool geometry at level 1 (square). The difference between maximum and minimum value in table 6.33, reflects the contribution of corresponding process parameters on grey relational grade. The response data is graphically illustrated in figure 6.32 and figure 6.33

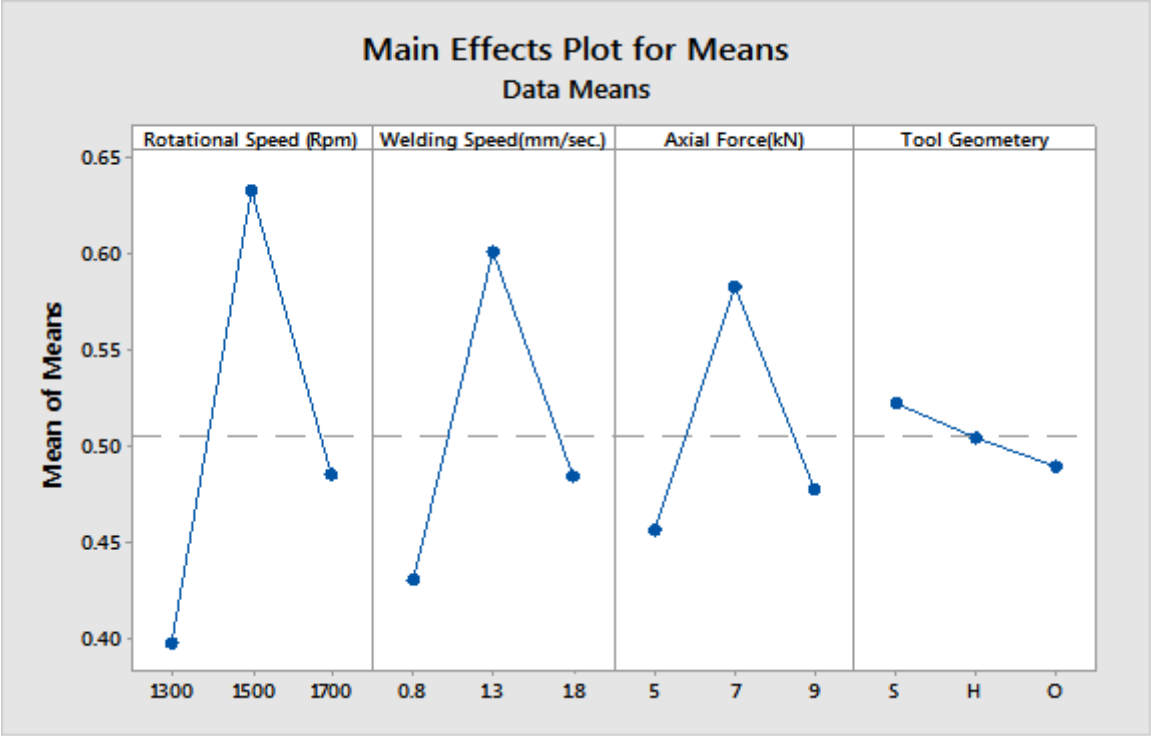

Figure 6.32 Main effect plot for grey relation grade (Means)

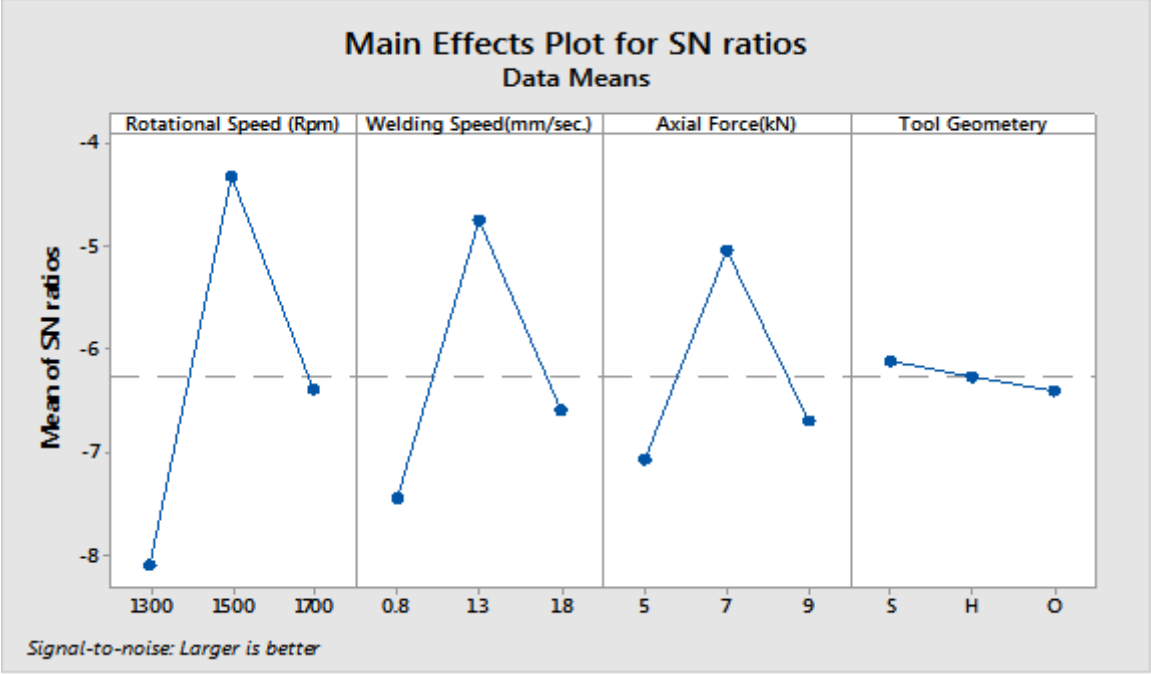

Figure 6.33 Main effect plot for grey relation grade (SN Ratio)

In figure 6.32 and figure 6.33 the slop of the grey relational graph represents the effect of friction stir welding process parameter. It was observe that, change in slope reflects the effect of process parameter. The figure 6.32 and figure 6.33 shows that rotational speed has the highest impact followed by welding speed and axial force. The tool geometry has a least impact on grey relational grade, as the graph represents a low slope line.

6.1.3.4 Effect of Rotational Speed on Grey Relation Grade

Figure 6.32 and figure 6.33 shows the effect of tool rotational speed on grey relation grade of friction stir welded AA7075/10%wt.SiC composite joints. The maximum grey relation grade was obtained at the rotational speed of 1500 rpm. At a lower rotational speed (1300 rpm) and higher rotational speed (1700 r/min), the tensile strength of joint was poor. When the rotational speed was increased from 1300 rpm, correspondingly the grey relation grade also increased and reached a maximum at 1500 rpm. If the rotational speed was increased above 1500 rpm, the grey relation grade of the joint was decreased. A lower tool rotational speed (1300 rpm) produced a lower heating condition as well as poor stirring action by the tool pin and improper consolidation of work material by the tool shoulder. Hence, a lower grey relation grade was obtained.

6.3.1.5 Effect of Welding Speed on Grey Relation Grade

Figure 6.32 and 6.33 present the effect of welding speed on grey relation grade of friction stir welded AA7075/10%wt.SiC composite joints. The grey relation grade of FSW joints was less at the low welding speed of 0.8 rpm. The grey relation grade was increased with increase in welding speed until the maximum of 1.3 mm/s. Further, increase in welding speed decreased the grey relation grade of FSW joints. It can be observed that a higher welding speed decreases the frictional heat input to the work material, which creates poor plastic flow of the metal and causes some voids like defects in the welded joint. This restricts grain growth and causes reduction in the width of the weld. Hence, poor grey relation grade is obtained.

6.3.1.6 Effect of Axial Force on Grey Relation Grade

Figure 6.32 and figure 6.33 analyzed the effect of axial force on grey relation grade of friction stir welded AA7075/10%wt.SiC composite joints. The lowest strength was obtained at axial load of 5 kN and 9 kN. The grey relation grade of composite joint

was increased with increase in axial load up to a maximum load of 7 KN. Further, increase in axial load decreased the grey relation grade of the joint.

6.3.1.7 Effect of Tool Pin Profile on Grey Relation Grade

Figure 6.32 and figure 6.33 shows the different values of grey relation grade for different types of tool pin profile. It is observed that the square type tool pin profile gives the maximum value of grey relation grade. The square type of tool pin profile produces good material stir quality during welding. Since, the tool has four edges, the point of each edge acts as an individual cutting tool that causes maximum deformation in the material. Hence, good surface finish and defect free joints are formed.

6.3.2 ANOVA for Grey Relational Grade

The purpose of ANOVA is to investigate the effect of process parameters and their influence on grey relational grade. ANOVA analysis is carried out for a level of significance of 5%, i.e. for 95% a level of confidence. If the calculated F-ratio is more than the tabulated value i.e. 5.14 for parameter and 4.53 for interactions at confidence level, then the effect is significant. P% gives the significant percentage contribution on grey relational grade. The calculated grade in table was analyzed with ANOVA and presented in table 6.34.

Table 6.34 Pooled ANOVA for Means (GRG)

Source	DOF	Seq SS	Adj SS	Adj MS	F Ratio	P	% PC
Rotational Speed	2	0.255693	0.255693	0.127847	98.61	0	41.44
Welding Speed	2	0.138658	0.138658	0.069329	53.48	0	22.66
Axial Force	2	0.082917	0.082917	0.041458	31.98	0	13.72
Tool Geometry	2	0.004932	0.004932	0.002466	1.90	0.229	
Rotational Speed*Welding Speed	4	0.108329	0.108329	0.027082	20.89	0.001	18.21
Rotational Speed* Axial Force	4	0.010824	0.010824	0.002706	2.09	0.201	
Welding Speed* Axial Force	4	0.014041	0.014041	0.003510	2.71	0.133	
Residual Error	6	0.007779	0.007779	0.001296			4.00
Total	26	0.623173					100

6.3.3 Interaction Plots for Grey Relational Grade

Figure 6.34 and figure 6.35 disclose pattern of line segments crossing each another or slight variation in the interaction plot paths, there is no actual 'disorder interaction' between rotational speed and welding speed or between rotational and axial force and profile plot paths crossed due to random variation. From the study of Table 6.27, it is apparent that potential of the model, R^2 is greater than 0.90. Normal probability plot of residuals as shown in figure 6.36 shows no drastic deviation with the normality. This result confirms the basic assumption used in analysis (errors are normally distributed).Percetage contributions of process parameters represented by figure 6.37.

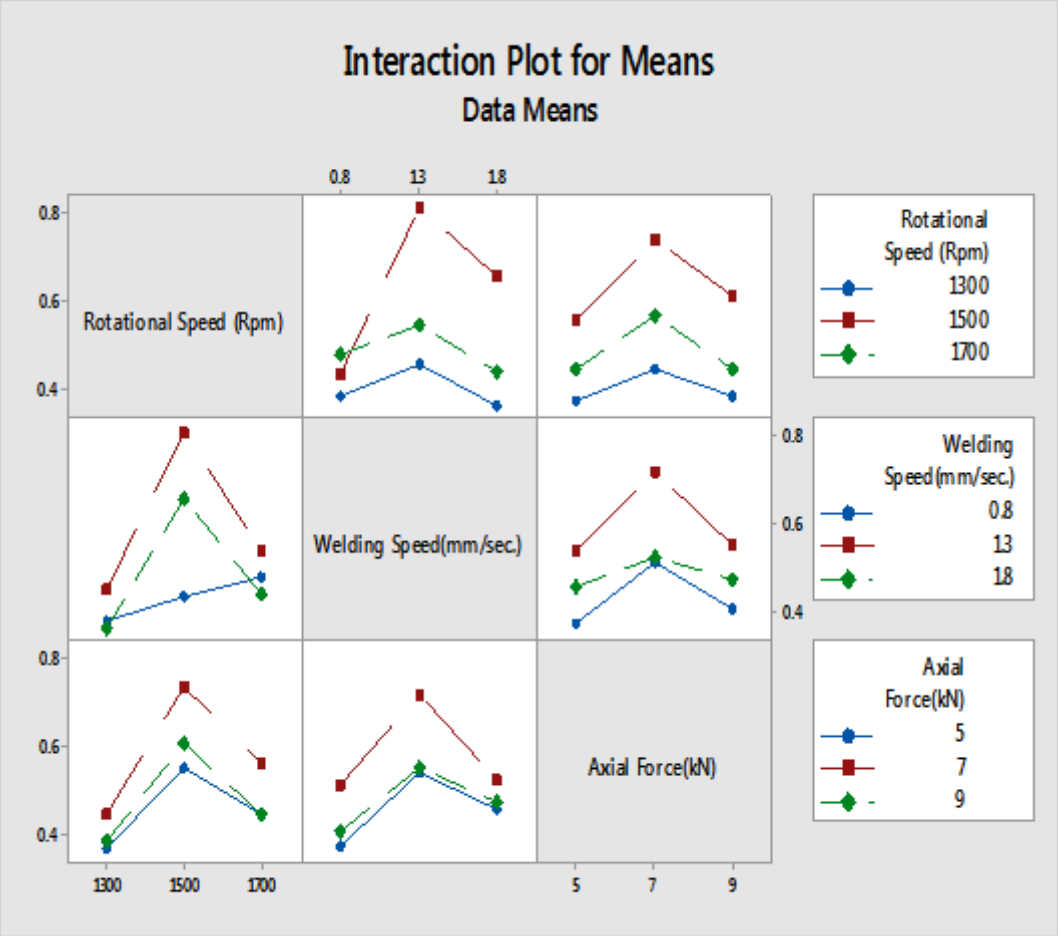

Figure 6.34 Interaction plot for Grey Relation Grade (Means)

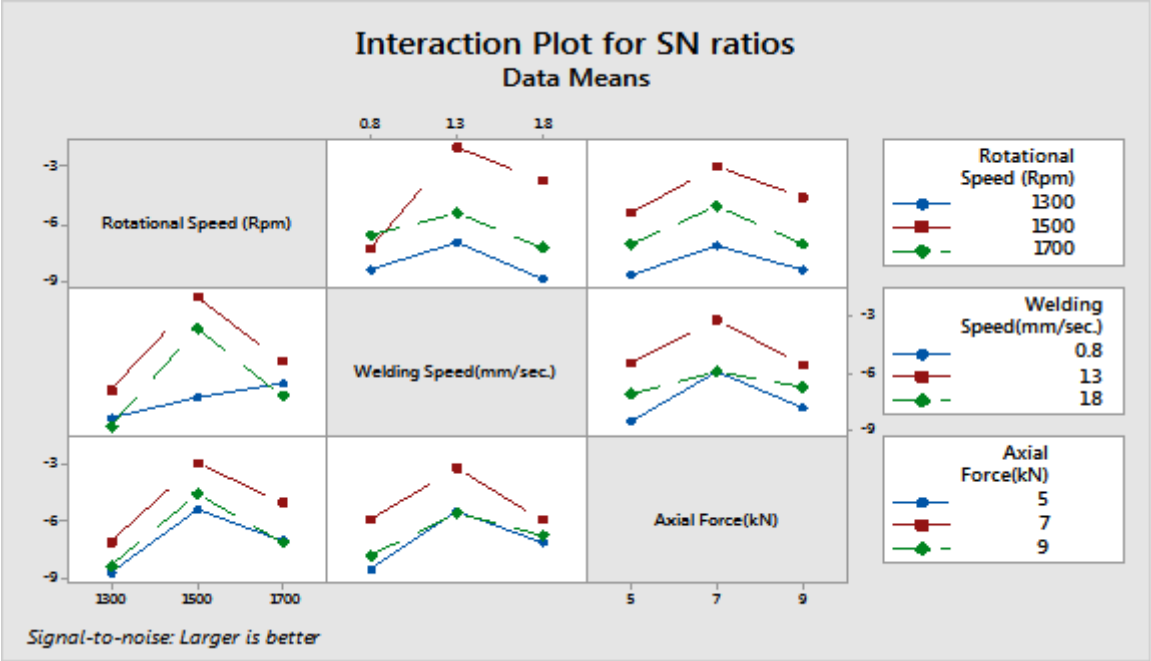

Figure 6.35 Interaction plot for Grey Relation Grade (SN Ratio)

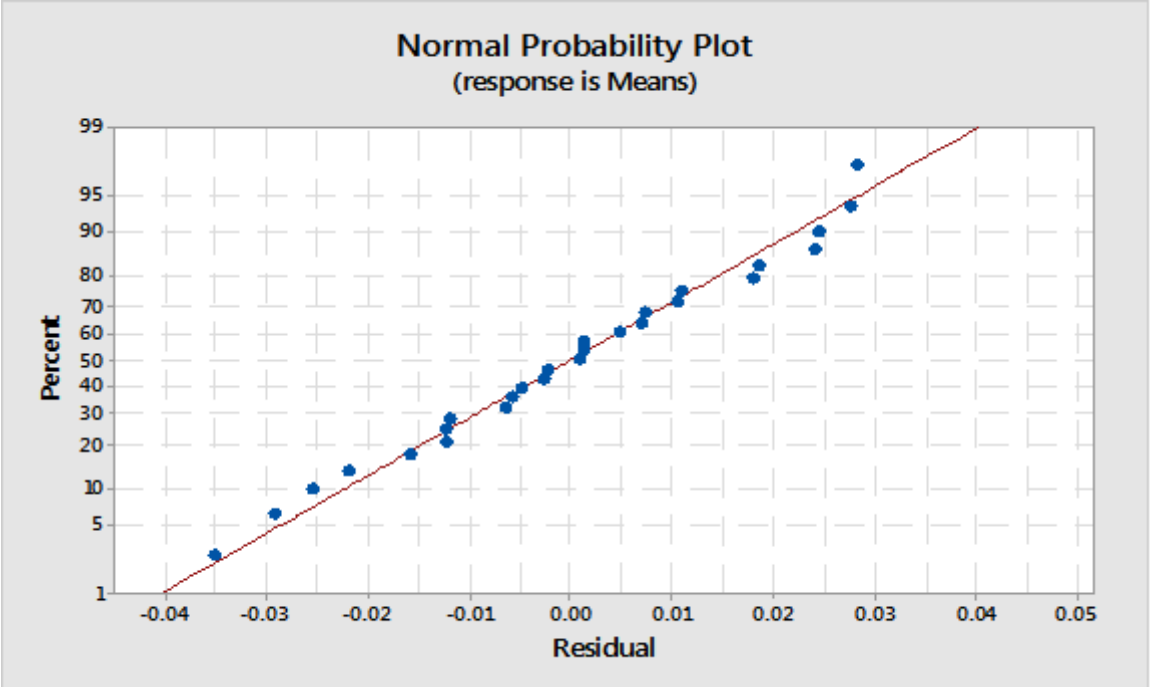

Figure 6.36 Normal probability plots of the residuals for GRG

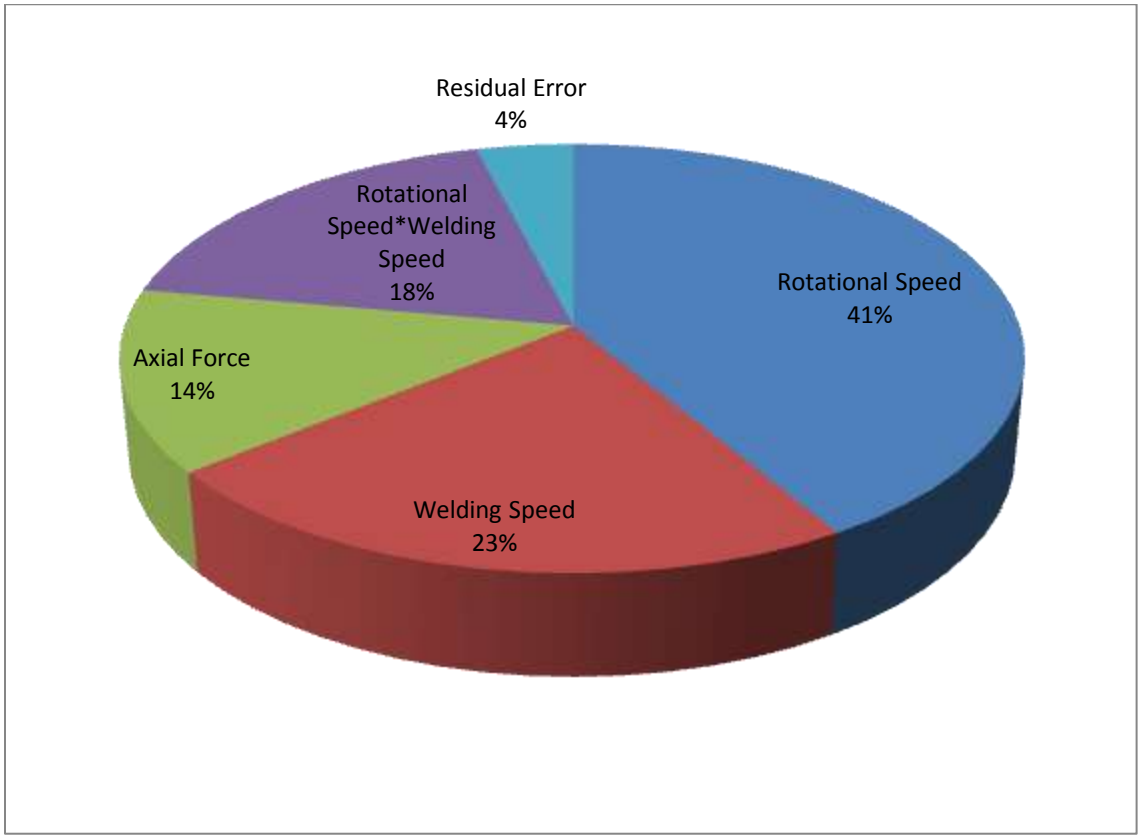

Figure 6.37 Percentage contributions of process parameters

6.3.4 Optimization of Process Parameters for Grey Relational Grade

The confirmation experiments were conducted at the selected optimum levels ($A_2B_2C_2D_1$) to verify the quality characteristics for friction stir welding of Al7075/10%wt.SiC composite. After the optimal level has been selected, one could predict the optimum grey relational grade using the following equation [118].

$$\mu_{predicted} = \mu_m + \sum_{i=1}^{n}(\mu_o - \mu_m)$$

Where, μ_m is the mean response, μ_o is the mean response at optimal level. Here, *n* is the number of factor that affects the GRG. It is very essential to perform a confirmatory experiment in the parameter design, particularly when less numbers of data

are utilized for optimal. The confirmation experiment is used to verify the improvement in the quality characteristics.

$\mu_{predicted\ mean\ grade} = A_2+B_2+C_2-2T$

Where

T = overall mean of grade = 0.5055

Where, the values of A_2, B_2 and $C_2$are taken from the response table.6.33

A_2 = average value of grey relational grade at the second level of rotational speed = 0.6336

B_2 = average value of grey relational grade at the second level of welding speed = 0.6019

C_2 = average value of grey relational grade at the second level of axial force = 0.5830

Substituting the values of various terms in the above equation,

$\mu_{predicted\ mean\ grade} = 0.6336+0.6019+0.5830 – 2(0.5055)$

$\mu_{predicted\ mean\ grade} = 0.8075$

The 95% confidence interval of confirmation experiment (Cl_{CE}) was calculated by following equation [41]:

$$Cl_{CE} = \sqrt{F_{\propto}(1, f_e)V_e\left[\frac{1}{n_{eff}} + \frac{1}{R}\right]}$$

Where, V_e is the error variance, F_{α} (1, f_e) is the F-ratio at a confidence level of (1-α) against DOF, 1 and error degree of freedom f_e. α is confidence level [118].

$$n_{eff} = \frac{N}{1 + [Total\ DOF\ associated\ in\ the\ estimate\ of\ mean]}$$

Where, N is the total number of results = 81 and R is the sample size for confirmation experiment = 3.

$$n_{eff} = \frac{81}{1 + [2 + 2 + 2]}$$

$$n_{eff} = 11.571$$

Error variance V_e = 0.001296 (From ANOVA)

f_e= error DOF= 6 (From ANOVA)

F (1, 6) = 5.14 (Tabulated F-ratio) [118].

So, $CL_{CE} = \pm 0.03$

Predicted optimum range for confirmation experiment is:

Predicted GRG + CI_{CE}> GRG > Predicted GRG - CI_{CE}

0.8075+0.03 > GRG > 0.8075-0.03

0.8375 > GRG > 0.7775

6.3.5 VERIFICATION OF OPTI MAL PARAMETERS THROUGH CONFIRMATION TEST

The confirmation experiments were conducted at optimum level (A_2, B_2, C_2, D_1). The confirmation experimental results at optimal level are shown in table 6.35. The grey relational grade at optimal levels is 0.8268. The obtained result is within the 95% confidence interval of the predicted optimum condition. Table 6.35 indicates that, grey relational grade value of confirmation experiment is improved by 10.85% from the initial value. This shows that, the grey relational analysis of multi response problems is an important technique for optimizing the tensile strength and hardness in the welding of AA7075/10%SiC composites.

Table 6.35- Comparison between initial and optimum welding parameters

Welding process parameter	Initial welding parameter	Optimum welding parameters	
		Predicted	Experimental
Level	$A_1 B_1 C_1 D_1$	$A_2B_2C_2D_1$	$A_2B_2C_2D_1$
Grey relational grade	0.7371	0.8075	0.8268

CHAPTER-7

CONCLUSION

7.1 CONCLUSION

1. AA7075/10%wt.SiC (particulate size 20-40 μm) successfully fabricated using mechanical stir casting process under the controlled conditions.
2. Microstructures of AA7075/10%wt.SiC reveal a fairly uniform and homogeneous distribution of reinforcing particles of SiC with matrix.
3. The X-RD patterns of cast composite sample confirm the presence of the base element aluminum and the other constituents of matrix alloy. The presence of hard phase constituents SiC are confirmed at respective peaks.
4. SEM fractography examination of AA7075/10%wt.SiC composite shows that distribution of reinforcement particles is homogeneous and products for secondary chemical reaction on reinforcement particles or matrix interface are not observed.
5. EDAX analysis confirms that the main elements like Mg, Si, Zn and Cu are present in major quantity.
6. Thermal analyses confirm that there are no degradation and material loss in the fabricated composites.
7. The fabricated AA7075/10%wt.SiC composite has an improvement of 44.23%, 51.37% and 41.56% in tensile strength, hardness, and impact strength, respectively, when compared to the Al 7075 alloy.
8. The optimal level of process parameters for optimum response quality targets was obtained as $A_2B_2C_2D_1$, Tool rotational speed of 1500 rpm (level 2), Welding speed 1.3 mm/sec (level 2), Axial force 7 KN (level 2) and Tool geometry is square (level 1).
9. Analysis of variance for tensile strength reveals that tool rotational speed has maximum influence (44.42%) followed by welding speed (23.57%) and axial

force (16.04%) were affecting the quality of welded composites. The interaction of tool rotational speed and welding speed is found be significant (14.09%).

10. Analysis of variance for Percentage elongation reveals that tool rotational speed has maximum influence (38.09%) followed by axial force (23.82%) and welding speed (23.59%) were affecting the the quality of welded composites. The interaction of tool rotational speed and welding speed is found be significant (12.08%).
11. Analysis of variance for hardness reveals that tool rotational speed has maximum influence (45.22 %) followed by welding speed (23.30%) and axial force (14.74 %) were affecting the the quality of welded composites. The interaction of tool rotational speed and welding speed is found be significant (15.15%).
12. Analysis of variance for welded joint efficiency reveals that tool rotational speed has maximum influence (44.26 %) followed by welding speed (23.57%) and axial force (16.19 %) were affecting the the quality of welded composites. The interaction of tool rotational speed and welding speed is found be significant (14.09%).
13. Grey relation analysis is used for predicting the mechanical properties (tensile strength and hardness) for welding of AA7075/10%wt.SiC composites.
14. Analysis of variance for Grey relation grade reveals that tool rotational speed has maximum influence (41.44 %) followed by welding speed (22.66%) and axial force (13.72 %) were affecting the the quality of welded composites. The interaction of tool rotational speed and welding speed is found be significant (18.21%).
15. The value of grey relation grade 0.7371with initial parameters ($A_1B_1C_1D_1$) is improved to 0.8268 with optimal parameters ($A_2B_2C_2D_1$). This increment in grade reflects that welded joint quality is improved using optimal process parameters.

7.2 INDUSTRIAL APPLICATION OF FSW PROCESS

Friction Stir Welding finds tremendous applications in the wide range of industrial sectors like Parts of automobile, aerospace, marine, electronics etc. This technique specially used for automotive industry requiring high strength to weight ratio. Some of the renowned industries which use FSW process are Honda, Boeing and Apple etc. Honda Accord used FSW, to perform lap welding of steel with aluminum for one of its sub-component in the chassis [112]. Apple, in one of its products called iMac, used FSW to weld the front panel with the back panel which has a thickness of 5 mm [113]. Similarly, various industries have already used the process in either joining of aluminum or for different materials. Welding of dissimilar materials majorly finds applications in many industries, as aluminum or any lighter material alone cannot cater the strength and stiffness requirement. Like, a combination of aluminum-steel is used in aerospace and automobile sectors to manufacture chassis, pillars, bumpers etc. [114]. FSW is used for high weld strength applications like aerospace, automobile and marine industries, and it also finds its application in electronic industry, where only aesthetics of the product is important, for e.g. iMac computer of Apple etc. This versatility in application tells about the potentiality and capability of the process.

7.3 **LIMITATIONS AND SCOPE FOR FUTURE WORK**

In this research the effects of different welding process parameters on welding responses (Tensile strength, Hardness, Percentage elongation and Weld joint efficiency) are studied. But work has the following limitations.

- This work require post heat treatment of friction s
- tir welded joints.
- Although of butt friction stir welded joints successfully fabricated but lap friction stir welded joints may be explored.

To minimize these limitations this work needs extension in the following direction.

- The effect of post heat treatment of friction stir welded joints with different ageing treatments to improve the tensile strength may be explored in detail.
- FSW is capable of joining of hybrid combination Al-Cu composites for manufacturing of household utensils, industrial power protection.
- Study of heat transfer analysis can be extended to lap friction stir welded joints.
- Impact on material removal rate (MRR) of tool and work piece may be explored.

REFERENCES

[1] D. Kim, W. Lee, and J. Kim,"Formability of evaluation of friction stir welded 6111-T4 sheet with respect joining material direction". International Journal of Mechanical Science, doi:10. 1016/j.i jmecsci. 2010.

[2] J. Masounave and F.G. Hamel, "Fabrication of Particulate Reinforced Metal Composites", International, Montreal, Que, Canada, September, 1990, p 79-86.

[3] T.S Mahmoud, A.M. Gaafer and T.A. Khalifa,"Effect of tool rotational and welding speeds on micro-structural and mechanical characteristics of friction stir welded A319 cast Al alloy", Materials Science and Technology, 2011 24(5): 553-559.

[4] K. Elangovan, and Balasubramanian.,"Influences of tool pin profile and tool shoulder diameter on the formation of friction stir processing zone in AA6061 aluminium alloy. Materials & Design 2008,29: 362–373.

[5] R.Palanivel, P. K Mathews, and N.Murugan, "Influences of tool pin profile on the mechanical and metallurgical properties of friction stir welding of dissimilar aluminum alloys". Int. Journal of Engg. Science and Technology,2010 2(6): 2109–2115.

[6] V. Agarwal and D. Dixit, "Fabrication of Aluminium Base Composite by Foundry Technique", Tr ans. Jpn Inst. Metall., 1981, 22(8), p 521–526

[7] L. Karthikeyan, K.Senthi, K.A, Padmanabhan, "On the roll of process variables in the friction stir cast aluminium A319 alloy", Materials & esign,2010, 31(2): 761−771.

[8] T.Azimzadegan, S.Serajzadeh, "An investigation into microstructures and mechanical properties of AA7075-T6 during friction stir welding", Journal of Materials Engineering Performance, 2010, 19(9):1256−1263.

[9] K.Elangovan, V.Balasubramanian, S.Babu, "Predicting tensile Strength of friction stir welded AA6061 aluminum alloy joints by a mathematical model". Materials & Design, 2009, 30(1): 188−193.

[10] S.N.Sundaram, N. Murugan,"Tensile behavior of dissimilar friction stir welded joints of aluminium alloys". Materials & Design, 2010, 31(9): 4184−4193.

[11] Asadi, Akbari, "Optimization of AZ91 friction Stir welding parameters using Taguchi method Materials" Design and Applications Mech. 2015. DOI:10.1177/1464420715570987 pil.sagepub.com

[12] P.Hema1 , N.Raviteja , K.Ravindranath,"Prediction and Parametric Optimization On Mechanical Properties of Friction Stir Welding Joints of AA 6061 and AA 2014 Using Genetic Algorithm" International Journal of Innovative Research in Science, Engineering and Technology, 2016 DOI:10.15680/IJIRSET.2016.0503093

[13] M Saeidi, B Manafi, MK Besharati Givi, G Faraji, "Mathematical modeling and optimization of friction stir welding process parameters in AA5083 and AA7075 aluminum alloy joints". Volume: 230 issue: 7, page(s): 1284-1294 Article Issue published: July 2016.

[14] S. Verma, J. P. Mishra,"Study on temperature distribution during Friction Stir Welding of 6082 aluminum alloy", Materials Today: Proceedings 4 (2017).

[15] Y.Bozkurt, Z.Boumerzoug,"Tool material effect on the friction stir butt welding of AA2124-T4 Alloy Matrix MMC", Journals of Material Research and Technology (2017).

[16] Yinfei, Shen, "Influences of friction stir welding parameters tensile on morphology and strength of high density polyethylene double-pin lap joints produced by tool", Journal of Manufacturing Processes (2017).

[17] D.K. Yaduwanshi, S. Bag, S. Pal,"Numerical modeling and experimental investigation on plasma-assisted hybrid friction stir welding of dissimilar materials", Materials and Design (2016).

[18] Rao.Prasad, Mano Misra, Damodaram Ramachandran, "Low temperature friction stir welding of P91 steel" Defence Technology (2016).

[19] S. SreeSabari, S. Malarvizhi, V. Balasubramanian, "Experimental and numerical Investigation on under-water friction stir welding of armour grade AA2519-T87 aluminium alloy", Defence Technology (2016).

[20] Sanghoon Noh, Masami Ando, Hiroyasu Tanigawa, Akihiko Kimura, “Friction stir welding of F82Hsteel for fusion applications”, A Journal of Nuclear Materials (2016).

[21] Nikul Patel, K.D.Bhatt, Vishal Mehta, “Influence of Tool Pin Profile and Welding Parameter on Tensile Strength of Magnesium Alloy AZ91 during FSW”, Procedia Technology (2016).

[22] Chinmay Shah, BhupeshGoyal, Vijay Patel,“Optimization of FSW process parameters for AlSiCp PRMMC usingANOVA”, Materials Today: Proceedings (2015).

[23] S. M. Bayazida, H. Farhangia, A. Ghahramania, “Investigation of friction stir welding Parameters of 6063-7075 Aluminum alloys by Taguchi method”, Procedia Materials Science (2015).

[24] Z. Shen, Y. Chen, M. Haghshenas, A.P. Gerlich,“Role of welding parameters on interfacial bonding in dissimilar steel/ aluminum friction stir welds”, Engineering Science and Technology (2015).

[25] R.I. Rodriguez, J.B. Jordon, P.G. Allison, T. Rushing, L. Garcia, “Microstructure and Mechanical properties of dissimilar friction stir welding of 6061-to-7050 aluminum alloys”, Materials & Design (2015).

[26] V. Jaiganesh., B.Maruthu, E.Gopinath.,“Optimization of process parameters on friction stir welding of high density polypropylene plate”,Procedia Engineering (2014).

[27] P.Sadeesh , K.Venkatesh, M Rajkumar, P.Avinash,“Studies on friction stir welding of AA 2024 and AA 6061 dissimilar metals”,Procedia Engineering (2014).

[28] Gurmeet Singh, Amardeep S. Kang, Kulwant Singh, Jagtar Singh,“Experimental Comparison of friction stir welding process and TIG welding process for 6082-T6 Aluminium alloy”,Materials Today: Proceedings 4 (2017).

[29] WM.Thomas, “Friction Stir Welding”. International Patent Application No. PCT/ GB92/02203 and GB Patent Application No. 9125978.8. U.S. Patent No. 5 (1991) 460;317.

[30] C.J. Dawes, “An Introduction to Friction Stir Welding and its Development”, Weld. Met. Fabr., 1995, **63**, p 2–16

[31] W.M. Thomas and E.D. Nicholas, Friction Stir Welding for the Transportation Industries, Mater. Des., 1997, **18**, p 269–273

[32] Munro RG. Material Properties of Titanium Diboride. Journal of Research of National Institute of Standards and Technology. 105(5), 2000, 709–20

[33] I.N. Tansel, M. Demetgul, H. Okuyucu, and A. Yapici, "Optimizations of Friction Stir Welding of Aluminum Alloy by Using Genetically Optimized Neural Network", Int. J. Mach. Tool. Manuf., 2009, 44, p 1205–1214

[34] Kennedy, A.R and Brampton, B. "The reactive wetting and incorporation of B4C particles into molted aluminum", Scr. Mater. 44(7), 2001, 1077-1082.

[35] Ramesh, C.S., Keshavamurthy, R., Chennabasappa, B.H., and Abrar Ahmad. "Microstructure and mechanical properties of Ni-P coated Si3N4 reinforced Al6061 composites", Mater. Sci. Eng., A 502(2), 2009, 99-106

[36] S. Lim, S. Kim, C.-G. Lee, and S. Kim, "Tensile Behavior of Friction-Stir-Welded Al 6061-T651", Metall. Mater. Trans. A, 2004, 35, p 2829–2835

[37] A. Barcellona, G. Buffa, L. Fratini, and D. Palmeri, On Microstructural Phenomena Occurring in Friction Stir Welding of Aluminium Alloys, J. Mater. Process. Technol., 2006, 177, p 340–343

[38] Y.S. Sato, H. Takauchi, S.H.C. Park, and H. Kokawa, "Characteristics of the Kissing-Bond in Friction Stir Welded Al Alloy 1050, Mater. Sci. Eng. A, 2005, 405, p 333–338

[39] X.H. Wang and K.S. Wang, "Microstructure and Properties of Friction Stir Butt-Welded AZ31 Magnesium Alloy", Mater. Sci. Eng. A, 2006,

[40] T. Clyne and P. Withers, "An Introduction to Metal Matrix Composites, Cambridge Solid State Science Series, Cambridge University Press", 1995, p 1–10

[41] B. Ralph, H.C. Yuen, and W.B. Lee, "The Processing of Metal Matrix Composites—An Overview", J. Mater. Process. Technol., 1997, 63, p 339–353

[42] J. Hashim, L. Looney*, M.S.J. Hashmi "Metal matrix composites: production by the stir casting method Journal of Materials Processing Technology" (1999), P 1-7

[43] R.S. Mishra, Z.Y. Ma, "Friction stir welding and processing", Materials Science and Engineering R 50 (2005).

[44] J.P. Pathak, J.K Singh and S. Mohan, "Synthesis and characterization of Aluminium-Silicon carbide composite", Ind.J.Engg.and Mater.Science.13(2006) 238-246

[45] A. Kalkanh and S. Yilmaz, "Synthesis and Characterization of luminium Alloy 7075 Reinforced with Silicon Carbide Particulates", Mater. Design, 2008, 29, p 741–756

[46] Reddy A.C and Ziton E Matrix Al-alloys for silicon carbide particle reinforced metal matrix composites Indian Journal of Science and Technology Vol. 3 No. 12 (Dec 2010) ISSN: 0974- 6846

[47] Rajesh Kumar Bhushan & Sudhir Kumar & S. Das "Fabrication and characterization of 7075 Al alloy reinforced with SiC particulates" Int J Adv Manuf Technol (2013) 65:611–624 DOI 10.1007/s00170-012-4200-6

[48] Bharath Va, Madev Nagaralb, V Auradib and S. A. Koric Preparation of 6061Al-Al2O3 MMC's by Stir Casting and Evaluation of Mechanical and Wear Properties3rd International Conference on Materials processing and Characterization (ICMPC 2014)

[49] Ravi "Fabrication and Mechanical Properties of Al7075-SiC-TiC Hybrid Metal Matrix Composites" International Journal of Engineering Science Invention ISSN (Online): 2319 – 6734, ISSN (Print): 2319 – 6726 www.ijesi.org ||Volume 6 Issue 10|| October 2017 ||

[50] Miss. Laxmi1, Mr. Sunil Kumar2 Fabrication and Testing of Aluminium 6061 Alloy & Silicon Carbide Metal Matrix Composites" International Research Journal of Engineering and Technology (IRJET) e-ISSN: 2395 -0056 Volume: 04 Issue: 06 June-2017

[51] Ramesh B T,Vinayak Koppad, Hemanth Raju T "Fabrication of Stir casting Setup for Metal Matrix Composite" IJSRD - International Journal for Scientific Research & Development| Vol. 5, Issue 06, 2017 | ISSN (online): 2321-0613

[52] Akash Kunjir1 , Onkar Lonkar2 , Lalit Kate3 , Pranjal Javalkar4 , P.B.Pawar5) "Fabrication of Low Cost Stir Casting Setup for Preparing Al Based MMC's" Int.J. of Advanced Research Vol.7, Issue 1, ISSN (online): 2018 ISSN (online): 2319-8454

Mohit Kumar Sahu Raj Kumar Sahu "Fabrication of Aluminum Matrix Composites by Stir Casting Technique and Stirring Process Parameters Optimization" · May 2018

[53] Ch Hima Gireesh, K. G. Durga Prasad, and Koona Ramji 2 "Experimental Investigation on Mechanical Properties of an Al6061 Hybrid Metal Matrix Composite", ID , Received: 14 May 2018; Accepted: 7 August 2018; Published: 13 August 2018)

[54] Rajasekar Thiyagarajan, Vignesh Ganesan, Milon Selvam Dennison, Nelson A.J.R4 "Preparation and characterization of aluminium metal matrix composite by using stir casting technique" International Research Journal of Engineering and Technology (IRJET) e-ISSN: 2395-0056 Volume: 05 Issue: 03 | Mar-2018 Page 62

[55] G. Diju Samuel, J. Edwin Raja Dhas, G. Ramanan and M. Ramachandran "Production and microstructure characterization of AA6061 matrix activated carbon particulate reinforced composite by friction stir casting method" 2017 ISSN:0976-0083

[56] L.M. Marzoli, A.v. Strombeck, J.F. Dos Santos, C. Gambaro, "Friction stir welding of an AA6061/Al2O3/20p reinforced alloy". Composites Science and Technology 66 (2006) 363–371

[57] Hu seyin Uzun "Friction stir welding of SiC particulate reinforced AA2124 Aluminum alloy matrix Composite" Materials and Design 28 (2007) 1440–1446

[58] F. Sarsılmaz, "Statistical Analysis on Mechanical Properties of Friction-Stir-Welded AA 1050/AA 5083 Couples", Int. J. Adv. Manuf. Technol. 2009, 43(3–4), p 248–255

[59] S. Rajakumar, C. Muralidharan, and V. Balasubramanian, "Optimization of the Friction-Stir-Welding Process and the Tool Parameters to Attain a Maximum Tensile Strength of AA7075-T6 Aluminium Alloy", J. Eng. Manuf., 2010, 224, P 1175–1191

[60] M. Jayaraman, R. Sivasubramanian, and V. Balasubramanian, "Establishing Relationship Between the Base Metal Properties and Friction Stir Welding Process Parameters of Cast Aluminium Alloys", Mater. Des., 2011, p 4567–457.

[61] K. Kalaiselvan N. Murugan Siva Parameswaran "Production and characterization of AA6061–B 4C stir cast composite" Materials and Design 32(7):4004-4009 · August 2011

[62] Ramesh Babu, S. / Karthik, P. / Karthik, S. / Kumar, S. Arun / Marris, Joel Optimization of Process Parameters during Friction Stir Welding of Dissimilar Aluminium Alloys (AA 5083 & AA 6061) Using Taguchi L9 Orthogonal Applied Mechanics and Materials 2014 p-592-594

[63] Asif, M.M, Shri Krishna, K.A & Sathiya, "Optimization of process parameters of FSW of UNS S31803 duplex Stainsless steels joints.Advances in manufacturing"(2016)P 55-63.

[64] H.G.Rana,V.J.Badheka,A.Kumar "Fabrication of Al7075 / B4C Surface Composite by Novel Friction Stir Processing (FSP) and Investigation on Wear Properties" Procedia Technology Volume 23, 2016, Pages 519-528

[65] S Jacob, S Shajin and C Gnanavel "Thermal analysis on Al7075/Al2O3 metal matrix composites fabricated by stir casting process" International Conference on Emerging Trends in Engineering Research IOP Publishing IOP Conf. Series: Materials Science and Engineering 183 (2017) 012010 doi:10.1088/1757-899X/183/1/012010

[66] S. Verma, Meenu, J. P. Mishra,"Study on temperature distribution during Friction Stir Welding of 6082 aluminum alloy", Materials Today: Proceedings 4 (2017).

[67] Yahya Bozkurt, ZakariaBoumerzoug,"Tool material effect on the friction stir butt welding of AA2124-T4 Alloy Matrix MMC",Journals of Material Research and Technology (2017).

[68] Gurmeet Singh, Amardeep S. Kang, Kulwant Singh, Jagtar Singh,"Experimental comparison of friction stir welding process and TIG welding process for 6082-T6 Aluminium alloy",Materials Today: Proceedings 4 (2017).

[69] Mr. Praveen G. Kohak1, Dr. R. R. Navthar2 "Optimization of Process parameters of Friction Stir Welding for Similar HE-30 Aluminium Alloy" International Research Journal of Engineering and Technology (IRJET) e-ISSN: 2395-0056 Volume: 04 Issue: 07 | July -2017 ISSN: 2395-0072

[70] V. M. Magalhães, C. Leitão & D. M. Rodrigues "Friction stir welding industrialisation and research status"Journal of Science and Technology of welding and joining Volume 23, Issue 5 2018

[71] Jain S, Sharma N & Gupta R. "Dissimilar alloys (AA6082/AA5083) joining by FSW and parametric optimization using Tauguchi, grey relation and weight method", 'Engg.Solid Mechanics"6(1) P 51-66 2018

[72] Mohammed Yunus and Mohammad S. Alsoufi "Mathematical Modelling of a Friction Stir Welding Process to Predict the Joint Strength of Two Dissimilar Aluminium Alloys Using Experimental Data and Genetic Programming" 2018

[73] Chintamani Mahananda Siddharth Jeet Sasmita Kar "Review on Application of Friction Stir Welding" National Conference on Emerging Trends in Engineering, Science and Manufacturing (ETESM-2018), at indira gandhi institute of technology (IGIT) Sarang, Dhenkanal, (Odisha)India.

[74] Pradeep GRC, Ramesh A and Veeresh Kumar GB. Studies on mechanical properties of Al6063–SiC. Int J Adv Eng Appl 2011; 1: 71–73.

[75] Huang J-h, Dong Y-l, Wan Y, et al. Investigation on reactive diffusion bonding of SiCp/6063 MMC by using mixed powders as interlayers. J Mater Process Tech 2007; 190: 312–316.

[76] Karamis MB, Tasdemirci A and Nair F. Failure and tri-bological behaviour of the AA5083 and AA6063 compo-sites reinforced by SiC particles under ballistic impact. Compos Part A: Appl S 2003; 34: 217–226.

[77] Mc Danels DL."Analysis of stress–strain, fracture, and ductility behavior of aluminum matrix composites containing discontinuous silicon carbide reinforcement". Metall Mater Trans A 1985; 6(16): 1105–1115.

[78] Ibrahim IA, Mohamed FA and Lavernia EJ. "Particulate reinforced metal matrix composites—a review". J Mater Sci 1991; 5(26): 1137–1156

[79] Lloyd DJ. Particle reinforced aluminum and magnesium matrix composites. Int Mater Rev 1994; 1(39): 1–23.

[80] Surappa MK. "Microstructure evolution during solidification of DRMMCs". State of art. J Mater Process Tech 1997; 63: 325–333.

[81] Pradeep GRC, Ramesh A and Veeresh Kumar GB. 'Studies on mechanical properties of Al6063–SiC". Int J Adv Eng Appl 2011; 1: 71–73.

[82] Huang J-h, Dong Y-l, Wan Y, et al. "Investigation on reactive diffusion bonding of SiCp/6063 MMC by using mixed powders as interlayers". J Mater Process Tech 2007; 190: 312–316.

[83] Karamis MB, Tasdemirci A and Nair F. Failure and tribological behaviour of the AA5083 and AA6063 composites reinforced by SiC particles under ballistic impact.Compos Part A: Appl S 2003; 34: 217–226.

[84] A.K. Banerji, M. K. Surappa and P. K. Rohargi, Abrasive wear of Cast Aluminum Alloys Containing dispersions of Zircon Particle, „Metall. Trans. Vol. 14B, 1983, PP.273-283

[85] Daoud, M.T. Abou El-Khair, and A.N. Abdel-Azim: Effect of Al2O3Particles on the Microstructure and Sliding Wear of 7075 Al Alloy Manufactured by Squeeze Casting Method, Journal of Materials Engg. And Performance Volume 13(2) April 2004-135

[86] K. Dhingra, "Metal replacement by composite", JOM 1986, Vol 38 (03), p. 17

[87] A. K. Kuruvilla, V.V. Bhanuprasad, K. S. Prasad and Y.R. Mahajan, "Effect of different reinforcements on composite-strengthening in aluminum", Bull. Mater. Sci., Vol. 12(5), 1989, pp 495-505.

[88] Alan A. Baker, A. A. Baker: A Proposed Approach for Certification of Bonded Composite Repairs to Flight-Critical Airframe Structure CRC Advanced Composite Structures (CRCACS) and Defence Science and Technology (DSTO) Air Vehicles Division, Melbourne, Australia, 04 Sept., 2010.

[89] Aman Aggarwal & Hari Singh, "Optimization of machining techniques – A retrospective And literature review" S¯adhan¯a Vol. 30, Part 6, December 2005, pp. 699–711. © Printed in India.

[90] A. Ravikiran, M.K.Surappa "Effect of sliding speed on wear behaviour of A356 Al-30 wt.%SiCp MMC In: Wear, 206 (1-2). pp. 33-38.

[91] A.Wang & H.J.Rack, "Transition wear behaviour of SiC-particulate and SiC whisker reinforced 7091 Al metal matrix composites", Journal of Material Science and Engineering A, Vol. 147, 1991, pp 211-224.

[92] Chin- Chun Chang, Ji-Gang Yang, Chi Ling and Chang-Pin Chou, "Optimization of Heat Treatment Parameters with the Taguchi Method for the A7050 Aluminum Alloy" IACSIT International Journal of Engineering and Technology, Vol.2, No.3, June 2010, ISSN: 1793-8236 269

[93] C.Y. Chung and K.C. Lau. "Mechanical Characteristics of Hipped SIC Particulate-Reinforced Aluminum Alloy Metal Matrix Composites", 0-7803-5489-3/99/$10.00109 99 IEEE. P. 1023-28

[94] D. Charles, "Addressing the Challenges of Aircraft Components design & Manufacturing from MMCs", J. Aerospace Engg (Proc. I. Mech E) pp 1-13, 1992.

[95] Deonath, R. T. Bhat and P. K. Rohatgi, "Preparation of Cast ALLOY-Mica ParticleComposites": J. Mater. Sci., Vol. 15, 1980, pp.1241-1251.

[96] D. H. Kim, E.J. Lavernia and J. C. Earthman, "Fatigue Crack growth behaviour of a Continuous alumina fiber reinforced Magnesium alloy", High performance Composites for the 1990"s eds. S.K. Das, C. P. Ballard and F. Marikar, TMS-New Jersey, 1990, pp117-126.

[97] D. Huda, M.A. El Baradie & M.J.S. Hashmi, "Metal Matrix Composites: Materials aspects. Part II"Journal of material processing technology, Vol.37 (1993), 528-541.

[98] D. J. Lloyd, "Particulate Reinforced Composites Produced by Molten mixing," High Performance Composites for the 1990"s, eds. S. K. Das, C.P. Ballard and F. Marikar, TMS-New Jersey, 1990, pp 33-46.

[99] D. Lu, J.F. Li, Y. Rong, A. Grevstad , S. Usui, School of Mechanical Engineering Shandong University, Jinan, China, Temperature and stress analysis in micro-cutting of Ti-6Al-4V and Al7050-T6

[100] D.Mahto and Anjani Kumar, Optimization of Process Parameters in Vertical CNC Milling Machine Using Taguchi"s Design of Experiments, Journal of Arab Research Institute in Sciences & Engg. (Industrial Engg.), ARISER, Vol. 4 No. 2 (2008), pp. 61-75, (UAE).

[101] D.Z. Yang, S. L. Dong, J. F. Mao and Y. X. Cui, "Fabrication Microstructure and Properties of A SiCw/Al-Li-Cu-Mg-Zr Composite",Key Engineering Materials, Vols. 104-107, Metal Matrix Composites, Part1.

[102] G. M. Newaz, H. Neber- Aeschbacher and F. H. Wohlber eds., Trans. Tech. Publications, Switzerland,1995, pp 627-632

[103] P.fluger, A. R. Lewis,. 1996, „Weld Imperfections", Proceedings of a symposium at Lockheed Palo Alto Research Laboratory, Palo Alto, California.

[104] A Arici, S. Selale (2007), "Effects of Tool Tilt Angle on Tensile Strength and Fracture Locations of Friction Stir Welding of Polyethylene", Science and Technology of Welding and Joining, Volume 12, pp. 536-539.

[105] Erica Anna Squeo, Giuseppe Bruno, Alessandro Gugliel, FabrizioQuadrini,(2009), "FrictionStir Welding of Polyethylene Sheets".

[106] S. Saeedy, M. K. BesharatiGivi "Feasibility of Friction Stir Welding on Medium Density Polyethylene Blanks" ASME 2010 10th Biennial Conference on Engineering Systems Design and Analysis, Volume 4 pp. 238-249.

[107] Mustafa Aydin, "Effect of Welding Parameters on Fracture Mode and Weld Strength Friction Stir Spot Welds of Polypropylene Sheets",New tech Ganati, Paper No. ESDA 2010-25344, pp. 841-844.

[108] S. Saeedy, M K Besharati, "Effects of Critical Process Parameters of Friction Stir Welding of Polyethylene" Proceedings of the Institution of Mechanical Engineers, Part B: Journal of Engineering Manufacture, (2011) vol. 225, pp. 1305-1310.

[109] G. H. Payganeh, N. B. Mostafa Arab, Y. DadgarAsif, "Effects of Friction Stir Welding Process Parameters on Appearance and Strength of Polypropylene Composite Welds" International Journal of the Physical Sciences, Vol. 6(19), pp. 4595-4601.

[110] Yoshihiro K., (2013), "Honda develops robotized FSW technology to weld steel and aluminum and applied it to a massproductionvehicle", Industrial Robot: An International Journal, Vol. 40 (3) pp. 208 – 212

[111] https://www.apple.com/in/imac/design/, as accessed on march 19, 2015 at 8:19 AM

[112] http://www.aluminiumleader.com/en/around/transport/cars, as accessed on march 19 at 8:33 AM

[113] http://materion.com/~/media/Files/PDFs/TechnicalMaterials/Bond%20Integrity%20in%20 Aluminum-Copper%20Clad%20Metals.pdf, as accessed on march 19, 2015 at 4:00 PM

[114] Bo li, Zhang Z., Shen Y., Hu W., Luo lei, (2014), ―Dissimilar friction stir welding of Ti6Al4V alloy and aluminum alloy employing a modified butt joint configuration: Influence of process variables on the weld interfaces and tensile properties‖, materials and design, vol. 53, pp. 838-848

[115] Hassan S.F., Gupta M.,(2003) ―Development of high strength magnesium copper based hybrid composites with enhanced tensile properties‖, material science and technology, vol. 19-2, pp253-259

[116] Minitab 17 Program guides and help (2014)

[117] P.L. Ross, ”Taguchi Technique for Quality Engineering”, New York:Mc Graw-Hill book Company,1988.

[118] J. Deng, “Introduction to Grey System Theory”, The Journal of Grey System, 1, pp. 1-24, 1989

BRIEF BIO DATA OF RESEARCH SCHOLAR

I Dhairya Partap Singh, carried out PhD work in the field of Metal Matrix Composite from faculty of Engineering and Technology, YMCA University of Science and Technology, Faridabad, Haryana, India. I did my Master of Technology in Manufacturing and Automation Engineering from YMCA, Faridabad and B. Tech in Mechanical Engineering from Uttar Pradesh Technical University Lucknow, Uttar Pradesh.

I have fourteen months technical experience in reputed industry and eight years teaching experience. I am working as an Assistant Professor in Mechanical Engineering Department at BSA College of Engineering and Technology, Mathura, Uttar Pradesh. I have published 14 research papers in International and National journals and conference proceedings

LIST OF PUBLICATIONS

List of Published Papers

S.NO	Title with date of publication	Journal With Volume & Issue	ISSN/ISBN number	Page no
1	Fabrication and Optimization of Process Parameters for Friction Stir Welding AA7075/10%wt.SiC Composite by Taguchi Method December 2018	Journal of Experimental & Applied Mechanics Vol, 9, Issue 3	ISSN: 2230-9845 (Online), ISSN: 2321-516X (Print) Volume 9,Issue 3	07-17
2	Multi Response Optimization in Friction Stir Welding Al 7075/SiC/10% Metal Matrix Composite. April 2018	Journal of Automobile Engineering and Applications Volume 5, Issue 1	ISSN: 2455-3360	30- 38
3	Optimization of Process Parameters for Friction Stir Welding AA7075/10%wt.SiC Fabricated Composite May 2018	International Journal of Advances in Engineering Sciences Vol. 8, Issue 1	Print-ISSN: 2231-2013 e-ISSN: 2231-0347	01-11
4	Optimization of process parameters for friction stir welded AA7075 SiC Composite joints by Taguchi Method. Jan.2016	YMCAUST International Journal of Research Vol. 4, Issue 1	ISSN: 2319-9377	67-74
5	Evaluating Optimal Process Parameters in Friction Stir Welding of Composites by GRA approach April, 2016	International Journal of Engineering & Technology Research Vol. 4, Issue 2	ISSN Online: 2347 -4904, Print: 2347-8292,	08-16

LIST OF PAPERS IN CONFERENCE PROCEEDINGS

S.No	Title of the paper	Name of Journal	Year	Page No
1.	Evaluating Optimal Process Parameters in Friction Stir Welding of Composites by GRA approach.	AICTE, New Delhi Sponsored International Conference on Technology & Trust (ICTT'17)	2017	37-46
2.	Role of Friction Stir Welding Process Parameters of AA7075.	CSI Sponsored 3rd Inter National Conference on evolution in Science and Technology ASSOCHAM (INDIA)	2014	61-70
3	Review of Friction Stir Welding for Aluminium Metal Matrix Composites	NCETME-2014	2014	26-30
4	Optimization of process parameters for Friction stir Welding AA7075/10%wt. SiC Composite by Taugchi method	NCSMMT-2018	2018	55-61
5	Study on Mechanical behaviour of Particulate Reinforced Aluminu Matrix composites developed by Stir Casting route	Proceedings of the National Conference on Trends and Advances in Mechanical Engineering, YMCA University of Science & Technology, Faridabad, Haryana	2017	293-298

List of Accepted Papers

S.No	Title of the paper	Name of Journal	Volume & Issue	Year	Page No
1.	Optimization of Process Parameters for Friction Stir Welding of cast alloy A7075 by Taugchi Method	International Science Index	------	2019	-----